



Norwegian University
of Life Sciences

Master's Thesis 2018 60 ECTS

Chemistry, Biotechnology and Food Science

Roland Kallenborn

Development of an optimized gas chromatography / triple quadrupole mass spectrometry method for the quantitative determination of nitro- and oxygen containing polycyclic aromatic hydrocarbons (N-/ O-PAHs) in atmospheric samples

Aina Osen Skarshaug

Chemistry

Chemistry, Biotechnology and Food Science

Preface

This master`s thesis was written at the Norwegian University of Life Studies (NMBU) in the faculty of Chemistry, Biotechnology and Food Science (KBM). The project was given in a collaboration with the Norwegian Institute for Air Research (NILU). The main supervisor was professor Roland Kallenborn from NMBU and the co-supervisor was Pernilla Bohlin Nizzetto, PhD, from NILU. I am most grateful for the task that was given me by my supervisors at the NMBU and NILU. It has been interesting and challenging to perform this study and I have learned so much over the past year, more than I could imagine.

A special thanks must be directed to supervisor Roland Kallenborn. Roland has provided me with knowledge and guidance throughout the process, and has always made himself available whenever I, as a frustrated and confused student, have needed his expertise. Roland have also done me the great service of sometimes throwing me in at the deep end of the pool, which has resulted in a sometimes steep learning curve, and a far more excessive knowledge of the GC/MS instrumentation than I would otherwise have obtained. When he learned of my pregnancy he was most supportive, and he has given me much flexibility to work on this thesis in a way that has made me as functional as possible when I have struggled with some physical challenges during this pregnancy. As I deliver this thesis in my 37th week of pregnancy, I could not have hoped for a more understanding and supporting supervisor and faculty.

Thank you also to Pernilla and the others at NILU, who have been very nice and gave me a great deal to think about, and work with, in the formation of this study. The work done at NILU in Kjeller is highly interesting and I am very glad to have been able to access some of the knowledge and resources there. At NMBU a lot of committed, helpful and very resourceful people work, and everyone I have met have been forthcoming and nice. Anne Marie Langseterand and Amir Musa Muhamed Ali are such people, and I thank you for your patience, time and help; you have made my life so much easier.

In this process my family and friends have been so supportive, and I thank you all. Thank you all babysitters and lovely people making dinner for poor, tired students. Thank you to my husband Erik, for always rubbing my feet and saying I am right. And thank you Anna, my clever daughter, for all your patience.

Ås, June 2018

Aina Oser Skarshøy



Norwegian University
of Life Sciences



Norsk institutt for luftforskning
Norwegian Institute for Air Research

Abstract

Nitrated and oxygenated polycyclic aromatic hydrocarbons (nitro-/oxy-PAHs) are organic pollutants which are released to the atmosphere from incomplete combustion processes, or formed by degradation of their parent PAH compounds. Nitro- and oxy-PAHs are present in the atmosphere at trace levels, but are shown to have potential of being highly carcinogenic and mutagenic and therefore represent a significant health threat even at low concentrations. In this study, three methods of identifying the presence of nitro- and oxy-PAHs have been researched and tested.

Before negative ion chemical ionization (NICI) became broadly available for GC/MS analysis, electron ionization (EI) ion sources were used for identification and quantification of PAHs. EI provides more excessive fragmentation, and therefore a higher sensitivity for the identification than the ionization method, which is usually applied for nitro- and oxy-PAH analysis today, NICI. The EI ion source was tested with a 60 m WAX-column in order of achieving improved sensitivity and selectivity compared to formerly applied methods. This method did not offer sufficient sensitivity or selectivity to provide an alternative to the established methods, however, as the EI ion source gave too excessive fragmentation for identification, and the chromatograms had many peaks, implying impurities from the column.

Multiple reaction monitoring (MRM) is a detection method where a precursor ion is selected and exposed to a dissociation reaction, in which it produces a product ion. This method increases the sensitivity, as several steps are monitored and the detection requires presence of both precursor ion and product ion. It was preceded by a product ion scan with NICI ion source and 50 m DB-5 column. The NICI ion source did not fragment enough to produce sufficient product ion yield to create an MRM-method. The EI ion source was not tested, as it provided too low sensitivity to be an alternative.

Selected ion monitoring combined with a NICI ion source is the most common method for trace analysis of nitro- and oxy-PAHs. This method allows focused detection of compound on the basis of monitoring a quantifier and a qualifier ion and separate compounds in different time windows, which gives the opportunity to detect compounds on basis of both retention time and the most abundant ions of the compound. The SIM-method was optimized with a 50 m DB-5 column. An efficient temperature program and SIM-program was developed on basis of experimentation and identification in full scan mode. The SIM-method was validated and used for quantification of two air samples. The method had sufficient linearity, limits of detection, limits of quantification and sensitivity to quantify 25 and identify 30 nitro- and oxy-PAHs. The method has possibilities of improvement, accuracy and sensitivity for late eluent compounds should be improved, and the linearity range, limits of detection and limits of quantification can possibly be lowered with further optimization and method development.

Sammendrag

Nitrerte og oksygenerte polysykliske aromatiske hydrokarboner (nitro-/oksy-PAHer) er organiske forurensninger som blir sluppet ut i atmosfæren fra ufullstendige forbrenningsprosesser, eller som blir dannet ved nedbrytning av PAHer. Nitro- og oksy-PAHer er tilstede i atmosfæren i svært små mengder, men de kan ha kraftige kreftfremkallende og mutagene egenskaper, og utgjør dermed en helsemessig trussel selv ved lave konsentrasjoner. I denne oppgaven har det blitt gjort undersøkelser av, og forsøk med tre metoder for identifikasjon og kvantifisering av, nitro- og oksy-PAHer.

Ionekilder med elektronionisasjon (EI) ble benyttet for identifikasjon og kvantifisering av PAHer før negativ ion kjemisk ionisering (NICI) ble utbredt i GC/MS-analyser. EI gir langt mer omfattende fragmentering enn NICI, noe som gir bedre følsomhet ved identifisering. EI-ionekilde ble testet sammen med en 60 m WAX kolonne, for å undersøke om dette kunne gi bedre følsomhet og selektivitet enn tidligere benyttede metoder for analyse av nitro- og oksy-PAHer. EI ionekilden fragmenterte for omfattende til å oppnå identifikasjon, og kromatogrammene hadde mange utslag, noe som tyder på urenheter fra kolonnen. Metoden ga ikke tilstrekkelig følsomhet eller selektivitet til å kunne utgjøre et alternativ til etablerte metoder.

Multipel reaksjonsovervåking (MRM) er en deteksjonsmetode der et forløper-ion blir valgt og utsatt for dissosiasjonsreaksjoner, der det produseres et produkt-ion. Metoden øker følsomheten ved overvåking av flere steg, og deteksjonen krever tilstedeværelse av både forløper-ionet og produkt-ionet. Det ble utført produkt-ioneskann med NICI ionekilde og 50 m DB-5 kolonne. NICI ionekilden fragmenterte ikke tilstrekkelige til å gi nok produkt-ioneutbytte til å lage en MRM-metode. EI ionekilden ble ikke testet, ettersom den ga for lav følsomhet til å utgjøre et alternativ.

Utvalgt ioneovervåking (SIM) kombinert med NICI ionekilde er den vanligste metoden for nitro-/oksy-PAH analyse. Metoden gir mulighet til å fokusere deteksjon av komponenter ved å overvåke et kvalifiserer-ion og et kvantifiserings-ion, og ved å skille komponenter inn i ulike tidsvinduer. Dette gir muligheten til å detektere komponenter på grunnlag av både retensjonstid og de mest forekommende ionene for hver komponent. SIM-metoden ble optimert med en 50 m DB-5 kolonne. Et effektivt temperaturprogram og SIM-program ble utviklet på grunnlag av eksperimenter og identifikasjon i fullskannmodus. SIM-metoden ble validert og benyttet til kvantifisering av to luftprøver. Metoden har tilstrekkelig linearitet, deteksjonsgrenser og kvantifikasjonsgrenser og følsomhet til å kvantifisere 25 og identifisere 30 nitro- og oksy-PAHer. Metoden har forbedringsmuligheter; nøyaktighet og følsomhet for sent eluerte komponenter kan forbedres, og linearitetsområdet, deteksjonsgrensene og kvantifikasjonsgrensene har muligheter for å bli lavere om metoden blir ytterligere optimert og utviklet.

Content

Preface	1
Abstract.....	3
Sammendrag	4
1.0 Introduction.....	10
1.1 Aim of the study	11
1.2 Objectives	12
2.0 Background.....	13
2.1 Polycyclic aromatic hydrocarbons (PAH).....	13
2.1.1 Nitro-PAHs	13
2.1.2 Oxy-PAHs	16
2.2 Analysis of nitro- and oxy-PAHs	17
2.2.1 Extraction methods	17
2.2.2 The working principles of the GC-MS	19
2.2.3 Application of GC/MS for nitro-/oxy-PAH quantification in environmental samples	27
2.3 Former applied analyzing methods.....	27
2.4 Nitro- and oxy-PAH compounds and analysis in a environmental perspective.....	29
3.0 Methodology	30
3.1 Sampling	30
3.1.1 High volume air sampling.....	30
3.2 Method strategy	31
3.2.1 Testing WAX column (60m) with GC/EI-scan-MS for enhanced selectivity and sensitivity	31
3.2.2 Testing DB-5 column (50m) with GC/NICI-PIScan and MRM-MS for testing mass transition for increased selectivity.....	31
3.2.3 Optimizing DB 5 column (50m) with GC/NICI-SIM-MS for sensitive quantification of oxy- and nitro-PAHs in urban atmospheric samples	32
4.0 Method.....	33
4.1 EI analysis.....	33
4.2 CI analysis	34
4.2.1 SIM-method.....	35
4.2.2 MRM-method	36
4.3 Sampling	37
4.4 Sample preparation.....	38
4.4.1 Filter extraction.....	38
4.4.2 PUF extraction	38
4.4.3 Sample clean-up	39
5.0 Method validation and quality control	40
5.1 Analyte identification	40
5.1.1 Limit of detection.....	40
5.2 Analyte quantification.....	41

5.2.1 Internal standard method	41
5.2.4 Recovery	41
5.2.2 Limit of quantification	42
5.2.3 Sensitivity	42
5.2.5 Accuracy	43
5.2.6 Precision	44
6.0 Results	45
6.1 EI analysis	45
6.1.1 Chromatograms and m/z spectra	46
6.2 NICI analysis	48
6.2.1 Temperature	48
6.2.2 SIM-analysis	49
6.2.3 MRM-analysis	55
7.0 Discussion	57
7.1 EI analysis	57
7.2 NICI analysis	58
7.2.1 Temperature	58
7.2.2 SIM-analysis	59
7.2.3 MRM-analysis	61
8.0 Conclusions	63
Bibliography	64
Appendix	71
Appendix I	72
Appendix II	75
Appendix III	86

Figures

Figure 1: High levels of emissions in urban areas leads to health risk for citizens. (Sosa, Porta, Lerner, Noriega & Massolo, 2017, p. 27).....	10
Figure 2: Metabolic generation of electrophilic metabolites of PAHs (Luch, 2005, p. 21).....	16
Figure 3: Sketch of the Soxhlet extractor (Laboratory size Soxhlet apparatus, 2013).....	18
Figure 4: Guidelines for choice of adsorbent for different types of SPE.....	19
Figure 5: An illustrational scheme of a principal GC-MS (Tröppner, 2017).....	20
Figure 6: Principle of chromatography: separation of a mixture based on difference in affinity towards a mobile and a stationary phase.....	20
Figure 7: Split/splitless injector (Chromedia, 2017).....	21
Figure 8: Quadrupole instrument consisting of source, focusing lenses, (quadrupole) cylindrical rods and detector (de Hoffmann & Stroobant, 2012, p. 90).....	22
Figure 9: Electron ionization ion source (de Hoffmann & Stroobant, 2007, p. 16).....	24
Figure 10: Chemical ionization ion source, the blue dots representing electrons, the green dots representing the reagent gas and the red dots representing the analyte molecules (Williams & Fleming, 2008, p. 183).....	25
Figure 11: Active high volume air sampler.....	30
Figure 12: Temperatures of all temperature programs.....	35
Figure 13: The chromatogram of 2-Nitrobiphenyl-d9.....	46
Figure 14: The mass spectra of peak at retention time 43,76 min in the chromatogram of 2-Nitrobiphenyl-d9.....	46
Figure 15: The chromatogram of 1-Indanone.....	47
Figure 16: The m/z spectra of peak at retention time 15,6 min in the chromatogram of 1-Indanone.....	47
Figure 17: The chromatogram of 9-Nitroanthracene.....	47
Figure 18: The mass spectra of peaks at retention time 24,68 min, 33,18 min and 40,4 min in the chromatogram of 9-Nitroanthracene.....	48
Figure 20: Effect of different temperature programs on the first compounds to elute.....	48
Figure 21: Effect of different temperature programs on the last compounds to elute.....	49
Figure 22: Spectra of 1 ng/ μ L SIM-method run showing all compounds.....	50
Figure 23: The Total Ion Chromatogram used for the Product Ion Scan showing very few peaks, except the ISTD-peaks of 17,1 min and 18, 0 min.....	55
Figure 24: The Total Ion Chromatogram used for the Product Ion Scan zoomed in at the first and second window, showing the baseline and the ISTD-peaks.....	55
Figure 25: The mass transfer of the ISTD-peak of 17,1 min in the Total Ion Chromatogram in Figure 23 and Figure 24.....	56
Figure 26: Chromatogram of four method blanks displayed on top of each other (file ONPAH-0078. ONPAH-0081, ONPAH-0084 and ONPAH-0108).....	85
Figure 27: Calibration curve for 1,4-Naphtoquinone.....	86
Figure 28: Calibration curve for 1-Nitronaphtalene.....	86
Figure 29: Calibration curve for 2-Nitronaphtalene.....	87

Figure 30: Calibration curve for 9-Fluorenone	87
Figure 33: Calibration curve for 4-Nitrobiphenyl	87
Figure 34: Calibration curve for 5-Nitroacenaphtene	88
Figure 35: Calibration curve for 9,10-Anthraquinone	88
Figure 36: Calibration curve for 4H-Cyclopentan[def]phenanthen-4-one	88
Figure 37: Calibration curve for 2-Methyl-9,10-Anthraquinone.....	89
Figure 38: Calibration curve for 2-Nitrofluorene.....	89
Figure 39: Calibration curve for 9-Nitroanthracene	89
Figure 40: Calibration curve for 9,10-Phenanthrenquinone	90
Figure 41: Calibration curve for 9-Nitrophenanthrene	90
Figure 42: Calibration curve for 2-Nitroanthracene	90
Figure 43: Calibration curve for Benzo[a]fluoren-11-one	91
Figure 44: Calibration curve for 2-Nitrofluoranthene	91
Figure 45: Calibration curve for 3-Nitrofluoranthene	91
Figure 46: Calibration curve for 4-Nitropyrene.....	92
Figure 47: Calibration curve for 1,8-Dinitropyrene.....	92
Figure 48: Calibration curve for 2-Nitropyrene.....	92
Figure 49: Calibration curve for 1-Nitropyrene.....	93
Figure 50: Calibration curve for 2,7-Dinitrofluorene.....	93
Figure 51: Calibration curve for 7-Nitrobenz[a]anthracene	93
Figure 52: Calibration curve for 6-Nitrocrysene	94
Figure 53: Calibration curve for 6H-Benzo[c,d]pyren-6-one	94

Tables

Table 1: The nitro-PAHs with component information and parent PAH	15
Table 2: The oxy-PAHs with component information and parent PAH.....	17
Table 3: Temperature program EI analysis	33
Table 4: Information of calibration standard and internal standard identification criteria (National Center for Biotechnology Information, 2018)	34
Table 5: Varying parameters of all temperature programs.....	35
Table 6: SIM program information with compound identification	36
Table 7: Product Ion Scan method information	37
Table 8: Sample information.....	37
Table 9: Result of GC/MS analysis of calibration standard with EI ion source	45
Table 10: Calibration parameters of the 25 compounds that could be quantified with this SIM-method, including LOD and LOQ.....	51
Table 11: Calculated LOQ for the not quantifiable compounds	51

Table 12: Calculated amount of C12 standards from the spiked laboratory blanks, with calculated percentage share of true value	52
Table 13: Concentration of analyte in each sample, and average response factor of each analyte compound. Results highlighted in bold marked with * is above the LOD, results highlighted in bold marked with ** is above the LOQ.....	53
Table 14: The accuracy of the standard calibration compounds	54
Table 15: Average response and standard deviation of the internal standard signals	54
Table 16: Comparison of maximum concentrations of nitro- and oxy-PAHs measured in different studies in different locations	60
Table 17: Summary of findings about the SIM-method and suggestions for further development	61
Table 18: Solvent information with CLPs and safety precautions.....	72
Table 19: Stock standard information	72
Table 20: Equipment information.....	73
Table 21: Overview of EI analysis of standard solutions with Chromatographic peaks and according m/z peaks ranked in order of magnitude	75

1.0 Introduction

Airborne pollution is a highly applicable topic, as it is more or less globally accepted fact that the temperature of the Earth is raising as a consequence of human emission and the United Nations is taking as much action as possible to achieve climate neutrality. (United Nations, 2012, p. 15) Working parallel to the political and public interest in climate changes are scientific progress in the understanding of the impact emissions and pollution have on human health and on wildlife around the globe.

Atmospheric particulate matter with a diameter of less than 2,5 μm ($\text{PM}_{2.5}$) is recognized as one of the most hazardous groups of airborne pollutants, because of their ability to drift far into the lungs when inhaled (Liu et al., 2017, p. 1). Polycyclic aromatic hydrocarbons (PAH) is a group of one of the most toxic air pollutants, as they are strongly associated with human lung cancer (Dang et al., 2014, p. 387). Nitrated PAHs (nitro-PAHs) and oxygenated PAHs (oxy-PAHs) are important groups of PAH derivatives. Some of these PAH derivatives show more toxicity than their parent PAH, because of their direct-acting mutagenicity and carcinogenicity (Alves et al., 2017, p. 495). PAHs released into the atmosphere is carried by $\text{PM}_{2.5}$, witch works as a carrier for toxic organic compounds (Liu et al., 2017, p. 1), as illustrated in Figure 1.

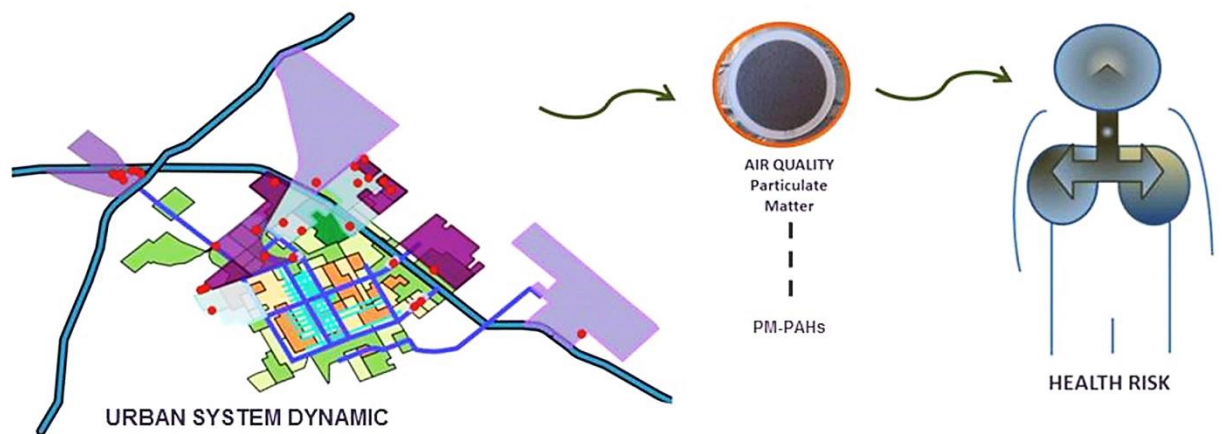


Figure 1: High levels of emissions in urban areas leads to health risk for citizens. (Sosa, Porta, Lerner, Noriega & Massolo, 2017, p. 27)

PAHs are mainly formed by incomplete combustion processes and in 2007 the global emission of PAH were expected to surpass 500 Gg. High levels of PAH have been observed in the atmosphere as a result of the high global emissions (Lin et al., 2015, p. 164). The highest concentrations of PAHs are found in urban areas, with high human populations, high vehicular traffic and little scattering of atmospheric pollutants. This makes the cities associated with the most risk of PAH exposure (Srogi, 2007, p. 170). The most risk is of PAH, nitro- and oxy-PAH exposure seem to be at traffic sites, as these sites are more exposed than urban background site or suburban sites (Alves et al., 2017, p. 496).

Benzo[a]pyrene (BaP) is one of the PAH carcinogens used as a trace compound for atmospheric PAHs. The EU uses the monitoring of this trace compound as a measure of the current PAH level in the air, and has a target value of 1 ng/m³ as annual average (Alam et al., 2015, p. 428). BaP is one of the most carcinogenic PAHs and is therefore used to indicate PAH level, as the other high priority PAHs are ranked according to carcinogenic properties relative to BaP (Dang et al., 2014, p. 387). In order of effective monitoring of PAHs, nitro-PAHs and oxy-PAHs, the selection of representative trace compounds (such as BaP) which provide information of the level of present contaminants causing a threat to health and environment need to be made.

1.1 Aim of the study

The topic of this thesis is method optimization for an analyzing method fit for the analysis of airborne nitrated and oxygenated derivatives of polycyclic aromatic hydrocarbons. These components are not generally exposed for surveillance, but advancement in the health sciences proves this might be a future necessity.

Oxy-PAHs have been studied by selection of trace compounds as 7H-benz[de]anthracene-7-one (BA), benzo[a]fluoren-11-one (BF) and benz[a]anthrazene-7,12-dione (BAD). These trace compounds are known to be produced both by combustion and photochemical reaction, and they have known ability to produce toxic reactive oxygen species after entering the respiratory system (Filippo, Pomata, Riccardi, Buiarelli & Gallo, 2015, p. 129). Wang et al. (2016) used the nitro- and oxy-PAH compounds representing the maximum concentrations as target chemicals in their study of the low molecular weight nitro- and oxy-PAHs (Wang et al., 2016, p. 569). This approach has the obvious advantage of providing the maximum level.

Oxy-PAHs are considered toxic both for humans and the environment, and their main primary source is fossil fuel combustion, wood combustion and metalwork furnaces (Filippo et al., 2015, p. 126) making trace analysis of these kind of pollutants tracers for fossil fuel combustion and environmentally threatening emissions.

Nitro-PAHs are mainly present in the atmosphere due to exhaust from diesel vehicles or secondary atmospheric reactions. Nitro-PAHs are strongly mutagenic and carcinogenic in the human cell, showing a great toxicity (Lin et al., 2015, p. 164), making trace analysis of their presence in the air a necessity.

1.2 Objectives

The main objectives of this master's thesis were:

- Conducting a study of the possibilities for analysis of nitrated and oxygenated polycyclic aromatic hydrocarbons with gas chromatography / mass spectrometry instrumentation using different ionization techniques (i.e., electron ionization and chemical ionization)
- Explore the possibilities of Multiple reaction mode (MRM) based Electron ionization for the quantitative analysis of nitrated and oxygenated polycyclic aromatic hydrocarbons
- Developing a highly sensitive trace analytical method for the determination of nitrated and oxygenated polycyclic hydrocarbons in urban air samples based on gas chromatography / mass spectrometry and negative ion chemical ionization (GC/NICI-SIM-MS).

2.0 Background

2.1 Polycyclic aromatic hydrocarbons (PAH)

Polycyclic aromatic hydrocarbons is a collective term describing a group of chemical components consisting of at least two or more benzene rings. PAHs are considered pollutants with mainly origins from anthropogenic incomplete combustion processes (Norwegian Environmental Agency, 2017). PAHs are a group of environmental contaminants, characterized by several chemical and physical characteristics, such as aggregation phase, life time and concentration level. The current scientific knowledge on environmental and health risks support the urgent need for continuous PAH monitoring and mitigation actions (Cecinato, Balducci, Mastroianni & Perilli, 2012, p. 1915). PAHs carcinogenic, mutagenic and teratogenic properties make them today a major health concern (Tomaz et al., 2017, p. 145).

PAH emissions from aluminum production is today considered an important source to PAH emission on the environment in Norway, as well as PAH release from the transport sector (Fossil fuel combustion), firewood burning and leaching from contaminated soil. Emissions from aluminum production have decreased significantly during the past decade, due to modernization of infrastructures, but they are still an important contributor to the overall PAH pollution in Norway (Norwegian Environmental Agency, 2017).

PAHs has always been present in the environment, because of their natural occurrence (i.e., uncomplete combustion of wood materials). The level of occurrence vary very much since its dependent on a variety of influencing factors, such as weather conditions, emission source and presence of influencing reactants like CO and O₃ in the atmosphere (Barrado, Garcia, Castrillejo & Barrado, 2012, p. 386).

PAH emission reduction is a global priority today, since the hazard effects of PAHs on humans and environments are considered as severe. The World Health Organization (WHO) reports a number of PAHs both as carcinogenic (Harrison et al., 2016, p. 1176).

The measurement of PAHs are often focused on the high-boiling fraction of the samples, since this is the fraction known to be possible hazardous for human health. Major transformation products such as nitrate containing (nitro-PAHs), methylated and halogenated PAH components are found to have increased toxicity compared to their respective mother component (Cecinato et al., 2012, p. 1918).

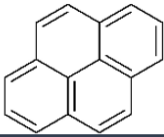
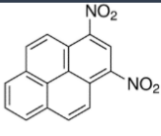
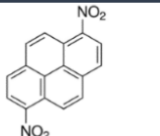
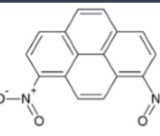
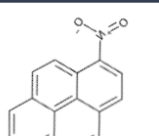
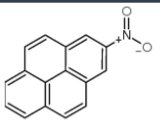
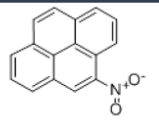
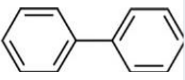
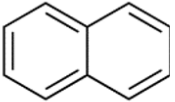
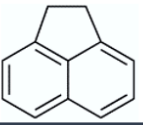
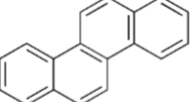

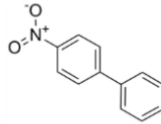
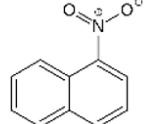
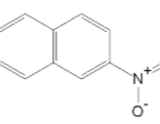
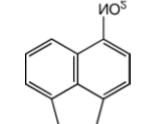
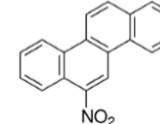
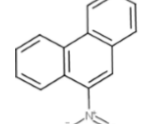
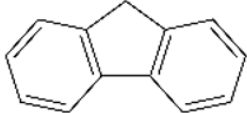
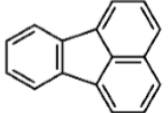
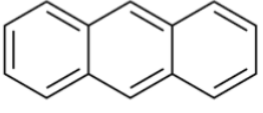
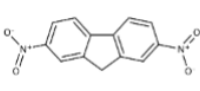
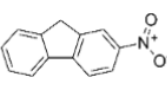
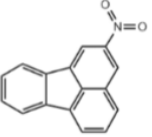
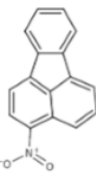
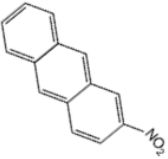
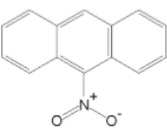
2.1.1 Nitro-PAHs

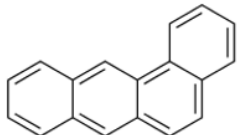
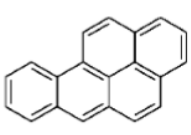
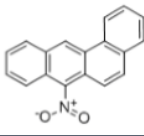
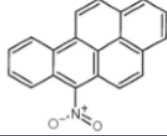
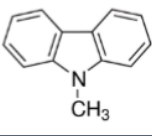
Nitro PAHs possess toxic properties for mammals (incl. humans), as they are strong mutagens. The mutagenic potency of nitro-PAHs does not require enzymatic activity. Nitro-PAHs occur both as products

of photochemical reactions and as direct emission, as they are produced and emitted from diesel engines (Cecinato et al., 2012, p. 1918). Nitro-PAHs has been found to be ubiquitously distributed, even though most of the measurements has been performed in urban areas. These findings match the multiplicities of the emission sources and the studies conducted show the impact the occurrence of nitro-PAHs have on populations (de Castro Vasconcellos, Sanchez-Ccoyllo, Balducci, Mabilia, & Cecinato, 2008, p. 88).

Specific Nitro-PAH isomers are formed depending on route of formation (Bamford, Bezabeh, Schantz, Wise & Baker, 2003, p. 576). Atmospheric occurrence of nitro-PAHs such as 2-nitropyrene and 2-nitrofluoranthene may be explained by hydroxyl radical (OH) induced nitration of the parent PAH in the presence of NO_2 . The hydroxy radical is not present without the sunlight. The parent PAH may be nitrated in the atmosphere during dark hours, but the presence of N_2O_5 or NO_3 is necessary for nitration to occur. This reaction will form 4-nitropyrene instead of 2-nitropyrene. In general, The ratio of formation of nitro-PAHs with respect to their parent PAH is expected to be about 3 % for native pyrene and, 30 % for native fluoranthene and about 100 % for native pyrene during the night (de Castro Vasconcellos et al., 2008, p. 88). The nitro-PAH isomers formatted in the atmosphere differs from the ones directly emitted from combustion processes, (Zielinska & Samy, 2006, p. 883) since the formation route effect the product, this is visible when studying the nitro-PAHs in correspondence with their parent PAHs, as in table 1.

Table 1: The nitro-PAHs with component information and parent PAH

Parent PAH						
	Pyrene					
Nitro-PAH						
	1,3-dinitropyrene	1,6-dinitropyrene	1,8-dinitropyrene	1-Nitropyrene	2-Nitropyrene	4-Nitropyrene
Molecular weight	292.25	292.25	292.25	247.25	247.25	247.25
Molecular formula	$C_{16}H_8N_2O_4$	$C_{16}H_8N_2O_4$	$C_{16}H_8N_2O_4$	$C_{13}H_9NO_2$	$C_{13}H_9NO_2$	$C_{13}H_9NO_2$
Parent PAH						
	Biphenyl	Naphthalene	Acenaphthene	Chrysene	Phenanthrene	
Nitro-PAH						
	4-nitrobiphenyl	1-Nitronaphthalene	2-Nitronaphthalene	5-nitroacenaphthene	6-nitrochrysene	9-Nitrophenanthrene
Molecular weight	199.21	173.17	173.17	199.21	273.29	223.23
Molecular formula	$C_{12}H_9NO_2$	$C_{10}H_7NO_2$	$C_{10}H_7NO_2$	$C_{12}H_9NO_2$	$C_{18}H_{11}NO_2$	$C_{14}H_9NO_2$
Parent PAH						
	Fluorene	Fluoranthene	Anthracene			
Nitro-PAH						
	2,7-Dinitrofluorene	2-Nitrofluorene	2-nitrofluoranthene	3-nitrofluoranthene	2-nitroanthracene	9-nitroanthracene
Molecular weight	256.21	211.22	247.25	247.25	223.23	223.23
Molecular formula	$C_{13}H_8N_2O_4$	$C_{13}H_9NO_2$	$C_{16}H_9NO_2$	$C_{16}H_9NO_2$	$C_{14}H_9NO_2$	$C_{14}H_9NO_2$

Parent PAH			
	Benz[a]anthracene	Benzo[a]pyrene	
Nitro-PAH			
	7-nitrobenz[a]anthracene	6-nitrobenzo[a]pyrene	9-Methylcarbazole
Molecular weight	273.29	297.31	181.23
Molecular formula	C ₁₈ H ₁₁ NO ₂	C ₂₀ H ₁₁ NO ₂	C ₁₃ H ₁₁ N

2.1.2 Oxy-PAHs

PAHs are typically oxidized in the atmosphere. The lifetime of these oxidation products often varies from hours to days. (Harrison et al., 2016, p. 1176) Four main categories of oxygenated PAHs have been investigated: phenols/diols, ketones/quinones, carboxaldehydes and oxygenated heterocycles (Cecinato et al., 2012, p. 1918). Oxygen containing products of PAHs, oxidized in the atmosphere are likely to be oxy-PAHs, such as quinones (Harrison et al., 2016, p. 1176).

Oxy-PAHs is mainly formed by oxygenating agents like O₃ or NO_x reacting with the mother PAHs, but they may also be formed directly by uncomplete combustion. In the human metabolism electrophilic metabolites of PAHs may be generated as illustrated in Figure 2.

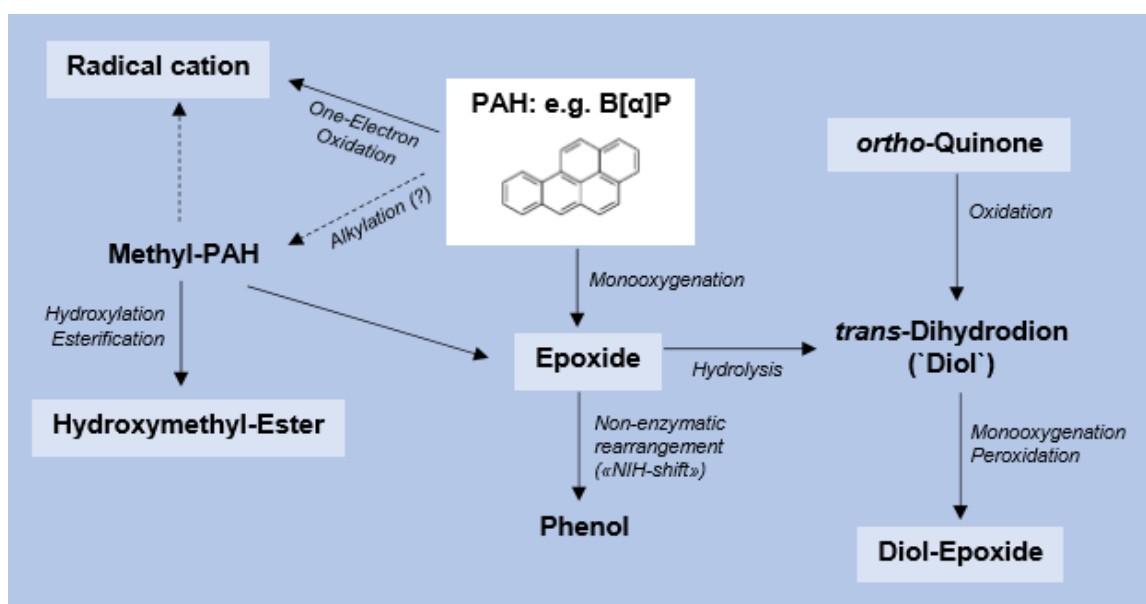
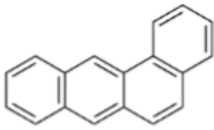
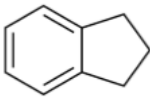
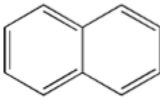
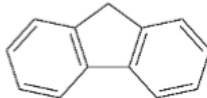

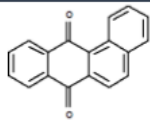
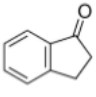
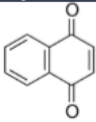
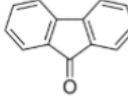
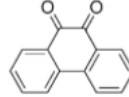
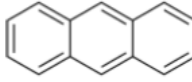
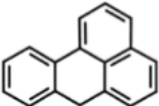
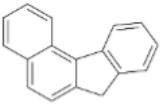
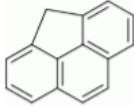
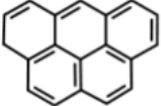
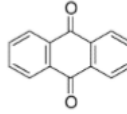
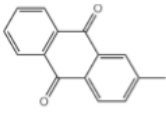
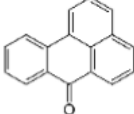
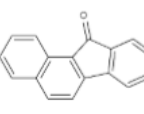
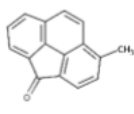
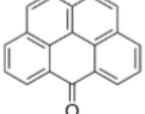


Figure 2: Metabolic generation of electrophilic metabolites of PAHs (Luch, 2005, p. 21)

Table 2: The oxy-PAHs with component information and parent PAH

Parent PAH						
	Benz[a]anthracene	Indane	Naphthalene	Fluorene	Phenanthrene	
Oxy-PAH						
	1,2-Benz[a]anthraquinone	1-Indanone	1,4-Naphthoquinone	9-Fluorenone	9,10-Phenanthrenequinone	
Molecular weight	258.28	132.16	158.15	180.20	208.21	
Molecular formula	C ₁₈ H ₁₀ O ₂	C ₉ H ₈ O	C ₁₀ H ₆ O ₂	C ₁₃ H ₈ O	C ₁₄ H ₈ O ₂	
Parent PAH						
	Anthracene	Benz[d,e]anthracene	Benzo[c]fluorene	Cyclopenta[d,e,f]phenanthren	Benzo[c,d]pyrene	
Oxy-PAH						
	9,10-Anthraquinone	2-Methyl-9,10-anthraquinone	Benzanthrone	Benzo[a]fluoren-11-one	4H-Cyclopenta[d,e,f]phenanthren-4-one	6H-Benzo[c,d]pyren-6-one
Molecular weight	208.21	222.24	230.27	230.26	204.22	254.28
Molecular formula	C ₁₄ H ₈ O ₂	C ₁₅ H ₁₀ O ₂	C ₁₇ H ₁₀ O	C ₁₇ H ₁₀ O	C ₁₅ H ₈ O	C ₁₉ H ₁₀ O

2.2 Analysis of nitro- and oxy-PAHs

The instrumental analysis of PAHs traditionally consist of a chromatographic unit coupled with a mass spectrometer. The mass spectrometry provide definite advantages considering identification of chemical compounds and the combination with a chromatographic unit represent the ability to separate similar compounds (Kasiotis & Emmanouil, 2015, p. 173).

MS fragmentation profiles of PAH isomers often share characteristic fragmentation pattern and m/z-value. Comparison with standards and chromatographic separation is mandatory for reliable identification and quantification (Anderson, Szelewski, Wilson, Quimby & Hoffman, 2015, p. 90).

2.2.1 Extraction methods

Albinet et al. developed a Quick Easy Cheap Effective Rugged and Safe (QuEChERS) extraction method for sample preparation of PAHs in atmospheric particulate matter (Albinet et al., 2013, p. 32), meaning filter samples. The QuEChERS-method was originally developed for extraction of pesticides in food samples, and gave the opportunity for making the extraction of samples of organic compounds more

effective (Albinet et al., 2013, p. 32). The QuEChERS-method consist of an time-efficient extraction step using vortex agitation and centrifugation for the sample preparation, followed by an solid phase extraction for the sample clean-up (Albinet et al., 2013, p. 34).

The extraction procedure applied on the gaseous phase samples (the PUFs) followed the procedure presented by Kristin Sundby in her master's thesis, using Soxhlet extraction for the sample preparation and solid phase extraction for further sample clean-up (Sundby, 2017, p. 24 – 25).

Soxhlet extraction

Soxhlet extraction is a well-established separation methods in analytical chemistry. It was invented in 1879 and was originally used to determine the amount of fat in milk (de Castro & Priego-Capote, 2010, p. 2384). The Soxhlet extraction method has since then been used on a wide range of target components in environmental research, as it works as a efficient way of separating analytes in complex sample matrixes and the method does not require excessive mechanization and manual labor (Chen & Urban, 2015, p. 75).

Conventionally set-up of the Soxhlet extractor will have the sample placed on a thimble holder which will gradually be filled up with extract. A siphon will lead the solute back as the liquid reaches the over-flow level, this will carry the analyte into the bulk liquid. This procedure will repeat itself until the extraction is complete (de Castro & Priego-Capote, 2010, p. 2384). A typical Soxhlet extraction set-up is illustrated in Figure 3.

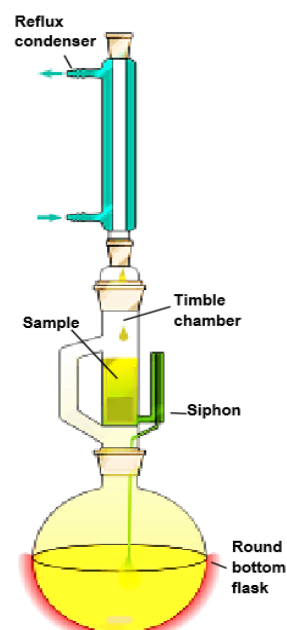


Figure 3: Sketch of the Soxhlet extractor (Laboratory size Soxhlet apparatus, 2013)

Solid Phase Extraction

Solid Phase Extraction (SPE) techniques are based on the separating of analytes between a solid and a liquid phase. SPE is used to either increase analyte concentration or to remove matrix interferences. SPE may be used for different types of analytes, as it can be conducted in Reverse-Phase , Normal-Phase and

Ion-Exchange mode (Nickerson, 2011, p. 75) as can be seen in Figure 4.

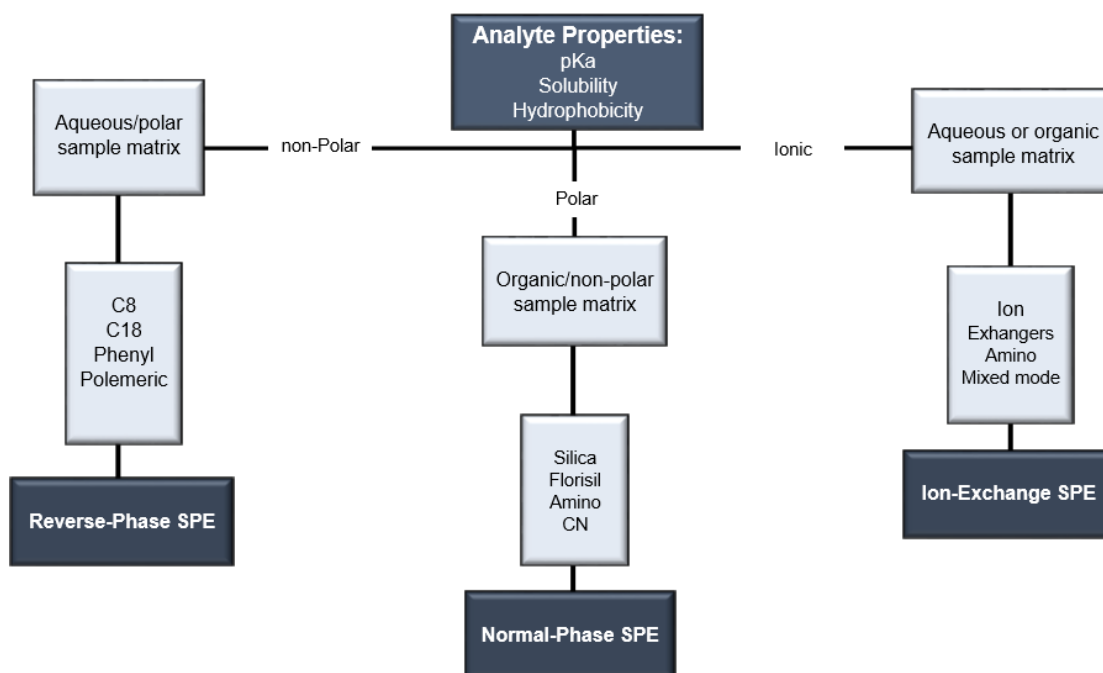


Figure 4: Guidelines for choice of adsorbent for different types of SPE

The SPE procedure goes through a conditioning step, where the solid packing material is conditioned by a suitable solvent which make the sorbent compatible with the liquid solution, before the sample is loaded or adsorbed. After the sample has been loaded a washing step follows, and the last step of elution. The adsorbed analytes are to be selectively detached from the extractant by a strong solvent during the elution step (Bart, 2005, p. 125).

2.2.2 The working principles of the GC-MS

The gas chromatograph coupled to a mass spectrometer (ref. Figure 5) makes an analytical method and instrument considered to be precise and accurate enough to meet the demanding needs of environmental analysis.

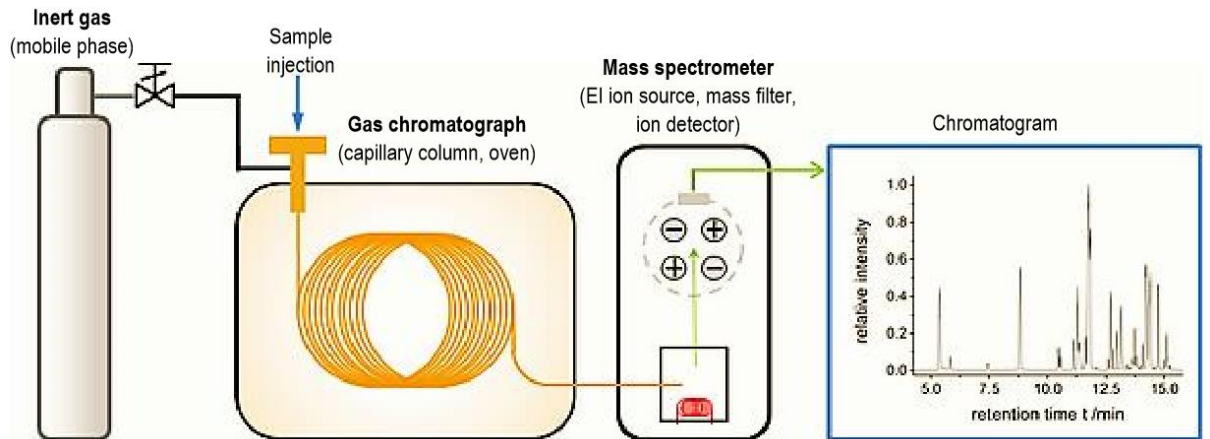


Figure 5: An illustrational scheme of a principal GC-MS (Tröppner, 2017)

Gas Chromatograph

Chromatography takes advantage of the difference in affinity towards a mobile phase and a stationary phase in the different components in a mixture, as shown in Figure 6. Gas chromatography uses a vaporized sample inserted onto the head of the chromatographic column. The sample is eluted through the column by an inert gaseous mobile phase. In other types of chromatography the mobile phase will interact with the molecules of the sample, in gas chromatography however, the mobile phase is only used for transportation and is thus often referred to as the carrier gas (Holler, Skoog & Crouch, 2007, p. 788-790).

Gas chromatography consist of two main categories, gas-liquid chromatography and gas-solid chromatography. Gas-solid chromatography consists of a solid stationary phase and a gaseous mobile phase, and is only in limited use because of challenges in the method such as heavy tailing of elution peaks and close to permanent retention of polar molecules. Gas-liquid chromatography is a popular separation method and is commonly shortened to gas chromatography (GC).

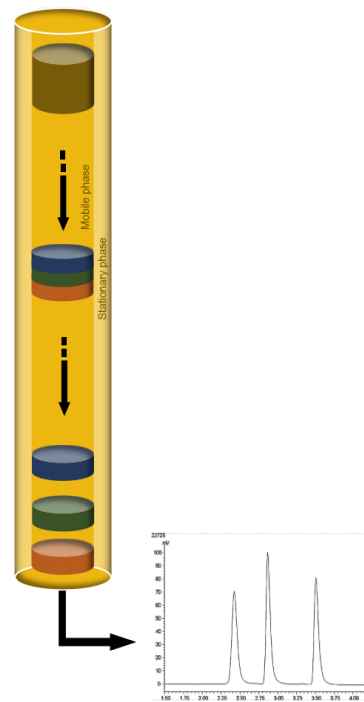


Figure 6: Principle of chromatography: separation of a mixture based on difference in affinity towards a mobile and a stationary phase

GC uses a gaseous mobile phase and a surface immobilized liquid phase. The liquid phase of the GC is either immobilized on the surface by an inert solid packing or on the walls of a capillary tubing (Holler, et al., 2007, p. 788). Gas-Liquid chromatography has high resolution, the ability of very quick analysis and detection range in the nanogram and picogram area (Greibrok, Lundanes & Rasmussen, 1998, p. 109).

GC Injection system

The injection system on to the chromatographic column must provide introduction of the sample in a suitable size and as an efficient vapor cloud. Inefficient sample introduction will lead to poor resolution and band spreading (Holler, et al., 2007, p. 791). Chromatographs are usually installed with a vaporizing injector which will introduce gasses, liquids and solids on the column (Greibrok et al., 1998, p. 115).

Capillary columns demands injection systems that meet their need of low volume injection (normally capillary columns only allow 50 – 100 ng analyte injected onto the column). The most common of these injectors are split injection, splitless injection and on column injection (Greibrok et al., 1998, p. 144). Split and splitless injection are proceeded with the same instrument, the split/splitless injector, as shown in Figure 7 and this is the most commonly used injector type, and the injector used in this thesis.

Split injection is ordinary vaporizing injection where the sample are vaporized, but split, so a part of the sample is introduced onto the column, and the rest is ventilated out of the injector. Normal split conditions may vary from 1:10 to 1:100, where 1 part is brought on to the column, while the rest is let out. With splitless injection the split vent is closed and the entire sample volume, or at least close to 100 %, is vaporized and injected onto the column. The injector use about 30 seconds to inject 1 mL gas onto the capillary column. To get 1 mL gas, 2 μ L sample solution must be injected and vaporized (Greibrok et al., 1998, p. 145).

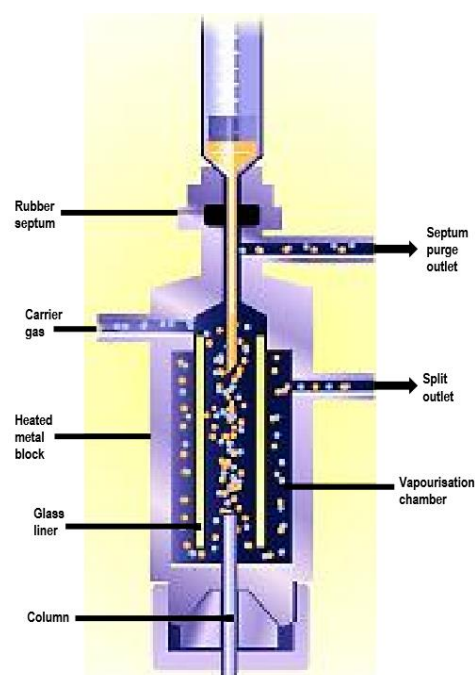


Figure 7: Split/splitless injector (Chromedia, 2017)

GC Column

There are two main types of often used columns used in GC: packed and capillary. Packed columns have a length in the area of 1 m to 5 m while capillary columns exist in the area from a couple of meters to 100 m. Construction material for most columns are fused silica, stained steel or less commonly glass and Teflon (Holler, et al., 2007, p. 791). The column is coiled to fit in the column oven, where a temperature just above or equal to the boiling point of the analyte will give a sensible elution time of about 2 min to 30 min. To achieve the best resolution the temperature needs to be as low as possible, this however, require a longer elution time (Holler, et al., 2007, p. 792).

Capillary columns consist of two basic categories, the wall-coated open tubular (WCOT) and the support-coated open tubular (SCOT) Where the capillary is internally lined with a thin film of support material. WCOTs are capillary tubes where the stationary phase has been coated on in a thin layer on the capillary tube. The definitely most commonly used column is the fused-silica wall-coated (FSWC) open tubular columns. These kind of columns are made with purified silica which contains very little metal oxides, they are given additional strength by an external layer of polyimide and they have much thinner capillary walls than glass columns. The FSWC capillary columns are strong and flexible, which gives them an advantage in instrumentation as they are efficiently coiled (Holler, et al., 2007, p. 801).

Mass spectrometer

Mass spectrometry (MS) is based on the production of ions, and finding the accurate weight of these ions. Mass spectrometers operate by taking the molecules M into gas phase, produce ions such as M^+ or MH^+ from the molecule and separate the ions by their mass-to-charge (m/z) ratio. Normally the charge on the ions are one, and the mass of the ions can be found directly from the MS spectra. Ionization methods as electrospray (ESI) or laser desorption (LD) do produce ions with multiple charges, however, but these methods will not be described throughout this thesis, as they are not available for this thesis. Some ionization methods use vibrational energy of such force they fragment into neutral fragments, which cannot be detected in the MS, and new ions, which can be used to obtain structural information (Williams & Fleming, 2008, p. 180).

In this study a GC/MS instrumentation with a quadrupole analyzer is employed. Quadrupole analyzers separate ions on basis of their m/z ratios by utilizing the stabilities of trajectories in oscillating electric fields. Quadrupole instrumentation consists of four parallel rods (de Hoffmann & Stroobant, 2012, p. 88) , as shown in Figure 8.

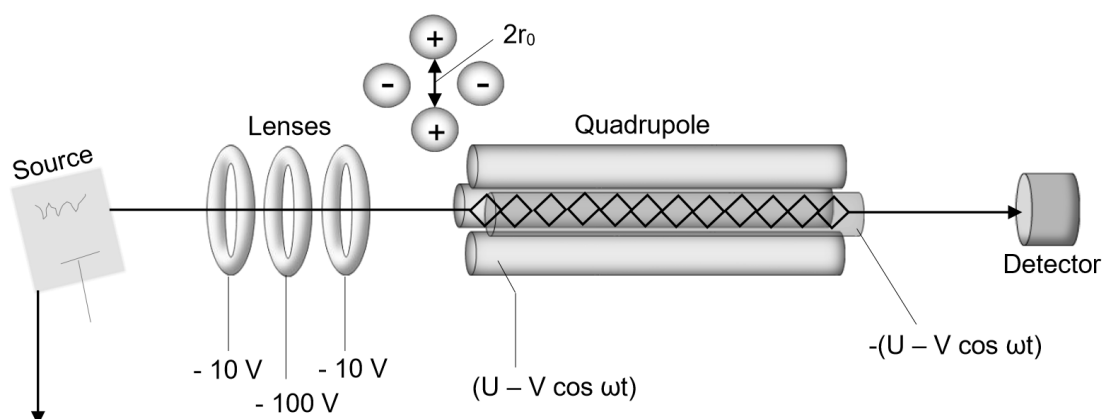


Figure 8: Quadrupole instrument consisting of source, focusing lenses, (quadrupole) cylindrical rods and detector (de Hoffmann & Stroobant, 2012, p. 90)

Ions entering the space between the rods of the quadrupole analyzer will be drawn to the rods with opposite charge of the ions – the ion will however change direction if the potential changes sign, forcing the ions to travel through the rods. The formula in Figure 9 describes the electric field influencing the ions travelling along the z-axis. This electric field is produced as a consequence of the potential of the quadrupole rods. This potential make a quadrupole alternative field, superposing a constant field.

$$\varphi_0 = (U - V \cos \omega t)$$

[Formula 1]

Φ_0 = the potential applied to the quadrupole rods

ω = the angular frequency

U = the direct potential

V = the zero-to-peak amplitude of the RF voltage

(de Hoffmann & Stroobant, 2012, p. 91)

Ionization methods

Electron ionization (EI) is one very commonly used method in which the molecular ion is fragmented, sometimes in such extent the molecular ion may not be detected (de Hoffmann & Stroobant, 2007, p. 15). A single electron may be removed from the molecule, producing a molecular ion, or the molecule may be broken to pieces, producing one or more fragment ions. A certain amount of energy is required to achieve ionization of the analyte molecule or fragments. The produced ions will have a certain amount of kinetic energy. The least amount of energy (U_{min}) required to produce ions of a diatomic analyte molecule is given by:

$$U_{min} = U_A + U_B + D_{AB} + W_{min}$$

[Formula 2]

U_A and U_B = the excitation energy of atom A and B of the diatomic molecule AB

D_{AB} = the dissociation energy

W_{min} = the minimum energy the relative motion of the ionic fragment will have

(Chaudhry & Kleinpoppen, 2011, p. 26)

The diatomic molecule is used as an illustrative simplification of the principle, the formula will be used in the same, although more complex form to describe a more complex molecule.

The electron ionization ion source consist of a heated filament which give off electrons that are accelerated towards an anode so they collide with sample molecules, as shown in Figure 9. The sample molecules must be in a gaseous phase (de Hoffman & Stroobant, 2007, p. 16 – 17). The EI ionization

method provide a fragmentation of the sample molecules, the fragments that are fragmented are detected and thus visible on the m/z spectra.

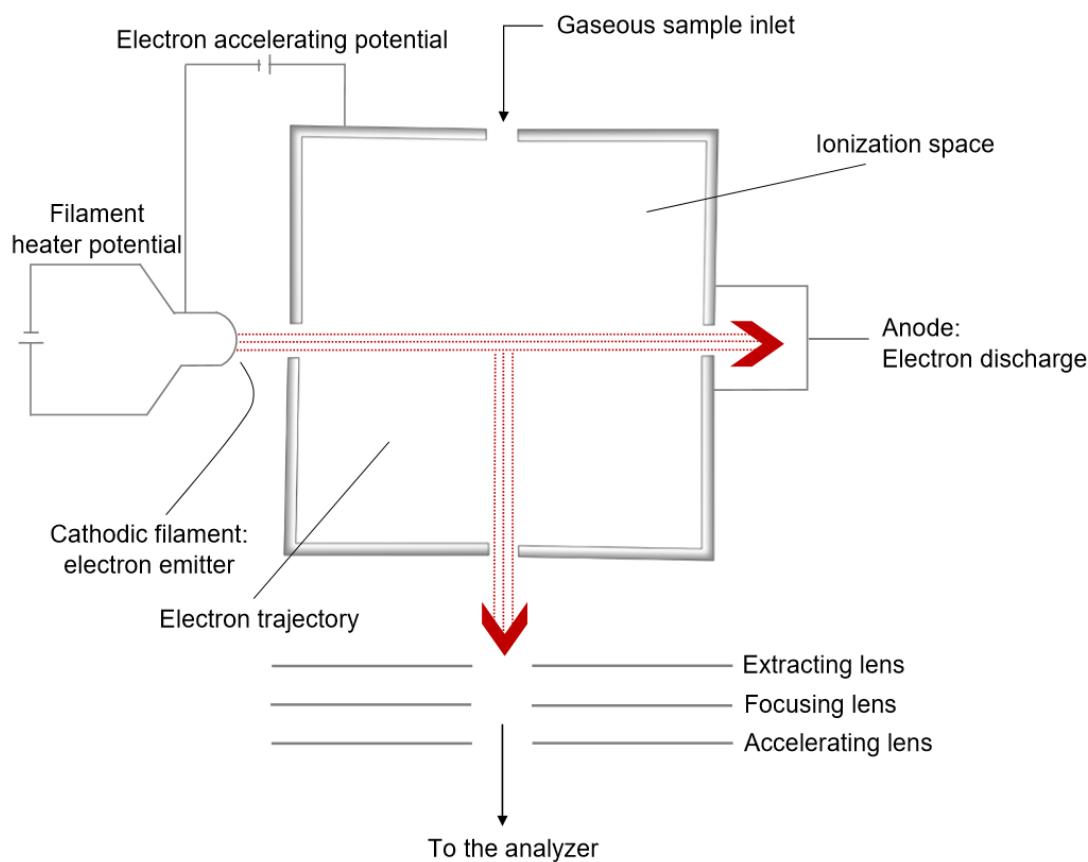


Figure 9: Electron ionization ion source (de Hoffmann & Stroobant, 2007, p. 16)

The fragmentation of the molecule is an advantage considering identification of analytes. The electron ionization method often gives good sensitivities, due to the production of high ion currents. An important disadvantage to this ion source is that it requires volatilization of the sample. Volatilization may cause some thermal degradation of the sample, and loss of analyte (Holler, et al., 2007, p. 557).

There exist softer ionization methods, which will not always provide fragmentation, but will ensure the production of the molecular ion. Chemical ionization (CI) is a ionization method which does provide ions without much excess energy. Chemical ionization is in use as a complimentary method to electron ionization for identification of the analyte, as it provides MS spectra without much disturbance and an easily recognizable molecular ion (de Hoffmann & Stroobant, 2007, p. 17). In chemical ionization a reagent gas is ionized and then leads to collide with sample molecules, M . The sample molecules are ionized by either proton transfer, which produces an $[M+1]^+$ ion, by electrophilic addition, which produces an $[M+15]^+$, $[M+24]^+$, $[M+43]^+$ or an $[M+18]^+$ ion (the latter is produced with NH_4^+), or by charge exchange with the reagent gas, this is very rare, however, and would produce an M^+ ion. There may be an $[M-1]^+$ ion due to possible hybrid abstraction, this peak may be dominating the spectra (Silverstein, Webster & Kielme, 2005, p. 3).

In an chemical ionization ion source the reagent gas is ionized by electron ionization. The ionized reagent gas molecules will then again collide with other reagent gas molecules. The ionized reagent gas will collide with the analyte molecules, creating analyte molecule ions, as shown in Figure 10. For the collisions to take place, the local pressure has to be sufficient (de Hoffmann & Stroobant, 2007, p. 18).

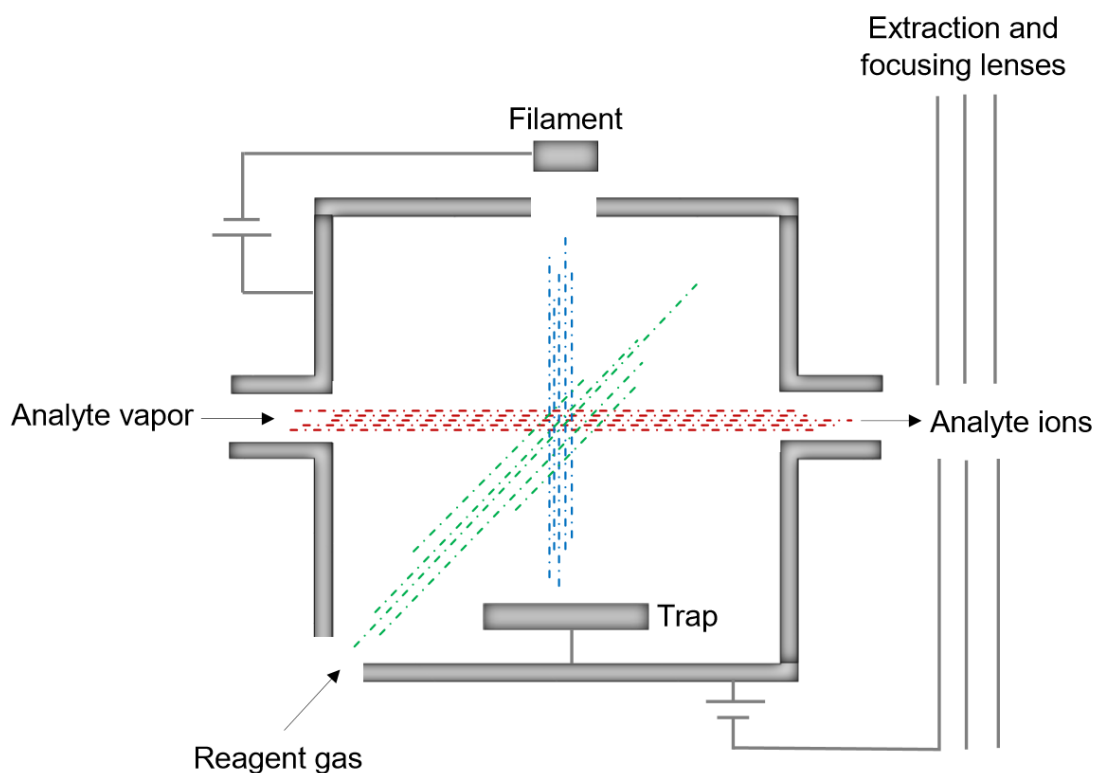


Figure 10: Chemical ionization ion source, the blue dots representing electrons, the green dots representing the reagent gas and the red dots representing the analyte molecules (Williams & Fleming, 2008, p. 183)

Formation of positive ions with chemical ionization is possible for most neutral components. To detect electronegative components, usage of their ability to produce negative ions may provide a certain selectivity as detection in a complex matrix goes (de Hoffmann & Stroobant, 2007, p. 24). Negative ions are produced by electron capture from molecules with acidic groups or electronegative elements under chemical ionization conditions. For efficient electron capture the chemical ionization conditions have to be at the high pressure range. At a high pressure electrons collide until an almost thermal energy state is reached. Electronegative molecules will be able to capture these electrons under such conditions and for this type of analytes the sensitivity may be as much as 10^3 times better than positive ion chemical ionization. The high level of sensitivity is due to the high rate of collisions with electrons the molecules undergo and the level of efficiency of the electron capture (Kitson., Larsen, & McEwen, 1996, p. 19).

Selected ion monitoring

Selected ion monitoring (SIM) in mass spectrometry is a method where the intensity of selected ion beams are recorded (IUPAC, 2014). SIM-mode is often used to provide an increase in the signal-to-noise ratio in the mass spectra. This increase is due to the reduction of noise as the dwell time in the measurement of a selected ion is increased. Also, the SIM-mode increases the transmission efficiency, resulting in an increased signal-to-noise ratio (Wells & Huston, 1995, p. 3650). There is an argument that the selection of ion beams might lead to loss of selectivity compared to full scan mass spectrometry. Another possible weakness of the method is the reliance on the analyst's ability to identify the molecular peak in the MS-spectra (Robbat & Wilton, 2014, p. 114).

Multiple reaction monitoring

In order to develop conditions that allow specific detections in tandem mass spectrometry, the multiple reaction monitoring (MRM) method is applied. MRM is mostly used as a recording method after separation by either liquid chromatography (LC) or gas chromatography (GC). The method is based upon the selection of the precursor ion(s) in the first stage of the m/z analysis of the mass spectrometer. The precursor ion(s) are to be transmitted into a collision cell and experience dissociation reactions. In the next phase of the m/z analysis the product ions are selected. The product ions were produced by the dissociation reaction in the collision cell. The consequence of this methodology is that such a molecule ion must be generated that it has the m/z -ratio to be selected in the first phase, *and* it must provide enough fragmentation to provide an ion which will be selected during the second phase, in order to make a signal to the detector (Kinter & Kinter, 2013, p. 9 -10).

Fixed product ion scan determines all parent ion m/z -ratios that will react and produce selected product ion m/z -ratios in one experiment. (IUPAC, 2014) Product ion scan is the result of collision-induced-dissociation (CID). The products will be either products of collision-activated-reaction (CAR) or simply fragmentation products, depending on the condition of the collision cell. CAR products will be apparent if there is used a reagent gas in the collision cell (de Hoffmann & Stroobant, 2007, p. 193). Product ion scan provide more information of analyte fragments, compared to the MRM method (Yao & Feng, 2016, p. 94).

When the MRM method is applied in MS-analysis coupled with an gas chromatographic unit, it will provide four degrees of specificity. The GC provides co-elution of the peaks, thus giving the first degree of specificity. Hence, the precursor mass, the product ion mass and the ratios of the relative abundance of the product ions each represent the next three degrees of specificity. However, to provide such specificity requires usage of stable-isotope-labeled internal standards (Tang & Poon, 2014, p. 119 – 120).

2.2.3 Application of GC/MS for nitro-/oxy-PAH quantification in environmental samples

Analysis of environmental samples measuring levels of contaminants in the atmosphere requires analysis of compounds both in gaseous and particulate phase, as most organic airborne contaminants divide between both these phases. When the samples have been prepared, the properties of the analyte (such as chemical stability, polarity, neutrality or hydrophobicity) determine the choice of separation method and detection (Cecinato, Balducci, Mastroianni & Perilli, 2012, p. 1916). For a chromatographic unit the column length, stationary and mobile phase, temperature and flow are parameters that may be optimized. The MS-system may use different kinds of ionization sources, as electron ionization or chemical ionization, and detection programs, such as full scan mode, SIM or MRM, to achieve the best detection of the target analyte.

Nitro-PAHs do account for a small fraction of the PAHs present in the atmosphere, and to identify and quantify these contaminants there is a necessity of detectors able to provide high sensitivity and selectivity. The NICI GC/MS is along the methods to provide satisfactory detection (Cecinato et al., 2012, p. 1918). This method is applied on oxy-PAHs as well (Filippo et al., 2015, p. 152).

2.3 Former applied analyzing methods

Environmental sample analysis has traditionally been analyzed by gas chromatography coupled with a mass spectrometer (GC/MS) (Zielinska & Samy, 2006, p. 885). The GC/MS is a natural choice because of the high resolution, but PAH compounds with five rings or more (high molecular weight PAHs) have low volatility, causing a low sensitivity for these compounds with GC/MS (Cochran et al., 2016, p. 6).

Nitro-PAHs has a history of being analyzed in electron ionization mode. The injections are often performed in cool-on-column and the most used capillary column was 60 meters long (5% phenylmethylsilicone fused-silica). Cool-on-column was the preferred injection technique because the nitro-PAHs has a tendency for thermal instability (Zielinska & Samy, 2006, p. 885). Selected ion monitoring (SIM) is applied for quantification of the individual compound. In the SIM-mode one or two ions is required for detection of the compounds, and the retention times the chosen ions are to be detected at may be limited, making SIM a more sensitive detection method than full scan MS (Zeigler, MacNamara, Wang & Robbat Jr., 2008, p. 110). The Negative Ion Chemical Ionization (NICI) ion source has however replaced EI in recent years due to significantly improved sensitivity of the analysis (Zielinska & Samy, 2006, p. 885).

Negative Ion Chemical Ionization Gas Chromatography Mass Spectrometry (NICI GC/MS) analysis of nitro-/oxy-PAHs or PAHs was applied in a recent master's project at NMBU (Garstad, 2017). In Garstad's study the NICI GC/MS (GC/NICI-SIM-MS) method was developed for analyzing nitro-/oxy-PAHs in soil (Garstad, 2017, p. 8) based on an earlier published Quick Easy Cheap Effective Rugged and Safe (QuEChERS) sample preparation method developed by Albinet et al. (Albinet, Tomaz & Lestremau, 2013, p. 31 – 33). This method was compared with the NICI GC/MS method (called the MPIC-method) developed by Pourya Shapoury at the Max-Planck-institute for Chemistry (Mainz, Germany). In this comparison GC/NICI-SIM-MS is applied as described in chapter 3. (Garstad, 2016) for both the "IKBM-method" and the "MPIC-method" analysis.

Kristin Sundby conducted a follow-up study and refined the GC/NICI-SIM-MS quantification for nitro-/oxy-PAHs in 2017 at the Norwegian University of Science and Technology (Sundy, 2017). Sundby's main objectives included "*Validation of an analytical method for the quantitative determination of nitro- and oxy-PAHs in air samples by GC/NICI-MS*" (Sundy, 2017, p. 2). Sundby analyzed a mixture of Nitro- and oxy-PAHs in full scan mode to identify the targeted ions, then developed a specialized SIM-method targeting the selected ions. The method was successfully applied in Arctic air samples from Longyearbyen (Svalbard).

GC/NICI-SIM-MS was also applied in several earlier conducted studies, such as Crimmins and Baker's study of hourly PAH and nitro-PAH concentrations measurements from 2006 (Crimmins & Baker, 2006, p. 6767), the study of nitro-PAHs in diesel particulate-related standard reference material by Bezabeh et al. from 2002 (Bezabeh, Bamford, Schantz & Wise, 2002, p. 383) and Chaspoul, Barban and Gallice's study of the simultaneous GC/MS analysis of PAHs and nitro-PAHs, published in 2006 (Chaspoul, Barban & Gallice, 2006, p. 160 – 161).

Cochran et al. published a study in 2012 where mother PAHs, nitro-, oxy- and hydroxy-PAHs were quantified. In this study Cochran et al. applied an optimized NICI GC/MS method on the nitro-PAHs and the oxy-PAHs, and an EI GC/MS method on the oxy-PAHs and the hydroxy-PAHs. The analysis was conducted with the SIM-mode or a combination of the SIM-mode and the total ion current (TIC) mode (Cochran et al., 2012, p. 96). In this study it was concluded that the GC/MS analysis of nitro- and oxy-PAHs with a NICI ion source gave low values for the limit of detection (LOD), whereas the GC/MS analysis of oxy-PAHs with an EI ion source gave significantly lower LOD-values (Cochran et al., 2012, p. 97).

Thomas et al. conducted a qualitative study of potentially genotoxic compounds, including nitro- and oxy-PAHs. Thomas et al. mainly analysed the samples on a GC/MS with an EI ion source, but some selected samples were analysed on a GC/MS with a NICI ion source. In the qualitative study the analysis conducted with an EI ion source proved far more successful. Thomas et al. points at the lack of reference

spectra for identification of the analytes in the NICI MS-spectra might be a reason for the rather less success this method provided in this experiment (Thomas et al., 2002, p. 257).

Adhikari, Wong and Overton had a study published in June 2017, comparing a optimized GC/MS/MS-MRM method with a conventional GC/MS/MS-SIM method used for the analysis of PAHs and alkyl-PAHs in oil residues subtracted from environmental samples. The study focused on compounds used as fingerprints and biomarkers in environmental sampling. The study conducted full scan analysis of standard compounds, as well as using reference literature to find the strongest m/z-peak and retention time in each spectra, using these as precursor ions in the product ion scan. The product ion spectra was obtained to optimize the MRM-transitions (Adhikari, Wong & Overton, 2017, p. 941). This study gave a strong indication on a encasement of sensitivity, elimination of interferences, and increment of reliability on quantification results ((Adhikari, Wong & Overton, 2017, p. 949).

2.4 Nitro- and oxy-PAH compounds and analysis in a environmental perspective

Quantitative analysis of explicit chemicals and groups of chemicals is necessary to investigate the environmental status on a consistent level. When specific chemicals of the nitro- and oxy-PAH families are quantitatively monitored, information like contamination source and degradation rate may be obtained. (Zeigler et al., 2008, p. 109). Degree of health threatening and environmentally hazardous emission to the atmosphere must be investigated so they can be controlled.

PAHs and the nitro and oxy PAH-derivatives represent a significant health threat to areas of high population density, making the monitoring of the concentration levels and the distribution of these compounds essential (Lin et al., 2015, p. 164). PAH derivatives have been reported in less extent than their precursors, due to difficulty in the analysis of these compounds (Cochran et al., 2016, p. 6), making the development of such analysis an interesting topic.

3.0 Methodology

The method consists of sampling, sample preparation and clean-up, and instrumental analysis of airborne nitro- and oxy-PAH pollution. The theoretical background of the applied procedures of this master's thesis is presented in this chapter.

3.1 Sampling

Atmospheric organic pollutants partitions between particulate and gaseous phase, which makes it necessary to sample both gaseous and particulate matter in order of measuring all the pollutants (Cecinato, 2012, p. 1916). High volume filtration is the common method for aerosol samples (Simoneit, 1999, p. 160). The United States Environmental Protection Agency as well as the Norwegian Environmental Agency (Miljødirektoratet) recommends high volume air samplers for collecting PAH-samples. High volume air samplers have been the preferable method for air sampling when PAHs were monitored (Tsapakis & Stephanou, 2003, p. 4935)

Passive air samplers is based upon the access to free air flow through the sampler and the principle of molecular diffusion of gaseous compounds in the surrounding air of an adsorbent. This kind of air samplers are used as a semi-quantitative method, on the basis of the uncertainty of the amount of air that has been flowing through the sampler. Passive air samplers are exposed for a long period of time (weeks/months), in order of collecting measurable amounts of analytes (Hak, Halse & Halvorsen, 2016, p. 8).

3.1.1 High volume air sampling

Active high volume air samplers are traditionally used in PAH partition measurement. High-volume samplers work by first trapping the particle phase sample on a filter, then sampling the gas phase with a solid sorbent. The filter may be a glass or quartz filter, while polyurethane foam (PUF), Tenax or amberlite XAD resin are examples of solid sorbents (Temime-Roussel, Monod, Massiani & Wortham, 2004, p. 1913-1914).

The filter on the active air sampler mostly capture organic contaminants bound to airborne particles. The solid sorbents mainly capture gaseous contaminants. The active air sampler is driven by a

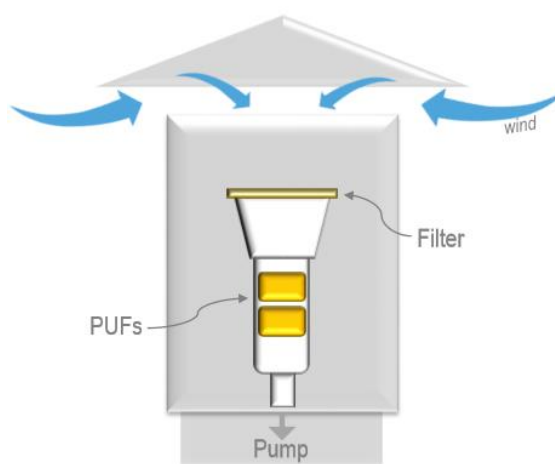


Figure 11: Active high volume air sampler

pump, as can be seen on Figure 11 (Schlabach et al., 2009, p. 14).

3.2 Method strategy

Developing and optimizing a GC/MS method for identification and quantification of nitro- and oxy-PAHs with high sensitivity and selectivity required the testing of equipment (GC columns) that may provide enhancement of these parameters. The GC columns tested in this thesis is a Agilent Technologies 60 m WAX column and a 50 m DB column. The detection methods tested were GC/EI-scan-MS, GC/NICI-PIS-MS and GC/NICI-SIM-MS. The strategies for testing these methods is presented in the following subchapters.

3.2.1 Testing WAX column (60m) with GC/EI-scan-MS for enhanced selectivity and sensitivity

The Agilent Technologies 60 m WAX column is a high polarity capillary GC column, regarded by the manufactory as ideal for food, flavor and fragrance analysis (Agilent Technologies, 2018). The column was tested for nitro- and oxy- analysis to examine the possibility of enhanced selectivity of these kind of analysis with a polar GC column for separation. Nitro- and oxy-PAHs are polar compounds (as can be seen in Table 1 and Table 2) and increment of the polarity of the stationary phase should increase the selectivity of the analysis (Dignac, Houot & Derenne, 2006, p. 129).

The column was tested along with a EI ion source. As described in section 2.2.2 the EI ion source provides excessive fragmentation of samples, providing complex source of identification of each analyte. This should provide an increment in sensitivity to the analysis. To identify the target compound a register of GC/EI-MS mass spectra for each target compound need to be made, and each target compound analyzed separately and identified on basis of the mass spectra.

3.2.2 Testing DB-5 column (50m) with GC/NICI-PIScan and MRM-MS for testing mass transition for increased selectivity

The Agilent Technologies Capillary DB-5 GC column is a non-polar column, classified by the manufactory as a low-bleed column with a high temperature limit (Agilent Technologies, 2018). The column shall have good inertness for active compounds and with the 50 m length it should increase chromatographic selectivity.

The column was tested by full scan analysis of analyte standards and internal standards with NICI ion source. After the standards was identified it was tested with GC/NICI-PIScan and MRM-MS with a PIScan program developed on basis of the full scan analysis.

3.2.3 Optimizing DB 5 column (50m) with GC/NICI-SIM-MS for sensitive quantification of oxy- and nitro-PAHs in urban atmospheric samples

The GC capillary column (described above in section 3.2.2) is similar to the one in use in Kristin Sundby master`s thesis from 2017, but considerably longer (Kristin Sundby used a Agilent J&W HP-5ms 30m column in her master`s thesis). The length of the column should increase the selectivity of the chromatograph, and thereby contribute to an increment in the sensitivity of the analysis.

In order of achieving a sensitive quantification the temperature program need to be optimized. A series of temperature programs with variations to the parameters hold time and temperature rise ratio was tested in order of optimization of the temperature program.

The SIM-program was developed according to retention times and m/z-values of the analyte standards and internal standards in the optimized temperature program. The SIM-program was tested and the windows were adjusted to avoid noise and separate compounds close in retention times, quantifier and qualifier ions.

4.0 Method

Solvents, standards and equipment are accounted for in Appendix I, Table 18, 19 and 20.

The instrumental analysis was somewhat disturbed by instrumentation problems, causing a decreased sensitivity and a necessity to run standards several times. The ion source was changed from EI to CI in march 2018. There had been problems with the injector and necessity of extra cleansing of the ion source since December 2017, these problems continued after the changing of the ion source. There was proceeded a full service on the instruments 18th of April, there accrued no additional instrumentation problems after this.

4.1 EI analysis

Stock standards of analyte compounds were diluted to concentrations of 10 ng/ μ L and 1 ng/ μ L. Stock standard concentrations and phase information are described in Appendix II, Table 19. Solvent in use for dilution was n-Hexane (Appendix II, table 18). N-Hexane was also used as method blank. All analyte compound standards were separated on a Agilent 7890B capillary gas chromatograph and subsequently analyzed on a Agilent Technologies Triple Quadrupole 7000C GC/MS System with Electron Ionization (Agilent Technologies, Santa Clara, USA) and Scan mode. The temperature applied temperature program is presented in Table 3.

Table 3: *Temperature program EI analysis*

	Rate [$^{\circ}$ C/min]	Value [$^{\circ}$ C]	Hold time [min]
Initial		70	2
Ramp 1	15	180	0
Ramp 2	5	280	5
Ramp 3	15	325	20

The calibration standards were analyzed separately and identified according to the three expected highest peaks in the m/z-spectra, as presented in Table 4. There was not found any reliable sources for identification of 1,3-Dinitropyrene, 6H-Benzo[c,d]pyren-6-one, 2-Nitropyrene, 2,7-Dinitrofluorene, 9-Methylcarbazole and 9-Nitrophenanthrene on GC/EI-MS. The deuterated standards (internal standards) 9-Fluorenone-d₈ and 2-Nitrobiphenyl-d₉ was identified according to their non-deuterated information, modified by the heavier masses of the deuterated standards.

In addition to the analysis of these calibration standards and deuterated internal standards, a selection of old 100 ng/ μ L calibration standards prepared for a master's thesis at NMBU in 2017 was diluted to

analyzed under the same conditions. These additional analysis were performed to compare the quality of the standards with those prepared for an earlier thesis.

Table 4: Information of calibration standard and internal standard identification criteria (National Center for Biotechnology Information, 2018)

Compound	Expected top peak	Expected 2 nd highest peak	Expected 3 rd highest peak
1-Indanone	104	132	103
9-Fluorenone	180	152	181
4H-Cyclopenta[def]phenanthren-4-one	204	176	205
1,2-Benz[a]anthraquinone	258	202	230
Benzanthrone	230	202	231
9,10-Anthraquinone	180	208	152
9,10-Phenanthrenquinone	180	152	208
1,4-Naphthoquinone	158	176	102
2-Methyl-0,10-anthraquinone	222	165	194
5-Nitroacenaphthene	152	199	153
Benzo[a]fluoren-11-one	230	200	202
2-Nitroanthracene	223	177	176
1,8-Dinitropyrene	292	263	293
1,6-Dinitropyrene	292	263	293
2-Nitrofluorene	165	211	164
3-Nitrofluoranthene	247	200	201
2-Nitrofluoranthene	247	201	200
6-Nitrochrysene	273	226	215
4-Nitrobiphenyl	199	152	169
6-Nitrobenzo[a]pyrene	297	251	267
7-Nitrobenz[a]anthracene	215	273	226
9-Nitroanthracene	223	176	177
4-Nitropyrene	201	247	200
1-Nitropyrene	201	247	100
2-Nitronaphthalene	127	173	115
1-Nitronaphthalene	127	115	173
2-Nitrobiphenyl	152	171	115

4.2 CI analysis

Stock standards of analyte compounds were diluted to a concentration of 1 ng/ μ L. The standard analyte compounds were analyzed as a mixture on the Agilent Technologies Triple Quadrupole 7000C GC/MS System with an Chemical Ionization ion source (Agilent Technologies, Santa Clara, USA) at the facilities of NMBU. n-hexane was the solvent in use for dilution. A Agilent DB-5 50 meter chromatographic column (Agilent Technologies, Santa Clara, USA) were used for the separation.

The mass-to-charge spectra of the standard mixture was compared to an archive spectra obtained by Kristin Sundby as part of her master thesis (Sundby, 2017, p. 37). The analyte compounds that could not be identified by such comparison were analyzed separately as single compounds at a 1 ng/ μ L

concentration in full scan mode. The compounds with a high level of uncertainty at this concentration were analyzed at a 10 ng/μL concentration.

4.2.1 SIM-method

The SIM-method was developed after a full scan run of a 10 ng/μL mix of the calibration standards and the internal standards. The temperature program for the SIM-method was experimentally developed by running the 10 ng/μL standard mix at full scan mode by different temperature programs. The tested temperature programs varied the rate of the temperature increment and the hold time at the different ramps. The different time programs are presented in Figure 12 and Table 5.

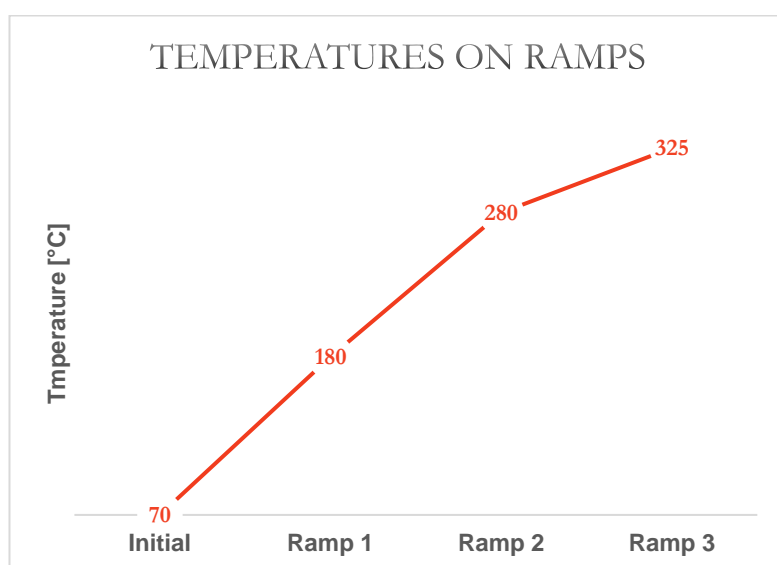


Figure 12: Temperatures of all temperature programs

Table 5: Varying parameters of all temperature programs

		Temperature program									
		1	2	3	4	5	6	7	8	9	10
Rate [°C/min]	Initial - Ramp 1	15	15	15	17	15	15	16	15	29	22
	Ramp 1- Ramp 2	5	5	5	6	6	7	7	7	7	5
	Ramp 2- Ramp 3	15	15	15	17	20	22	24	25	20	22
Hold time [min]	Initial	2	2	2	2	2	2	2	2	2	2
	Ramp 1	0	0	0	0	0	0	0	2	0	0
	Ramp 2	10	8	5	5	5	5	5	7	5	8
	Ramp 3	10	8	5	5	5	5	5	5	5	8

The SIM program was developed experimentally by detecting the standards retention times in the temperature program and setting up windows to exclude m/z-values causing interference. The NICI-SIM-program is presented in Table 6.

Table 6: SIM program information with compound identification

Chromatographic peak number	SIM window	Retention time [min]	Qualifier ion [m/z]	Quantifier ion [m/z]	Compound
1	1 (8,0 – 15,4)	8,8	105	107	6-Nitrobenzo[a]pyrene
2		11,4	158	159	1,4-Naphthoquinone
3		13,7	173	174	1-Nitronaphtalene
4		14,2	173	174	2-Nitronaphtalene
5		14,6	208	209	ISTD: 2-Nitrobiphenyl-d ₉
6		15,4	188	189	ISTD: 9-Fluorenone-d ₈
7	2 (15,4 – 18,5)	15,4	180	181	9-Fluorenone
8		16,5	148	149	1-Indanone
9		16,8	199	200	4-Nitrobiphenyl
10		18,4	266	264	RSTD: TCN
11	3 (18,5 – 21,0)	18,5	208	199	9,10-Anthraquinone
12		19,0	199	200	5-Nitroacenaphthene
13		19,5	204	205	4H-Cyclopentan[def]phenanthren-4-one
14		20,1	222	223	2-Methyl-9,10-Anthraquinone
15		20,2	211	212	2-Nitrofluorene
16		20,7	223	222	9-Nitroanthracene
17	4 (21,0 – 26,4)	21,2	208	209	9,10-Phenanthrenequinone
18		21,5	223	224	9-Nitrophenanthrene
19		22,7	223	224	2-Nitroanthracene
20		23,4	230	231	Benzo[a]fluoren-11-one
21		25,6	230	231	Benzathrone
22		26,3	247	248	2-Nitrofluoranthene
23	5 (26,4 – 31,2)	26,4	247	248	3-Nitrofluoranthene
24		26,8	247	248	4-Nitropyrene
25		27,2	258	259	1-Nitropyrene
26		27,5	247	248	1,8-Dinitropyrene
27		27,8	247	248	2-Nitropyrene
28		28,1	257	258	2,7-Dinitrofluorene
29		29,8	273	274	7-Nitrobenz[a]anthracene
30		30,5	254	255	6H-Benzo[c,d]pyren-6-one
31		30,8	273	274	6-Nitrochrysene
32		6 (31,2 – 34,0)	31,8	293	294
33	32,5		292	293	1,3-Dinitropyrene
34	33,0		292	293	1,6-Dinitropyrene

4.2.2 MRM-method

The Product Ion Scan program was build from the information obtained by the individual calibration standard and internal standard analysis after scanning (m/z – 50 – 600 amu). There was a lack of sensitivity when analyzing the calibration standards, therefore the standards were analyzed at a high concentration of 10 ng/μL. The PIS can was run on a 2 ng/μL mix of calibration standards and internal

standards. The mass-to-charge ratio of the qualifier ions and the quantifier ions were targeted according to retention time. The mass-to-charge ratios of some compounds were alike, and some retention times were very close to each other. The windows of the PIScan-method were set according to expected retention time and m/z-values of the precursor ions, as presented in table 7.

Tabell 7: Product Ion Scan method information

PIScan window (number)	PIScan window [min]	Expected compound in window		
1	4,0 – 13,5	9-Methylcarbazole	2-Methyl-9,10-anthraquinone	1,4-Naphtoquinone
2	13,5 – 17,9	1-Nitronphtalene	2-Nitronaphtalene	2-Nitrobiphenyl-d ₉
3	17,9 – 19,5	9-Fluorenone-d ₈	9-Fluorenone	
4	19,5 – 21,0	1-Indanone	4-Nitrobiphenyl	
5	21,0 – 24,0	9,10-Anthraquinone	5-Nitroacenaphtene	
6	24,0 – 24,15	9,10-Phenanthrequinone	Benzathrone	
7	24,15 – 25,4	4H-Cyclopentan[def]phenanthrene-4-one	2-Nitrofluorene	
8	25,4 – 30,0	9-Nitroanthracene	9-Nitrophenanthrene	Benzo[a]fluoren-11-one
9	30,0 – 34,0	2,7-Dinitrofluorene	2-Nitrofluoranthene	3-Nitrofluoranthene
10	34,0 – 37,5	2-Nitropyrene	1-Nitropyrene	4-Nitropyrene
11	37,5 – 39,0	1,2-Benz[a]anthraquinone	7-Nitrobenz[a]anthracene	6H-Benzo[c,d]pyren-6-one
12	39,0 – 44,0	6-Nitrochrysene	1,3-Dinitropyrene	1,6-Dinitropyrene
13	44,0 – 57,5	2-Nitroanthracene	6-Nitrobenzo[a]pyrene	

4.3 Sampling

The sampling was carried out by NILU in Kjeller, Norway. Two samples with one filter (glass fiber filter for collection of the particulate phase) sample and two PUFs (for collection of the gaseous phase) each was collected using high volume air sampling in April 2018 (Table 8). The samples were collected in Kjeller, Norway, at the facilities of the Norwegian Institute for Air Research (NILU). The samples was collected using Digital High Volume Air Samplers (Digital Elektronik AG, Hegnau, Switzerland). Information regarding sampling time and volume is described in table 8.

Table 8: Sample information

Sample name	Date of sampling	Volum [m ³]	Time [min]
PUF 1 / Filter 1	27.04.18 – 30.04.18	1918,5	4075,4
PUF 2 / Filter 2	26.04.18 – 27.04.18	628,2	1340,9

4.4 Sample preparation

The sample preparation followed the Quick Easy Cheap Effective Rugged and Safe (QuEChERS) extraction method presented by Albinet et al. (2013) and further developed by Kristin Sundby in her master's thesis in 2017.

4.4.1 Filter extraction

The sample filters were folded and put in centrifuge test tubes. A method blank filter was spiked with 30 ng of calibration standard mix and prepared and analysed in the same matter as the sample filters. 25 ng of the internal standards, 2-Nitrophenyl- d_9 and 9-Fluorenone- d_8 , were added to each filter before ACN were added to the filters until they were completely covered by the solvent (approximately 10 mL). The filters were mixed with the solvent in the vortex mixer (Vortex Genie 2 Vortex Mixer, Scientific Industries, New York, USA) for two minutes. After mixing, the test tubes were centrifugated in EBA 20 Centrifuge, Hettich Instruments, LP, Tuttlingen, Germany at 4500 rpm for five minutes. The extract was removed and contained in new test tubes. The procedure was repeated three times, whereas sufficient ACN (about 2 mL) was added between each repetition to keep the filters covered in solvent. After the last repetition the filters was removed from the test tubes and squeezed over the test tubes before the extract was removed. The total amount of extract was 12 - 14 mL.

The extract was concentrated to near dryness under a gentle stream of nitrogen (5.0, AGA AS, Porsgrunn, Norway) in the nitrogen evaporator Reacti-Vap I #TS-18825 Nitrogen Evaporation Unit, Thermo Scientific, Massachusetts, USA. The stainless steel needles of the nitrogen evaporator was rinsed in Acetone in a ultrasonic bath for ten minutes. The inner walls of the tube was cleansed, using 1 mL ACN, before the extract again was concentrated to near dryness. The extract was finally diluted in 200 μ L DCM.

4.4.2 PUF extraction

The PUFs were extracted using a Soxhlet extractor. Both the higher and lower PUFs of the same sample were added to one Soxhlet extraction unit. A method blank was spiked with 30 ng of calibration standard mix and prepared and analysed in the same matter as the sample PUFs. 25 ng of the internal standards, 2-Nitrophenyl- d_9 and 9-Fluorenone- d_8 , were added to each PUF before 350 mL DCM and three boiling stones were added to the round bottle for preventing boiling retardation. The Soxhlet extraction was run for 8 hours.

The extract was transferred to a 250 mL TurboVap tube. The Soxhlet round bottle were rinsed three times with 1 mL DCM, which were also transferred to the TurboVap tube. The TurboVap system was rinsed by running it with Acetone twice. The temperature in the TurboVap water bath was kept at 35°C. The solvent

was evaporated until it reached the censor stopping point, at 0,5 mL, and the sample were transferred to a sample vial. The TurboVap was cleaned three times with a few drops of DCM, which was also transferred to the sample vial.

4.4.3 Sample clean-up

The sample clean-up procedure was the same for both filter extract and PUF extract. The sample clean-up was carried out using solid phase extraction (SPE) on a SPE manifold with SiOH cartridges (Chromabond SPE SiOH glass cartridges, 3mL, 500mg, Teknolab, Ski, Norway) connected to a vacuum flask and a vacuum pump.

The SiOH cartridges was initially treated with n-hexane before the sample extract was added to the column. The first mL were removed, to eliminate alkanes, then the sample was eluted with 9 mL 35:65 (v/v) DCM-n-hexane. The sample was concentrated to near dryness under a gentle stream of nitrogen (5.0, AGA AS, Porsgrunn, Norway), using nitrogen evaporation. When the sample reached near dryness, it was dissolved in 500 μ L cyclohexane, before the sample volume were evaporated to 150 μ L. The stainless steel needles of the nitrogen evaporator (Reacti-Vap I #TS-18825 Nitrogen Evaporation Unit, Thermo Scientific, Massachusetts, USA) was rinsed in Acetone in a ultrasonic bath for ten minutes.

The samples were transferred to sample vials and added 25 ng of recovery standard (TCN, 4 ng/ μ L).

5.0 Method validation and quality control

Any method will be without value if it and its results cannot be tested and proved statistically satisfactory and comparable to other methods and results. In this section a selected set of measures and methods commonly used to provide validation information about chemical analyse methods and results is presented, to enable a measurability of the quality of the methods investigated in this study.

5.1 Analyte identification

Analyte identification requires distinguishing the analyte molecules in the spectra. This study applied comparison to known spectra of the molecule and expected retention times. The analyte cannot, however, be identified without a measure on how the analyte signal separate itself from the background noise of the spectra. The limit of detection serve as such a measure.

5.1.1 Limit of detection

The limit of detection (LOD) may be defined as the analyte concentration that will provide a significantly larger signal than the signal expected of a blank sample. (Helbæk, 2008, p. 163) The LOD can be mathematically expressed as:

$$X_{LOD} = \bar{X}_B + 3\sigma_B$$

[Formula 3]

\bar{X}_B = the mean at $n > 30$ blank samples

σ_B = the standard deviation

(Valcárcel, 2000, p. 206)

As LODs derive from a minimum of signal-to-noise (S/N) ratio related to the baseline noise (Oehme, 2007, p. 20) the LOD can be calculated from the S/N ratio of standards:

$$S_{LOD} = \frac{S_i}{N}$$

[Formula 4]

S_{LOD} = The corresponding signal to the LOD

S_i = The height of the analyte peak

N = The height of the noise band

(Lundanes, 2014, p.190)

The LOD concentration may be found by:

$$C_{LOD} = \frac{C_i}{S_i} * S_{LOD}$$

[Formula 5]

C_{LOD} = The concentration of the LOD

C_i = The concentration of the analyte

5.2 Analyte quantification

The GC/MS technique is commonly used to quantify molecular species. To be able to quantify the analyte satisfactorily, it is necessary to apply calibration techniques giving the most reliable quantification. The calibration method most trusted is the internal standard method, due to its ability to reduce uncertainties given from the sample preparation and sample introduction (Holler et al., 2007, p. 583). The quantification method has to be evaluated, however, and this chapter presents some chosen measures of quality.

5.2.1 Internal standard method

The internal standard quantification method is the most reliable method for quantification since the method corrects variation in sample preparation and separation steps, such as extraction and gas chromatography. The internal standard needs to be a compound similar to the analyte. The selected internal standard must be of a known quantity and are to be added to an precisely measured amount of sample (Sparkman, Penton, & Kitson, 2011, p. 214).

5.2.4 Recovery

Recovery is important to consider when sample preparation with several steps that may represent loss of analyte is acquired. The addition of a recovery standard that will make it possible to account for the losses in the sample preparation is necessary to make quantification trustworthy. The loss of analyte during sample preparation may be calculated by formula:

$$f_r = \frac{C_{ISTD} * A_{RSTD}}{C_{RSTD} * A_{ISTD}}$$

[Formula 6]

f_r = the response factor

C_{ISTD} = the concentration of the internal standard

A_{RSTD} = the peak area of the recovery standard

C_{RSTD} = the concentration of the recovery standard

A_{ISTD} = the peak area of the recovery standard

The recovery in each sample is further given by formula;

$$R (\%) = \frac{M_{RSTD} * A_{ISTD} * f_{r,avg}}{M_{ISTD} * A_{RSTD}} * 100\%$$

[Formula 7]

R (%) = the recovery in percentage

M_{RSTD} = the amount of recovery standard added to the sample

M_{ISTD} = the amount of internal standard added to the sample

(Oehme, 2007, p. 25)

5.2.2 Limit of quantification

The limit of quantification (LOQ) may be defined as the analyte concentration that will provide a signal in the lowest end of the calibration curves lower linear area. (Valcárcel, 2000, p. 355) The LOQ can be mathematically expressed as:

$$X_{LOQ} = \bar{X}_B + 10\sigma_B$$

[Formula 8]

(Valcárcel, 2000, p. 68)

The mathematical expression of the LOQ will therefore provide a value higher than that of the LOD (see formula 3).

5.2.3 Sensitivity

The sensitivity describes the ability a given method has to separate similar (but unlike) quantities of analyte, or to detect small presences of analyte. The reproducibility (precision) and the slope of calibration curve are the two main restrictive factors of the sensitivity (Holler et al., 2007, p. 19). The sensitivity has mathematical relations to the LOD and the LOQ. It can be shown that the LOD in the calibration curve may be expressed by the sensitivity (S):

$$C_{LOD} = \frac{3\sigma_B}{S}$$

[Formula 9]

Hence, the LOQ in the calibration curve will be expressed as:

$$C_{LOQ} = \frac{10\sigma_B}{S}$$

[Formula 10]

(Valcárcel, 2000, p. 68)

5.2.5 Accuracy

Accuracy is mathematically expressed by a systematic error. The systematic error appears as a difference with a positive or negative sign. Accuracy may also be mathematically presented as a relative, with use of percentage or a fraction. Accuracy is dependent upon the uncertainty, or precision, to express accuracy without the risk of showing mere coincidence of method or result.

Accuracy can be expressed as a result, by the difference:

$$e_{x_i} = \pm |x_i - \hat{X}'|$$

[Formula 11]

e_{x_i} = the accuracy of the result

x_i = the result

\hat{X}' = the value representing the true value

Or the relative difference:

$$(e_{x_i})_{rel} = \frac{\pm e_{x_i}}{\hat{X}'} * 100$$

[Formula 12]

Accuracy of a method will represent bias if the number of results (n) from the same method is < 30, as is expressed in equation:

$$e_{\bar{X}} = \pm |\bar{X} - \hat{X}'|$$

[Formula 13]

$e_{\bar{X}}$ = the accuracy of the mean of the n < 30 results

\hat{X}' = the mean of the < 30 results

Accuracy of a method will however represent the relative trueness if n > 30, as expressed in equation:

$$e'_{\mu} = \pm |\mu' - \hat{X}'|$$

[Formula 14]

e'_{μ} = the accuracy of the mean of the n > 30 results

μ' = the mean of the > 30 results

(Valcárcel, 2000, p. 53)

5.2.6 Precision

Precision may be defined as:

“degree of consistency among results obtained by applying the same analytical method separately to individual aliquots of the same sample”

(Valcárcel, 2000, p. 57)

Precision is dependent on the matter on which it is applied and on the way the results are gained. The precision of one isolated result is mathematically defined in formula:

$$d_{x_i} = \pm |x_i - \bar{X}|$$

[Formula 15]

d_{x_i} = the precision of the result

This formula can be alternated to describe the difference between the result and the mean at $n > 30$, instead of the mean at $n < 30$ (Valcárcel, 2000, p. 57). The same is of course true for formula below.

The standard deviation is used to describe the precision of a set of results:

$$s = \sqrt{\frac{\sum(x_i - \bar{X})^2}{n - 1}} = \sqrt{\frac{d_{x_i}^2}{n - 1}}$$

[Formula 16]

s = the standard deviation

((Valcárcel, 2000, p. 58)

6.0 Results

6.1 EI analysis

The MS-spectra of the GC/EI MS analyzed nitrated and oxygenated PAH calibration standards were compared to expected m/z values of the three highest peaks for each compound. The result is presented in Table 9.

Table 9: Result of GC/MS analysis of calibration standard with EI ion source

Component	m/z expected top peak	m/z expected 2nd highest peak	m/z expected 3rd highest peak	Match calibration standard
1-Indanone	104	132	103	<i>P2 peak at 15,6 min indicates match</i>
9-Fluorenone	180	152	181	No
4H-Cyclopenta[def]phenanthren-4-one	204	176	205	<i>P2 peak at 44,3 min indicates match</i>
1,2-Benz[a]anthraquinone	258	202	230	No
Benzanthrone	230	202	231	<i>Not probable, but weak match in P1 peak at 43,9 min</i>
9,10-Anthraquinone	180	208	152	<i>P2 peak at 42,7 min indicates match</i>
9,10-Phenanthrenquinone	180	152	208	No
1,4-Naphthoquinone	158	176	102	No
2-Methyl-0,10-anthraquinone	222	165	194	<i>P2 peak at 44,5 min indicates match</i>
5-Nitroacenaphthene	152	199	153	No
9-Nitrophenanthrene	<i>Missing reference data</i>			<i>No reference data</i>
9-Methylcarbazole	<i>Missing reference data</i>			<i>No reference data</i>
Benzo[a]fluoren-11-one	230	200	202	<i>Empty sample file</i>
2-Nitroanthracene	223	177	176	<i>Empty sample file</i>
1,8-Dinitropyrene	292	262	293	<i>Empty sample file</i>
1,6-Dinitropyrene	292	262	293	No
2,7-Dinitrofluorene	<i>Missing reference data</i>			<i>No reference data</i>
2-Nitrofluorene	165	211	164	No
3-Nitrofluoranthene	247	200	201	No
2-Nitrofluoranthene	247	201	200	No
6-Nitrochrysene	273	226	215	No
4-Nitrobiphenyl	199	152	169	No
6-Nitrobenzo[a]pyrene	297	251	267	No
7-Nitrobenz[a]anthracene	215	273	226	No
9-Nitroanthracene	223	176	177	No
4-Nitropyrene	201	247	200	No
2-Nitropyrene	<i>Missing reference data</i>			<i>No reference data</i>
1-Nitropyrene	201	247	100	No
2-Nitronaphthalene	127	173	115	No
1-Nitronaphthalene	127	115	173	No
6H-Benzo[c,d]pyren-6-one	<i>Missing reference data</i>			<i>No reference data</i>
1,3-Dinitropyrene	<i>Missing reference data</i>			<i>No reference data</i>
9-Fluorenone-d ₈	<i>Missing reference data</i>			<i>No reference data</i>
2-Nitrobiphenyl-d ₉	152	171	115	<i>P1 peak at 43,6 min indicates match</i>

In addition to the presented analysis in Table 9, a selection of old calibration standards prepared for a master's thesis at NMBU in 2017 was analyzed using the same method, as described in section 4.1. The

complete list of chromatographic peaks and according m/z-values of all the standards are presented in Appendix II, Table 19.

6.1.1 Chromatograms and m/z spectra

The chromatograms and mass spectra of three elected compounds are displayed in Figure 13, 14, 15, 16, 17 and 18 below. The spectra's representing 2-Nitrobiphenyl in Figure 13 and 14 is presented because this compound has a chromatogram with a clear peak representing the compound. The spectra's representing 1-Indanone in Figure 15 and 16 is shown because it is a calibration standard compound with a possible match and the spectra's of 9-Nitroanthracene is displayed in Figure 17 and 18 to exemplify the compounds with no match with the reference values.

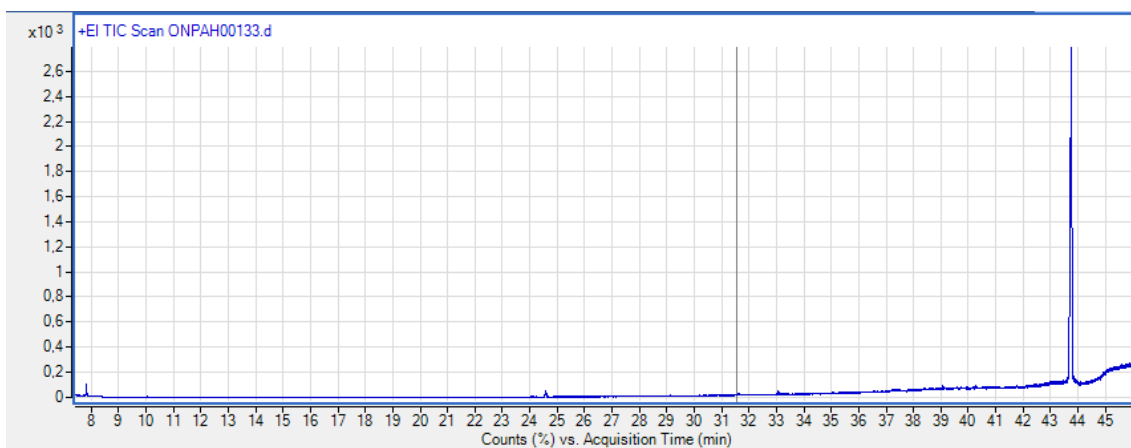


Figure 13: The chromatogram of 2-Nitrobiphenyl-d₉

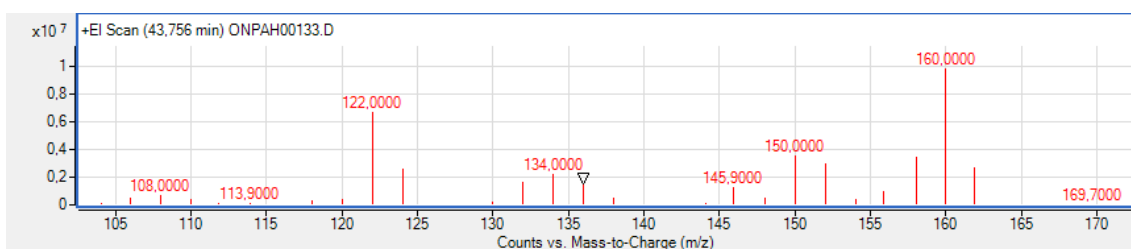


Figure 14: The mass spectra of peak at retention time 43,76 min in the chromatogram of 2-Nitrobiphenyl-d₉

The chromatogram of 2-Nitrobiphenyl- d₉ in Figure 14 has a even baseline and one clear main peak. This chromatogram is, along with the one of 9-Fluorenone-d₈ (the other deuterated internal standard) one of the two only compounds providing a clean chromatogram with only one main peak and is therefor presented. The mass spectra of 2-Nitrobiphenyl-d₉ have correlations with those given in the reference data in Table 4, although offset with a factor of nine, as it is deuterated.

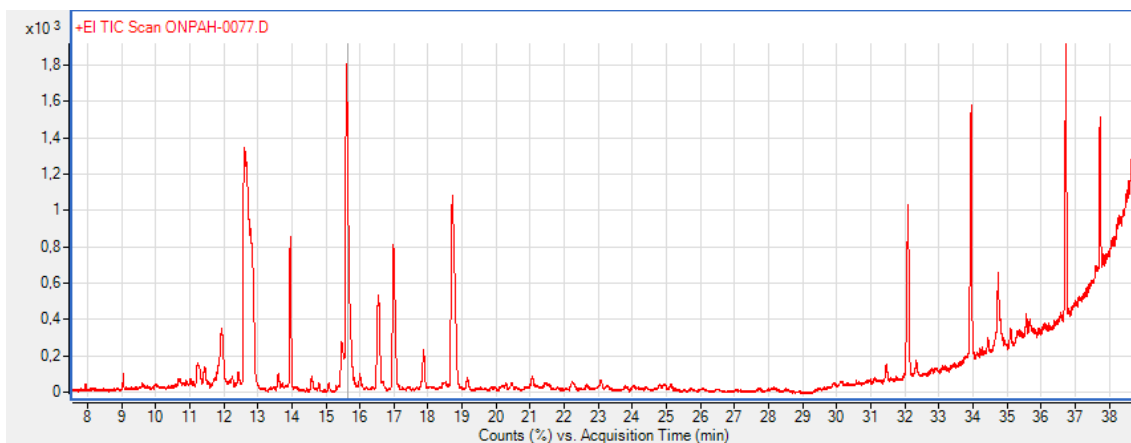


Figure 15: The chromatogram of 1-Indanone

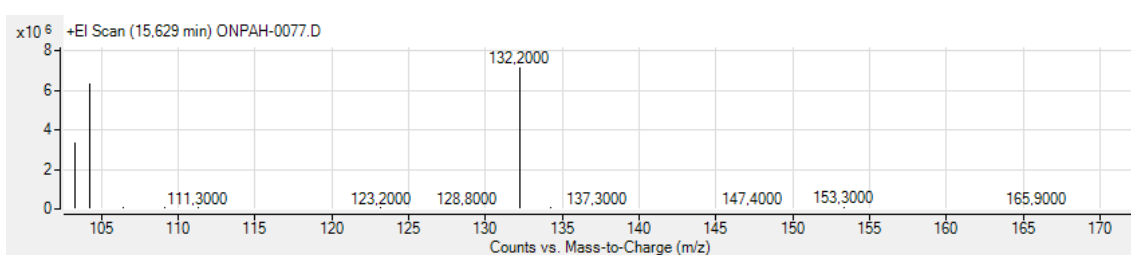


Figure 16: The m/z spectra of peak at retention time 15,6 min in the chromatogram of 1-Indanone

The chromatogram of 1-Indanone in Figure 16 show several peaks. The baseline is more uneven than that of 2-Nitrophenyl- d_9 , and some of the smaller peaks split and show a tailing and heading. The plenty of peaks and the faulting quality of the peaks may represent deterioration of the analyte through decomposition, contamination or solvent disturbance. All the peaks have been investigated, the result is presented in Appendix II, Table 19, and the peak at retention time 15,6 minutes show correlating values in the highest peaks in the mass spectra in Figure 16 to the reference values in Table 4.

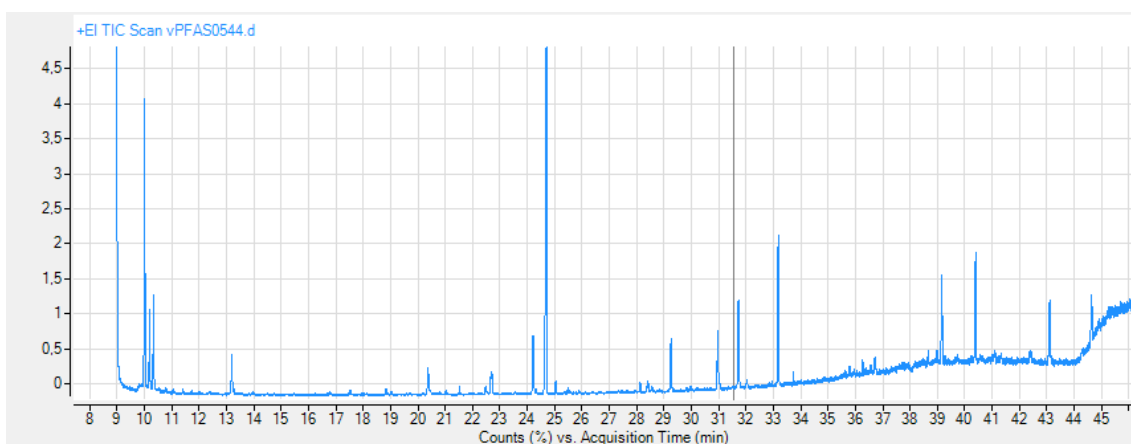


Figure 17: The chromatogram of 9-Nitroanthracene

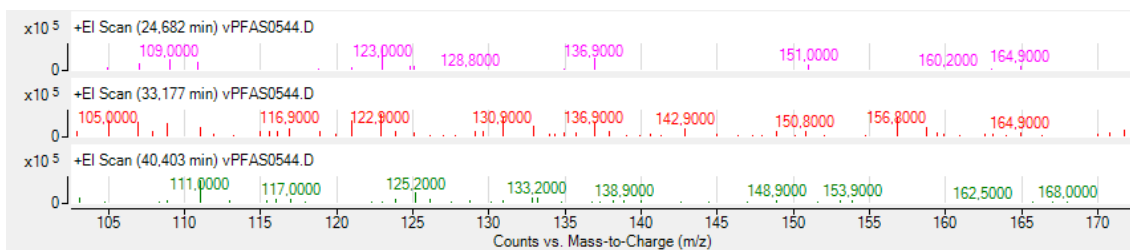


Figure 18: The mass spectra of peaks at retention time 24,68 min, 33,18 min and 40,4 min in the chromatogram of 9-Nitroanthracene

The chromatogram of the chosen representative to the spectra's of the compound with no found match to the reference data in Table 4, 9-Nitroanthracene, is provided in Figure 18. This compound and its spectra's were chosen to illustrate the phenomena quite randomly. The chromatogram in Figure 18 show many peaks, some clustering, with very different sizes and tendency to severe noise and an uneven baseline. Figure 19 provide an overview over three mass spectra's from three of these peaks, at retention time 24,7 min, 33,18 min and 40,4 min, accordingly. There is some fractioning, providing a number of peaks in the presented mass spectra`s.

6.2 NICI analysis

The most commonly used ion source for PAH analysis on GC/MS-instrumentation is NICI in SIM-mode, as shown in section 2.3. This thesis have been developing and testing a SIM-program and a PIScan-program (with the goal of developing a MRM-method) for GC/MS-NICI, the results is presented here.

6.2.1 Temperature

The ten different temperature programs tested in full scan mode gave different efficiency and sensitivity. The first compounds to elute had least difference in results, as is graphically illustrated in Figure 20.

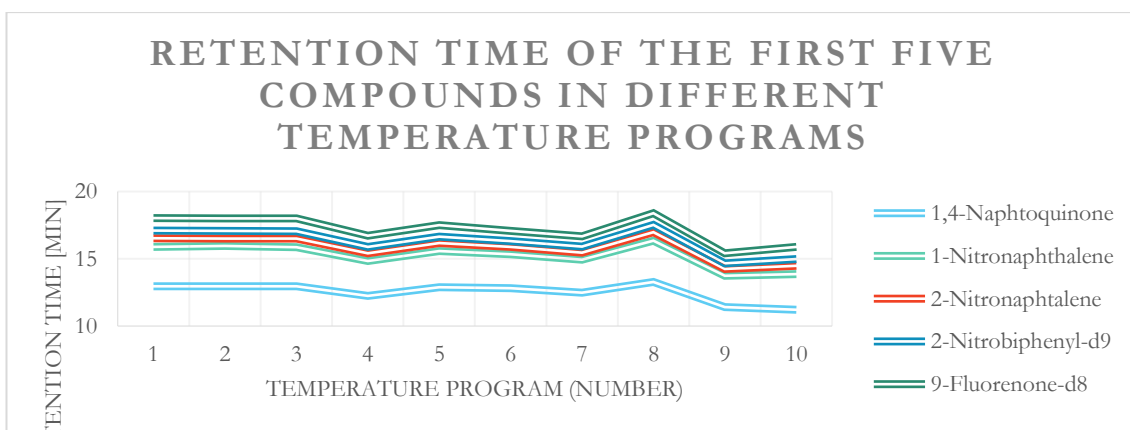


Figure 19: Effect of different temperature programs on the first compounds to elute

The different effect of the temperature programs were quite more visible on the last compounds to elute, as is presented graphically in Figure 21 below. Some programs did not elute all of the compounds, proving that increasing the temperature rate and increasing the hold time at Ramp 2 and Ramp 3 at the same time gave no increment in sensitivity.

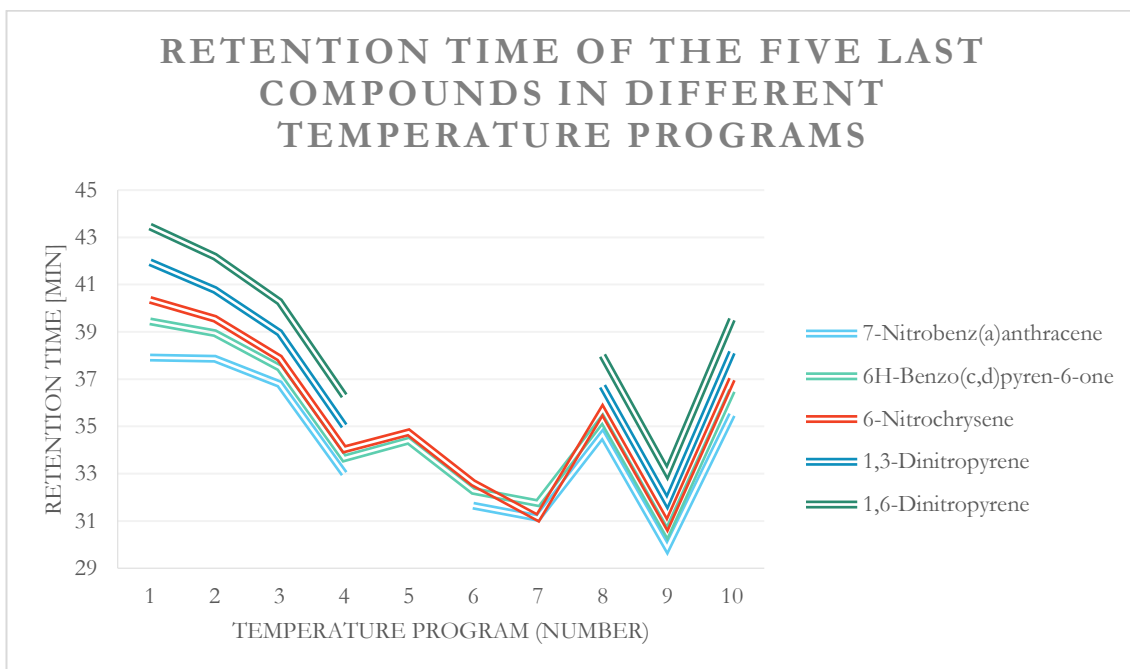


Figure 20: Effect of different temperature programs on the last compounds to elute

The temperature program used throughout the SIM-analysis, temperature program nine, had high rate at every step and a low hold time. The temperature program gave however no visible loss off sensitivity (see Figure 21) and the best efficiency to the analysis.

6.2.2 SIM-analysis

The SIM-method was developed from the obtained information from the full scan runs of standard compounds. The SIM-windows were adjusted to achieve separation sufficient for detection of as many compounds as possible and sensitivity for quantification of as many compounds as possible. The resulting spectra is presented in Figure 22.

There was a higher peak for 1-Indanone in the blank sample than in the standards, making the quantification of this compound impossible and detection in samples questionable. 6-Nitrobenzo[a]pyrene was not visible even in high concentration spectra (10 ng/ μ L), which made this compound not detectable. All thirty other target compounds were calibrated. The signals of 9-Methylcarbacole, Benzanthrone, 1,2-Benzo[a]anthraquinone, 1,3-Dinitropyrene and 1,6-Dinitropyrene could not be calibrated, however, as linearity could not be achieved for these compounds.

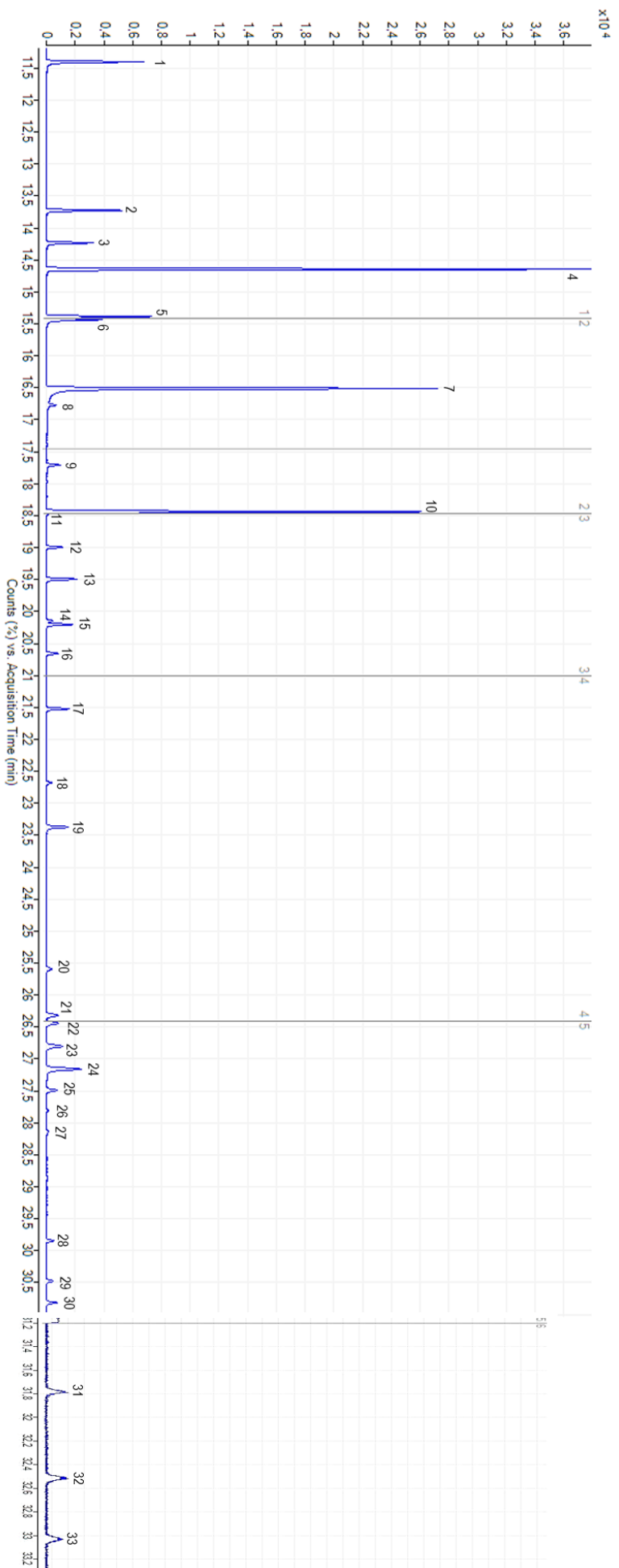


Figure 21: Spectra of 1 ng/ μ L SIM-method run showing all compounds. Note that the last window with the three latest compounds is enlarged for visual reasons. Peaks: 1: 1,4-Naphthoquinone, 2: 1-Nitronaphthalene, 3: 2-Nitronaphthalene, 4: 2-Nitrobiphenyl- d_8 (STD), 5: 9-Fluorenone- d_8 (STD), 6: 9-Fluorenone, 7: 1-Indanone, 8: 4-Nitrobiphenyl, 9: Impurity, 10: TCN (RSTD), 11: 9,10-Anthraquinone, 12: 5-Nitroacenaphthene, 13: 4H-Cyclopentadienylphenanthren-4-one, 14: 2-Methyl-9,10-Anthraquinone, 15: 2-Nitrofluorene, 16: 9-Nitroanthracene, 17: 9-Nitrophenanthrene, 18: 2-Nitroanthracene, 19: Benzofluoren-11-one, 20: Benzathione, 21: 2-Nitrofluoranthene, 22: 3-Nitrofluoranthene, 23: 4-Nitropyrene, 24: 1-Nitropyrene, 25: 1,8-Dinitropyrene, 26: 2-Nitropyrene, 27: 2,7-Dinitrofluorene, 28: 7-Nitrobenz[a]anthracene, 29: 6H-Benzofc,d]pyren-6-one, 30: 6-Nitrochrysene, 31: 1,2-Benz[a]anthraquinone, 32: 1,3-Dinitropyrene, 33: 1,6-Dinitropyrene

The twenty-five quantifiable compounds are presented with calibration parameters and LOD and LOQ in Table 10. LOD for the five detectable compounds is presented in Table 11. Calibration curves for the quantified compounds is available in Appendix III, Figure 27 - 53.

Table 10: Calibration parameters of the 25 compounds that could be quantified with this SIM-method, including LOD and LOQ

Compound	R ²	m	b	Levels used	Points used	LOD [pg]	LOQ [pg]	Linear range [pg/μL]
1,4-Naphthoquinone	0,9927	16,37	-2,370	5	10	20,0	66,7	6,5-1000
1-Nitronaphthalene	0,9977	0,03980	-0,0323	4	8	4,0	13,3	49-800
2-Nitronaphthalene	0,9456	0,03760	-0,03778	6	12	3,8	12,5	45-1000
9-Fluorenone	0,9944	0,01915	-0,01642	4	8	25,0	83,3	38-800
4-Nitrobiphenyl	0,9551	0,004548	-0,004070	5	10	40,0	133,3	40-800
9,10-Anthraquinone	0,9944	0,001601	-0,002237	4	8	40,0	133,3	38-800
5-Nitroacenaphthene	0,9906	6,349*10 ⁻⁴	-0,001040	4	8	46,2	153,8	75-800
4H-Cyclopentan[def]phenanthren-4-one	0,9944	0,01149	-0,01481	5	10	6,0	20,0	58-1000
2-Methyl-9,10-anthraquinone	0,9863	0,003545	-0,007201	4	8	66,7	222,2	91-1000
2-Nitrofluorene	0,9859	0,01636	-0,02962	4	8	40,0	133,3	81-800
9-Nitroanthracene	0,9948	0,01404	-0,02165	5	10	4,6	15,4	70-1000
9,10-Phenanthrenequinone	0,9950	4,853*10 ⁻⁵	-6,260*10 ⁻⁵	4	8	46,2	153,8	58-800
9-Nitrophenanthrene	0,9917	0,01423	-0,02265	4	8	66,7	222,2	72-800
2-Nitroanthracene	0,9429	0,002088	-0,002865	6	11	63,8	212,8	62-1000
Benzo[a]fluoren-11-one	0,9987	0,01590	-0,01018	4	8	6,3	20,8	29-800
2-Nitrofluoranthene	0,9605	3,680*10 ⁻⁴	-6,787*10 ⁻⁴	4	6	66,7	222,2	84-800
3-Nitrofluoranthene	0,9744	5,425*10 ⁻⁴	-8,445*10 ⁻⁴	4	7	63,2	210,5	69-1000
4-Nitropyrene	0,9270	2,427*10 ⁻⁴	-4,383*10 ⁻⁴	5	8	60,0	200,0	81-1000
1-Nitropyrene	0,9979	0,01289	-0,01325	4	8	46,2	153,8	46-800
1,8-Dinitropyrene	0,9403	0,001168	-0,001982	5	10	50,0	166,7	76-800
2,7-Dinitrofluorene	0,9976	2,725*10 ⁻⁴	-2,919*10 ⁻⁴	4	8	44,4	148,1	48-800
2-Nitropyrene	0,9731	0,001101	-0,002172	4	7	230,8	769,2	89-1000
7-Nitrobenz[a]anthracene	0,9607	0,002315	-0,002708	5	10	15,8	52,6	52-800
6-Nitrochrysene	0,9607	5,999*10 ⁻⁵	-8,059*10 ⁻⁵	5	10	16,7	55,6	60-800
6H-Benzo[c,d]pyren-6-one	0,9864	0,009314	-0,01064	5	10	13,0	43,5	52-1000

Table 11: Calculated LOQ for the not quantifiable compounds

Compound	LOQ [pg]
9-Methylcarbazole	200,0
Benzanthrone	240,0
1,2-Benz[a]anthraquinone	333,3
1,3-Dinitropyrene	375,0
1,6-Dinitropyrene	375,0

The response factors of all analyte compounds and internal standards were calculated alongside the percentage recovery, this was used to calculate the amount of analyte compound in the laboratory blanks and the samples. The percentage share of the known value of analyte added to the was calculated and is presented alongside the amounts of analyte in the laboratory blanks in Table 12.

Table 12: Calculated amount of C12 standards from the spiked laboratory blanks, with calculated percentage share of true value

Compound	Filter B1 [ng]	% of 30 ng	Filter B2 [ng]	% of 30 ng	PUF B1 [ng]	% of 30 ng	PUF B2 [ng]	% of 30 ng
1,4-Naphtoquinone	0,529	1,76	0,793	2,64	3,63	12,1	9,24	30,8
1-Nitronaphthalene	2,86	9,54	2,36	7,89	4,65	15,5	5,63	18,8
2-Nitronaphthalene	3,62	12,2	3,07	10,24	4,84	16,1	5,93	19,8
9-Fluorenone	26,0	86,73	29,5	98,4	24,4	81,4	51,0	170,1
4-Nitrobiphenyl	10,8	36,1	11,22	37,3	8,58	28,6	114,9	383,1
5-Nitroacenaphtene	19,0	63,4	18,5	61,8	17,4	58,0	307,4	1024,6
9,10-Anthraquinone	21,6	72,0	20,5	68,4	18,7	62,3	52,1	173,7
4H-Cyclopentan[de]phenanthren-4-one	30,8	102,5	39,1	130,2	21,2	70,6	32,5	108,5
2-Methyl-9,10-Anthraquinone	45,9	153,1	47,5	158,2	3,86	12,9	11,2	37,3
2-Nitrofluorene	9,87	32,9	9,99	33,3	7,56	25,2	10,6	35,5
9-Nitroanthracene	0,352	1,17	0,320	1,07	1,301	4,34	2,09	6,96
9,10-Phenanthrenquinone	11,9	39,7	14,01	46,7	20,7	68,9	150,3	500,9
9-Nitrophenanthrene	0,350	1,17	0,290	0,966	1,32	4,39	2,86	9,53
2-Nitroanthracene	47,3	157,8	52,4	174,6	32,4	108,1	16,0	53,3
Benzo[a]fluoren-11-one	17,3	57,5	17,8	59,2	8,08	26,9	17,5	58,2
2-Nitrofluoranthene	148,3	494,3	181,5	605,1	62,4	208,0	507,1	1690,4
3-Nitrofluoranthene	63,9	213,1	66,6	222,1	46,0	153,5	413,6	1378,5
4-Nitropyrene	57,5	191,8	61,6	205,3	22,6	75,5	378,4	1261,4
1,8-Dinitropyrene	44,6	148,7	58,2	194,0	31,1	103,6	32,9	109,8
2-Nitropyrene	28,2	94,1	36,3	120,8	27,3	91,0	22,9	76,3
1-Nitropyrene	36,4	121,2	39,3	130,9	23,3	77,8	33,7	112,2
2,7-Dinitrofluorene	36,6	122,1	40,8	135,8	27,0	89,9	34,5	115,1
7-Nitrobenz[a]anthracene	3,304	11,0	3,59	12,0	8,79	29,3	14,4	47,9
6-Nitrocrysene	11,8	39,3	13,0	43,4	49,4	164,6	1133,9	3779,8
6H-Benzo[c,d]pyren-6-one	17,8	59,3	18,3	61,1	12,5	41,6	17,3	57,7

The amount of analyte in each sample is presented in Table 13 with the average response factor of each analyte. Every value is the average of two analyzed parallels. The results which are calculated above the LOD and/or LOQ of the compound are highlighted and marked, the rest of the results are calculated to be too low for detection and quantification and count as not adequately present.

Table 13: Concentration of analyte in each sample, and average response factor of each analyte compound. Results highlighted in bold marked with * is above the LOD, results highlighted in bold marked with ** is above the LOQ

Compound	Filter P1 [pg/m ³]	Filter P2 [pg/m ³]	PUF P1 [pg/m ³]	PUF P2 [pg/m ³]	Average f _i
1,4-Naphtoquinone	1,72	11,4	4,67	8,19	0,0541
1-Nitronaphthalene	0,0306	0,0322	0,826	0,498	28,4
2-Nitronaphtalene	0,0425	0,0322	0,564	0,384	38,3
9-Fluorenone	3,69	5,35	208,0*	101,8*	60,8
4-Nitrobiphenyl	2,82	1,25	2,86	0,704	332,0
5-Nitroacenaphtene	54,4**	55,9**	40,0	5,00	2403,9
9,10-Anthraquinone	237,8*	126,5**	96,6**	1,3	870,6
4H-Cyclopentan[def]phenanthen-4-one	2,205	1,80	18,06**	10,5**	113,0
2-Methyl-9,10-Anthraquinone	0,981	1,48	9,52	6,31	494,2
2-Nitrofluorene	0,0865	0,0307	0,0312	0,0246	98,5
9-Nitroanthracene	0,201	0,0586	0,148	0,0775	106,8
9,10-Phenanthrenquinone	58,2**	20,2	6,46	22,4	27721,8
9-Nitrophenanthrene	0,199	0,570	0,0521	0,0553	106,9
2-Nitroanthracene	1,05	0,380	0,322	0,212	770,9
Benzo[a]fluoren-11-one	1,76	1,05	1,62	0,611	62,6
2-Nitrofluoranthene	206,4**	81,5**	10,8	4,45	25751,9
3-Nitrofluoranthene	66,2**	62,9	4,78	7,87	18974,2
4-Nitropyrene	67,0**	132,2**	8,05	48,9	17280,3
1,8-Dinitropyrene	1,16	1,94	0,279	0,454	1593,7
2-Nitropyrene	1,17	7,44	0,244	0,627	3900,9
1-Nitropyrene	3,88	1,80	0,58	0,315	85,7
2,7-Dinitrofluorene	4,06	1,81	4,80	4,55	4238,5
7-Nitrobenz[a]anthracene	0,498	1,27	0,108	0,183	659,0
6-Nitrocrysene	33,8	99,5	8,21	25,4**	49410,5
6H-Benzo[c,d]pyren-6-one	8,53	3,69	7,14	18,8**	120,9

The accuracy was calculated in MassHunter for each calibration step, the result is presented in Table 14.

Table 14: The accuracy of the standard calibration compounds

Compound	Accuracy L1 (50 pg/ μ L)	Accuracy L2 (100 pg/ μ L)	Accuracy L3 (200 pg/ μ L)	Accuracy L4 (400 pg/ μ L)	Accuracy L5 (800 pg/ μ L)	Accuracy L6 (1000 pg/ μ L)
1,4-Naphtoquinone	90,5	363,0	103,0	112,2	96,6	97,7
1-Nitronaphthalene	135,3	263,8	93,1	96,9	101,1	125,4
2-Nitronaphthalene	117,3	210,5	75,9	80,0	87,2	111,2
9-Fluorenone	111,1	238,8	88,0	97,1	103,7	125,6
4-Nitrobiphenyl	101,6	188,8	70,4	83,0	104,7	142,7
5-Nitroacenaphtene	169,8	223,3	89,7	91,4	102,5	127,8
9,10-Anthraquinone	152,7	232,7	91,4	94,1	101,8	125,3
4H-Cyclopentan[def]phenanthren-4-one	144,3	253,3	95,5	97,4	95,2	103,6
2-Methyl-9,10-Anthraquinone	202,3	225,5	92,5	84,8	82,5	102,5
2-Nitrofluorene	181,6	232,1	88,4	89,6	103,0	140,7
9-Nitroanthracene	160,0	207,4	89,3	93,1	103,2	99,3
9,10-Phenanthrenquinone	145,2	171,3	88,8	97,8	101,1	95,3
9-Nitrophenanthrene	164,2	207,8	89,7	92,7	102,2	98,3
2-Nitroanthracene	142,2	189,3	76,0	80,0	91,9	130,5
Benzo[a]fluoren-11-one	98,6	287,3	97,5	102,2	99,6	108,3
2-Nitrofluoranthene	168,5	200,5	80,3	80,9	102,4	174,7
3-Nitrofluoranthene	142,3	147,5	60,7	57,3	69,9	117,9
4-Nitropyrene	167,0	151,3	62,4	58,4	75,2	138,8
1,8-Dinitropyrene	165,7	171,0	71,4	74,4	106,7	228,3
2-Nitropyrene	182,9	129,1	59,0	47,1	59,9	128,0
1-Nitropyrene	129,7	265,1	93,3	98,1	100,8	124,6
2,7-Dinitrofluorene	128,2	265,7	94,2	97,8	100,8	130,8
7-Nitrobenz[a]anthracene	123,5	173,6	72,5	82,9	104,8	148,3
6-Nitrocrysene	126,7	170,9	74,6	81,8	104,9	145,2
6H-Benzo[c,d]pyren-6-one	144,3	283,2	101,2	95,8	91,8	105,7

The average response and standard deviations of the internal standards were calculated and are presented in Table 15.

Table 15: Average response and standard deviation of the internal standard signals

	9-Fluorenone-d8	2-Nitrobiphenyl
Average response (all samples and calibration standards)	1111,2	983268,8
Standard deviation (all samples and calibration standards). σ	231,75006	83350,8
$\frac{\sigma}{\text{Average response}}$	0,209	0,0848
Average response (calibration standards)	1276,0	1840577,7
Standard deviation (calibration standards), σ	138,1	73736,5
$\frac{\sigma}{\text{Average response}}$	0,108	0,0401

6.2.3 MRM-analysis

The PIScan method was built upon standard runs of the analytes and ISTDs, first in mix and with comparison to the values of Kristin Sundby master's thesis (2017, p. 28), later individual runs were proceeded on the uncertain components (se chapter 4.2.2).

The Product ion spectra provided very few peaks, even at a high concentration level (2 ng/ μ L), as can be observed in Figure 23. The only clear peaks represented the internal standards, 2-Nitrobiphenyl- d_9 at 17,1 minutes in window 1, and 9-Fluorenone- d_8 at 18,5 minutes in window 2 (see Figure 24). There is some smaller peaks, but these are very small and too few too use as basis to create a useful method on low concentrations of analyte. Very few peaks provided any mass transfers at all, a representation of the mass transfer of the 2-Nitrobiphenyl- d_9 -peak at 17,1 minutes is presented in Figure 25.

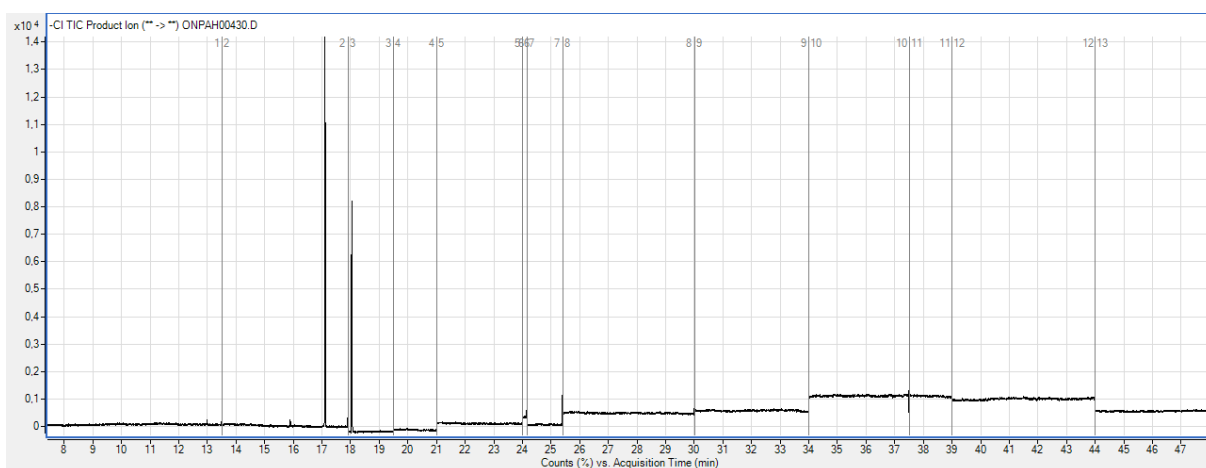


Figure 22: The Total Ion Chromatogram used for the Product Ion Scan showing very few peaks, except the ISTD-peaks of 17,1 min and 18,0 min

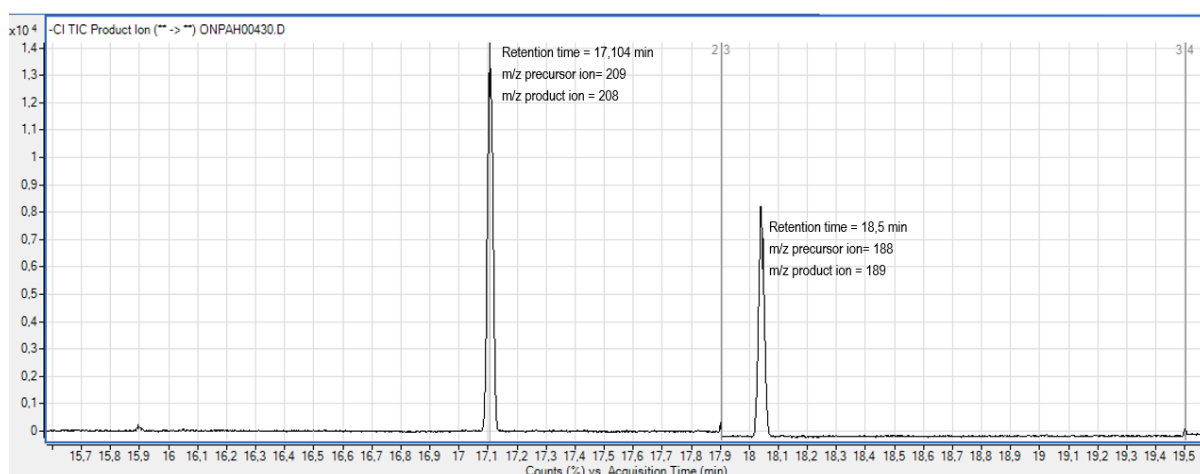


Figure 23: The Total Ion Chromatogram used for the Product Ion Scan zoomed in at the first and second window, showing the baseline and the ISTD-peaks

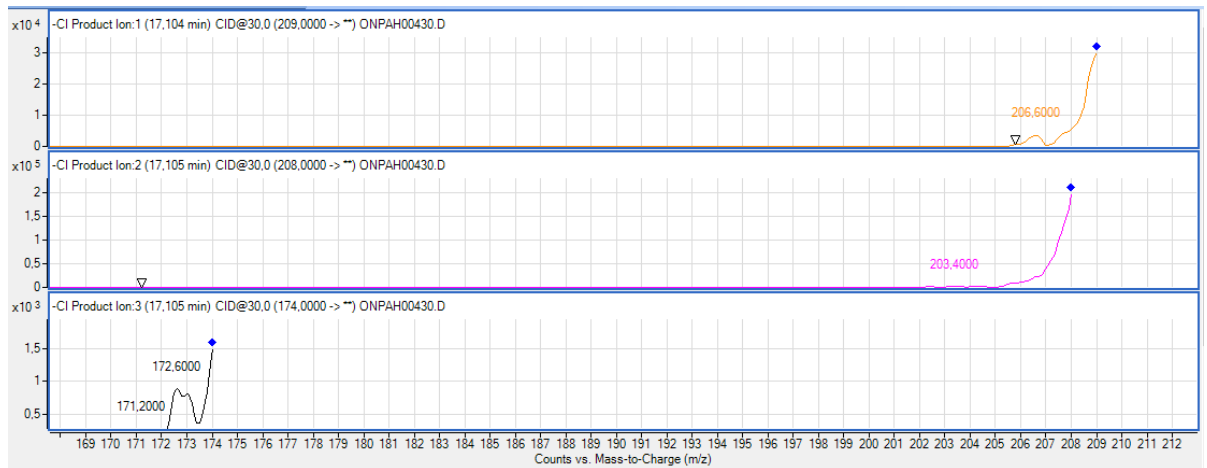


Figure 24: The mass transfer of the ISTD-peak of 17,1 min in the Total Ion Chromatogram in Figure 23 and Figure 24

7.0 Discussion

7.1 EI analysis

Most of the standard chromatograms have many peaks, making identification based on retention time difficult with the EI ion source (Appendix II, Table 21). The chromatogram of 1-Indanone is presented in Figure 15, serving as an example of a chromatogram with many peaks. The peaks represent different compounds separated by the GC, as a result of impurities, thermal degradation or other kinds of transformations to the compound. The blank sample chromatograms do not have apparent peaks (see four method blank chromatograms in Appendix II, Figure 26), making the solvent a less likely source of impurities. The temperature program was not optimized, leaving the effect of a “softer” temperature program with lower rates of temperature increment and different hold times unexplored in this experiment. The 60 meter WAX column was the only tested column, a shorter column of another type of column may provide elution of the compounds with less degradation or alteration. As can be seen in Appendix II, Table 21, many of the calibration standard compound chromatograms do contain many peaks.

The deuterated internal standards have chromatograms with few peaks. The deuterated compounds do thus seem to undergo less degradation and contain less impurities than the calibration standard compounds. The deuterated internal standards were prepared and diluted from 100 % solid phase standards, as may be seen from Appendix I, Table 19. They did therefore contain only the solvent with which they were diluted (n-Hexane), on contrary of the calibration standards (Appendix I, Table 19). As the blank chromatograms show no significant peaks, the impurities of the calibration standards may originate from the stock standard solvents. Degradation due to exposure to air over time or similar effects that may have caused damage to the calibration standard solutions would not have affected the deuterated standards, as they were prepared from 100 % compound in solid phase.

All scan chromatograms are in the range of 10^3 (with the exception of the blanks, illustrated in Appendix II, Figure 26, which is the range of 10^4). This is very low for a concentration of 1 ng/ μ L and imply a sensitivity problem when using the EI ion source with the parameters applied for this experiment. There were some problems regarding the instrumentation, as accounted for in section 4.0. The experiment was not repeated after the GC/MS service in April 2018, so it can not be excluded that the sensitivity issues may have a connection to these instrumentation problems.

Mass spectra (m/z-spectra) of the deuterated internal standards show the expected peaks of their counterpart 1H compound moved eight and nine units, according to the deuterated standards difference in mass compared to their 1H counterparts (as seen in Figure 15 and presented in Appendix II, Table 19). These compounds are as thereby easily identified with this method, and does not undergo to extensive

fragmentation, even though they are related to compounds (shown in Table 1 and Table 2) which do undergo far too extensive fragmentation to be identified (Figure 18 and Appendix II, Table 19). The deuterated compounds does thus seem to be more thermally stable than the 1H nitro- and oxy-PAHs, which are not identifiable by EI-MS, as they are too thermally unstable.

The mass spectra of 1-Indanone is presented in Figure 16, showing a rearranged match with the expected top peaks presented in Table 4. The highest (top) peak in the spectra is at $m/z = 132$, which is expected to be the second highest peak. The expected top peak at $m/z = 104$ is the second highest peak, and the third highest peak at $m/z = 103$ correlates with the expected third highest peak. The mass spectra does not show excessive fragmentation, in contrast to many of the mass spectra produced for the calibration standard compounds (Appendix II, Table 19). In order of using these fragmentation products as qualifier and quantifier ion in a targeted detection program however, it is necessary to further confirm this as the correct compound mass spectra of 1-Indanone. The mass spectra in Figure 16 currently only represent a possible match as it has resemblance to the expected mass spectra of 1-Indanone.

The three mass spectra of 9-Nitroanthracene in Figure 18 show more representative fragmentation patterns for the calibration standards, as may be seen in Appendix II, Table 19. None of the mass spectra of 9-Nitroanthracene give a match with the expected top peaks, giving reason to believe the fragmentation is too excessive for identification. This is the case with most of the calibration standard compound mass spectra (Appendix II, Table 19). Even though their nonpolar parent compounds was identified and quantified by EI-MS until NCI-MS became the preferred analyzing method (section 2.3) this study does indicate that this method is not suitable for increment of sensitivity when analyzing the nitro- and oxy-derivatives.

7.2 NCI analysis

The target compounds was all (including internal standards and recovery standard) analyzed in full scan mode for identification with GC/NCI-MS instrumentation. The chromatograms appeared clean of impurities, in difference to the EI chromatograms. Some peaks with mass spectra showing a lot of fragments and the highest peak at $m/z = 148$ and second highest peak at $m/z = 149$, the same top peaks as is the qualifier and quantifier of the target compound 1-Indanone. 1-Indanone was also significantly present in the blank samples, making the detection of this compound uncertain.

7.2.1 Temperature

The efficiency of the temperature program need to be as high as possible without the loss of analytes. The different temperature programs had severe differences in how many compounds that was eluted, as presented in Figure 20 and Figure 21. The temperature programs with the longest hold times produced chromatograms with many peaks. The number of peaks in the chromatograms exceeded the number of

analyte compounds, and accordingly there was unidentified peaks, implying the long hold time resulted in contaminations or degradation of the compounds. The rate of the rise in temperature is highest in temperature program 9, which eluted all analyte compounds and had the highest efficiency of the temperature programs. This program also had too high a number of peaks, even though the other programs with low hold time had a lower number of peaks in their chromatograms. The high temperature rise rate might lead to degradation of analyte, and it is possible this program therefore have loss of analyte, especially high mass nitro-compounds, which are associated with thermal degradation.

The main difference between temperature program 9 and the other temperature programs with low hold times and high rates of temperature rise is that the highest rate is at the first step for temperature program 9. All the other temperature programs have higher rate at the end of the program, as presented in Table 5, and the other temperature programs with low hold times have too few peaks, not being able to eluate all the compounds. This implies more loss and degradation of analytes with higher rate of temperature rise at the end of the temperature program. This may be explained by the temperature difference at the beginning and the end of the program, as all temperature programs start at an initial temperature of 70°C, and end at 325°C. Thermally unstable compounds seem to endure high rise in temperature in a lower temperature range more sufficient than in a higher temperature range.

7.2.2 SIM-analysis

With the developed SIM-method, thirty out of thirty-two target compounds were identified and LOQ was calculated. This represents an improvement compared to the method used by Kristin Sundby in her master's thesis, but the significant improvement is found in the number of quantifiable compounds. With this method twenty-five analyte compounds may be quantified, when the concentration is above the LOD and LOQ. The LOD-values and LOQ-values are on level with the ones presented in Kristin Sundby's master's thesis (2017), and thereby a bit higher than the ones used by the studies presented in Table 16 (see Table 10). For trace analysis of small concentrations in environmental samples the ability to detect analytes of low concentrations is severe. The possibility of further development of the method in order of achieving better detection would probably make it a useful tool for monitoring of nitro- and oxy-PAHs.

The targeted compounds which were calibrated and quantified had LODs in the range of 3,8 pg – 230,8 pg, and LOQs in the range of 12,5 pg - 764,2 pg (Table 10). It should be noted that the LOD and LOQ representing 2-Nitropyrene is a lot higher than the other compounds, and thereby not representative. The linearity range is somewhat higher than the ones obtained in Sundby's thesis (2017), which can be explained by the fact that the calibration curves in this study is built upon standards in the range of 50 pg/μL – 1000 pg/μL while Sundby had standards in the range of 25 pg/μL – 500 pg/μL. In order of

developing this method further, it could improve the linearity range to add calibration standards with a concentration of 25 pg/ μ L.

In Table 16, there is presented a comparison of the maximum concentrations of nitro- and oxy-PAHs measured in different sites in different studies. The maximum concentrations overwrites the concentrations measured in this study, mostly by far, with the exception of Sundby (Table 16). This may be correlated to sampling time, site and weather conditions. Wind and other influencing weather parameters is not taken into account in this study. The sampling volume and time was different for the two samples, but either PUF not filter samples seem to have a pattern implying that longer or shorter sampling time provides higher concentrations of analyte (Table 8).

Table 16: Comparison of maximum concentrations of nitro- and oxy-PAHs measured in different studies in different locations

Study	This study	Alves et al. (2017)	Alves et al. (2017)	Alves et al. (2017)	Sunby (2017)	Li et al. (2015)
Season	Spring	Summer	Summer	Summer	Winter/spring	Annual
Location	Kjeller, Norway (rural)	Oporto, Portugal (urban/rural)	Florence, Italy (urban/rural)	Athens, Greece (urban/rural)	Longyearbyen, Svalbard (urban/rural)	Wuwei, China (rural)
Maximum nitro-PAH concentration	208,0 pg/m ³	18,5 ng/m ³	5,80 ng/m ³	4,79 ng/m ³	64,2 pg/m ³	555,0 pg/m ³
Maximum oxy-PAH concentration	237,8 pg/m ³	4,01 ng/m ³	1,71 ng/m ³	0,674 ng/m ³	570,4 pg/m ³	27,5 ng/m ³

The calibration curves all have R²-values above 0,9 and use four or more levels in the building (Appendix III), so the quantification should be sufficiently statistically reliable. The accuracy is mainly close to 100 for most levels of all compounds, if level two (L2) is excluded (Table 14). L2 seem to have a systematic error, and has consequently to high response for its concentration (Table 14 and Appendix III). Both level one (L1) and level six (L6) have accuracies that differs from 100, but this does not seem systematic (Table 14 and Appendix III). These errors might originate from errors in the dilution and may be removed by more precise measuring when diluting. The standards deviations of the internal standards seem to be statistically small compared to the average values of the response (Table 15), adding to the reliability of the method.

The added amount of analyte in the spiked laboratory blanks does not correlate well with the calculated values. As the elsewhere studied and calculated method validation implies a valid method it is possible the recovery standard (TCN) gave too weak and unstable signal to provide accurate calculation of the recovery. It may also have been done manual errors in the computing. In order of further development of the method, investigation of the recovery standard and its relation to the internal standards should be performed.

The three latest eluted compounds (1,2-Benz[a]anthraquinone, 1,3-Dinitropyrene and 1,6-Dinitropyrene) are high mass compounds and are injected with a temperature of 225°C, which probably lead to a considerable loss of analyte in the injector. These compounds are not thermic stable, and will be affected by the high injection temperature. No measure has been taken in this experiment to avoid the loss of these high mass compounds, due to limitations in equipment and time. If these compounds are to be identified and quantified along with the other analytes targeted in this thesis, the injection temperature may be further decreased, but this may lead to a lot of contamination which would effect the chromatographic separation. High Pressure Injection can be tested, but the light mass compounds might be lost with such a method. To minimize loss in injected a pre-column could be tested, to improve the focus, in combination with a On-Column injector. An shorter column may lead to less band spreading, as the long column reduces sensitivity for the late eluted compounds, but this might decrease the sensitivity for the earlier eluted compounds. A long column with a thinner stationary phase might increase the sensitivity of the late eluted compounds without decreasing the sensitivity of the earlier eluted compounds, however. Such a column may decrease the alternating effect and the retention time and in this way provide improved sensitivity.

A summary of the status of the method and suggestions of measures that may be taken in order of developing and optimizing the method further is presented in Table 17.

Table 17: Summary of findings about the SIM-method and suggestions for further development

	Status	Suggestions for further development
LOD and LOQ	Higher than for several compared studies	Remove impurities and increase sensitivity
Linearity range	Starts at a high concentration level for most compounds	Expand linearity range by adding standards with lower concentrations
Accuracy	Laboratory blanks have too high deviation from known value, systematic error in one calibration level	Eliminate errors in sample preparation, test RSTDs
Sensitivity	Sensitivity is better for early eluted compounds than late ones	Test capillary column with thinner stationary phase and test on-column injection with a pre-column
Quantification	Could be done for additional compounds if method was further optimized	(see former suggestions) Improve probability by examining and testing RSTD

7.2.3 MRM-analysis

In the attempt to create a Product Ion Scan method the mass-to-charge ratios of some compounds were alike, and some retention times were very close, which may have caused trouble achieving satisfying

sensitivity. There is a possibility that trouble with the instrumentation caused a lack of sensitivity, making the foundation for the development of the program rather uncertain. The sensitivity achieved on the SIM-program after the GC/MS service imply a significance of the state of the instrument. The lack of present peaks in the Total Ion Chromatogram (Figure 23) suggest a need for method development, hence finding better or true precursor ions and studying means of improving the sensitivity of the method. In order of developing a MRM-method it is necessary to have a satisfactory production of product ions. The NICI ion source does not produce much fragmentation, and it is possible a "harder" ionization method with more excessive fragmentation will produce a sufficient product ion yield to develop an acceptable MRM method. EI ion source does provide more fragmentation, but in this experiment it was not tested, as the EI-analysis showed too low sensitivity to improve upon the MRM analysis.

Adhikari et al. achieved increased sensitivity and reduction of baseline noise by optimizing a MRM-method for fingerprint analysis of PAHs and alkyl-PAHs. Their study did not include nitrated or oxygenated PAHs and are by these means not direct comparable, as the electronegativity of the compounds are quite different. The difference in electronegativity may effect the fragmentation pattern and the thermal stability. The precursor ions used for the development of a MRM-method was in this thesis obtained mainly by reference material, such as Kristin Sundbys master's thesis (2017). In order of developing a efficient MRM-method the precursor ions should have been selected after analyzing each target compound individually. This would have been a time-consuming task, however, and the results obtained by the test method developed using the reference information were not promising. If the results obtained by Adhikari et al. are transferrable to more electronegative target compounds it will most likely be necessary to adjust and develop the method, considering such parameters as solvent, temperature program and capillary column.

8.0 Conclusions

The EI ion source did not provide sufficient sensitivity to improve identification and quantification of nitro- and oxy-PAHs. It may be tested with a less polar capillary column, but it seem to fragmentize the nitro- and oxy-PAHs in too great extent to work sufficient to provide an alternative for NICI ion source when analyzing these compounds.

The NICI ion source did not provide enough fragmentation to produce sufficient product ion yield to develop a MRM-method. The EI ion source should not be considered, even though it fragmentize sufficient, it did not provide the sensitivity necessary to be an alternative.

The NICI ion source SIM-method provided sensitivity enough to identify thirty of thirty-two compounds and quantify twenty-five, although most at higher concentrations than these compounds usually are found at. The SIM-method produced calibration curves sufficient for quantification, but the recovery standard should be investigated, and the method further optimized in order of lowering the LOD and LOQ. More precise dilution could improve the method. The method may allow more compounds to be detected and quantified if the instrumentation is modified. A less thermally destructive injection method and a different capillary column could be tested in order of prevent loss and degradation of analyte during analysis. The method was validated by quantification of two air samples, and was able to identify and quantify the nitro- and oxy-PAH compounds present in sufficient magnitude for identification and quantification with the method.

Bibliography

Adhikari, P. L., Wong, R. L. & Overton, E. B. (2017). Application of enhanced gas chromatography/triple quadrupole mass spectrometry for monitoring petroleum weathering and forensic source fingerprinting in samples impacted by the *Deepwater Horizon* oil spill. *Chemosphere*, 184, 939 – 959. doi: <https://doi.org/10.1016/j.chemosphere.2017.06.077>

Agilent Technologies (2018). *Capillary DB-WAX*. Obtained from: <https://www.agilent.com/en/products/gas-chromatography/gc-columns/capillary/db-wax>

Alam, M. S., I. J. Keyte, J. X. Yin, C. Stark, A. M. Jones and R. M. Harrison (2015). Diurnal variability of polycyclic aromatic compound (PAC) concentrations: Relationship with meteorological conditions and inferred sources. *Atmospheric Environment* 122, 427-438. doi: 10.1016/j.atmosenv.2015.09.050

Albinet, A., Tomaz, S. & Lestremau, F. (2013). A really quick easy cheap effective rugged and safe (QuEChERS) extraction procedure for the analysis of particle-bound PAHs in ambient air and emission samples. *Science of the Total Environment*, 450 – 451, 31 – 38. doi: <http://dx.doi.org/10.1016/j.scitotenv.2013.01.068>

Alves, C. A., A. M. Vicente, D. Custodio, M. Cerqueira, T. Nunes, C. Pio, F. Lucarelli, G. Calzolari, S. Nava, E. Diapouli, K. Eleftheriadis, X. Querol and B. A. M. Bandowe (2017). Polycyclic aromatic hydrocarbons and their derivatives (nitro-PAHs, oxygenated PAHs, and azaarenes) in PM_{2.5} from Southern European cities. *Science of the Total Environment*, 595, 494-504. doi: 10.1016/j.scitotenv.2017.03.256

Anderson, K. A., Szelewski, M. J., Wilson, G., Quimby, B. D. & Hoffman, P. D. (2015). Modified ion source triple quadrupole mass spectrometer gas chromatograph for polycyclic aromatic hydrocarbon analyses. *Journal of Chromatography A*, 1419, 89 – 98. doi: <https://doi.org/10.1016/j.chroma.2015.09.054>

Bamford, H. A., Bezabeh, D. Z., Schantz, M. M., Wise, S. A. & Baker, J. E. (2003). Determination and comparison of nitrated-polycyclic aromatic hydrocarbons measured in air and diesel particulate reference materials. *Chemosphere*, 50(5), 575 – 587. doi: [https://doi.org/10.1016/S0045-6535\(02\)00667-7](https://doi.org/10.1016/S0045-6535(02)00667-7)

Barrado, A.I., Garcia, S., Castrillejo, Y. & Barrado E. (2013). Exploratory data analysis of PAH, nitro-PAH and hydroxy-PAH concentrations in atmospheric PM₁₀-bound aerosol particles. Correlations with physical and chemical factors. *Atmospheric Environment*, 67, 385-393. doi: <https://doi.org/10.1016/j.atmosenv.2012.10.030>

Bart, J. C. J. (2005). *Additives in polymers : industrial analysis and applications*. Chichester: John Wiley & Sons

Bezabeth, D. Z., Bamford, H. A., Schantz, M. M. & Wise, S. A. (2002). Determination of nitrated polycyclic aromatic hydrocarbons in diesel particulate-related standard reference materials by using gas chromatography/mass spectrometry with negative ion chemical ionization. *Analytical and bioanalytical Chemistry*, 375(3). 381 – 388. doi: 10.1007/s00216-002-1698-8

Cecinato, A., Balducci C., Mastroianni D. & Perilli M. (2012). Sampling and analytical methods for assessing the levels of organic pollutants in the atmosphere: PAH, phthalates and psychotropic substances: a short review. *Environmental Science and Pollution Research*, 19(6). 1915–1926. doi: 10.1007/s11356-012-0959-0

Chaspoul, F., Barban, G., & Gallice, P. (2006). Simultaneous GC/MS analysis of polycyclic aromatic hydrocarbons and their nitrated derivatives in atmospheric particulate matter from workplaces. *Polycyclic Aromatic Compounds*, 25(2), 157 – 167. doi: 10.1080/10406630590922337

Chaudhry, A. & Kleinpoppen, H. (2011). *Analysis of Excitation and Ionization of Atoms and Molecules by Electron Impact*. New York: Springer.

Chen, S.-Y. & Urban, P. L. (2015). On-line monitoring of Soxhlet extraction by chromatography and mass spectrometry to reveal temporal extract profiles. *Analytica Chimica Acta*, 881, 74-81. doi: <https://doi.org/10.1016/j.aca.2015.05.003>.

Chromedia. (2017). *Splitless injection*. Obtained from: <http://www.chromedia.org/chromedia?waxtrapp=sbwgrDsHqnOxmOIIecCbCoFtFgC&subNav=tmfweDsHqnOxmOIIecCbCoFtFgChC>

Cochran, R. E., Dongari, N., Jeong, H., Beránek, J., Haddadi, S., Shipp, J. & Kubátová, A. (2012). Determination of polycyclic aromatic hydrocarbons and their oxy-, nitro-, and hydroxy-oxidation products. *Analytica Chimica Acta*, 740, 93 – 103. doi: <https://doi.org/10.1016/j.aca.2012.05.050>

Cochran, R. E., I. P. Smoliakova and A. Kubatova (2016). Detection of nitrated and oxygenated polycyclic aromatic hydrocarbons using atmospheric pressure chemical ionization high resolution mass spectrometry. *International Journal of Mass Spectrometry* 397, 6-17. doi: 10.1016/j.ijms.2016.01.001

- Crimmins, B. S. & Baker, J. E. (2006). Improved GC/MS methods for measuring hourly PAH and nitro-PAH concentrations in urban particulate matter. *Atmospheric Environment*, 40, 6764 – 6779. doi: <https://doi.org/10.1016/j.atmosenv.2006.05.078>
- Dang, J., X. L. Shi, J. T. Hu, J. M. Chen, Q. Z. Zhang and W. X. Wang (2015). Mechanistic and kinetic studies on OH-initiated atmospheric oxidation degradation of benzo[alpha]pyrene in the presence of O₂ and NO_x. *Chemosphere*, 119, 387-393. doi: 10.1016/j.chemosphere.2014.07.001
- de Castro, M. D. L. & Priego-Capote, F. (2010). Soxhlet extraction: Past and present panacea. *Journal of Chromatography A*, 1217(16), 2383-2389. doi: <https://doi.org/10.1016/j.chroma.2009.11.027>
- de Castro Vasconcellos P., Sanchez-Ccoyllo O., Balducci C., Mabilia R. & Cecinato A. (2008). Occurrence and Concentration Levels of Nitro-PAH in the Air of Three Brazilian Cities Experiencing Different Emission Impacts. *Water, Air, and Soil Pollution*, 190(1-4). 87-94. doi: 10.1007/s11270-007-9582-y
- de Hoffmann, E. & Stroobant, V. (2007). *Mass spectrometry – Principles and Applications* (3th ed.). West Sussex, England: John Wiley & Sons, Ltd.
- Dignac, M.-F., Houot, S. & Derenne, S. (2006). *Journal of Analytical and Applied Pyrolysis*, Vol.75(2), 128-139. doi: 10.1016/j.jaap.2005.05.001
- Garstad, J. B. (2017). *Gas chromatography-Mass spectrometry method validation for the quantitative determination of nitro- and oxy- containing polycyclic aromatic hydrocarbons (ND/ODPAHs) in soil samples*. (Master's Thesis). Ås: University of Life Sciences.
- Greibrokk, T., Lundanes, E. & Rasmussen, K. E. (1998). *Kromatografi – Seperasjon og deteksjon* (3th ed.). Oslo: Universitetsforlaget.
- Hak, C., Halse, A. K. & Halvorsen, H. L. (2016). Kartlegging av 2-4 ring PAHer og SO₂ rundt FeSi-/ Si-smelteverk - Passive luftmålinger rundt Finnfjord AS, oktober – desember 2014 og analyse av mikrosilikastøv. *NILU rapport 19/2016*. ISBN: 978-82-425-2847-6
- Harrison R. M., Alam M. S., Dang J., Ismail I. M., Bashi J., Alghamdi A., . . . Khoder M. (2016). Relationship of polycyclic aromatic hydrocarbons with oxy(quinone) and nitro derivatives during air mass transport. *Science of the Total Environment*, 572(Supplement C). 1175 – 1183. doi: <https://doi.org/10.1016/j.scitotenv.2016.08.030>

Helbæk, M. (2008). *Statistikk for kjemikere* (2th ed.). Trondheim: Tapir akademiske forlag.

Holler, F. J., Skoog, D. A. & Crouch, S. R. (2007). *Principles of Instrumental Analysis* (6th ed.). Belmont, USA: Brooks/Cole.

IUPAC. (2014) *Fixed product ion scan in mass spectrometry*. Obtained from:
<https://goldbook.iupac.org/html/F/F02406.html>

IUPAC. (2014). *Selected ion monitoring in mass spectrometry*. Obtained from:
<http://goldbook.iupac.org/html/S/S05547.html>

Kasiotis, K. M. & Emmanouil, C. (2015). PAHs Pollution Monitoring by Bivalves. I E. Lichtfouse, J. Schwarzbauer & D. Robert (Red). *Pollutants in Buildings, Water and Living Organisms* (p. 169 – 234). Switzerland: Springer International Publishing.

Kinter, M. & Kinter, C. S. (2013). *Application of Selected Reaction Monitoring to Highly Multiplexed Targeted Quantitative Proteomics : A Replacement for Western Blot Analysis*. New York: Springer.

Kitson, F. G., Larsen, B. S. & McEwen, C. N. (1996). *Gas Chromatography and Mass Spectrometry : A Practical Guide*. San Diego, California: Academic Press.

Laboratory size Soxhlet apparatus. (2013). Obtained from: http://www.tankonyvtar.hu/hu/tartalom/tamop412A/2011-0016_01_the_theory_and_practise_of_pharmaceutical_technology/ch14.html

Lin, Y., X. H. Qiu, Y. Q. Ma, J. Ma, M. Zheng and M. Shao (2015). Concentrations and spatial distribution of polycyclic aromatic hydrocarbons (PAHs) and nitrated PAHs (NPAHs) in the atmosphere of North China, and the transformation from PAHs to NPAHs. *Environmental Pollution* 196, 164-170. doi: 10.1016/j.envpol.2014.10.005

Liu, D., T. Lin, J. H. Syed, Z. N. Cheng, Y. Xu, K. C. Li, G. Zhang and J. Li (2017). Concentration, source identification, and exposure risk assessment of PM_{2.5}-bound parent PAHs and nitro-PAHs in atmosphere from typical Chinese cities. *Scientific Reports* 7(1), 1 - 12. doi: 10.1038/s41598-017-10623-4

Luch A. (2005). *The Carcinogenic Effects of Polycyclic Aromatic Hydrocarbones*. London: Imperial College Press

National Center for Biotechnology Information. (2018). *PubChem*. Obtained from <https://pubchem.ncbi.nlm.nih.gov/#>

Nickerson, B. (2011). *Sample Preparation of Pharmaceutical Dosage Forms : Challenges and Strategies for Sample Preparation and Extraction*. Boston, MA: Springer, US.

Niederer, M. (1998). Determination of Polycyclic Aromatic Hydrocarbons and Substitutes (Nitro-, Oxy-PAHs) in Urban Soil and Airborne Particulate by GC-MS and NCI-MS/MS. *Environmental Science and Pollution Research*, 5(4), 209 – 216. doi: 10.1007/BF02986403

Norwegian Environmental Agency. (2017). *Utslippene av PAH har gått ned*. Obtained from <http://www.miljostatus.no/tema/kjemikalier/prioritetslisten/pah/>

Oehme, M. (2007). *Quality control in organic trace analysis*. Applied Analytical Chemistry, Arlesheim and University of Basel, Basel.

Robbat, A. & Wilton, N. M. (2014). A new spectral deconvolution - Selected ion monitoring method for the analysis of alkylated polycyclic aromatic hydrocarbons in complex mixtures. *Talanta*, 125, 114 – 124. doi: <https://doi.org/10.1016/j.talanta.2014.02.068>

Schlabach, M., Breivik, K., Fjeld, E., Hirdmann, D., Pfaffhuber, K. A. & Stohl, A. (2009). Atmospheric transport of environmental pollutants to Lake Mjøsa. *SPFO-rapport 1059/2009*. ISBN: 978-82-425-2149-1

Simoneit, B. R. (1999). A review of biomarker compounds as source indicators and tracers for air pollution. *Environ Sci Pollut Res Int* 6(3): 159-169. doi: 10.1038/s41598-017-10623-4

Sosa, B. S., Porta, A., Lerner, J. E. C., Noriega, R. B. & Massolo, L. (2017). Human health risk due to variations in PM10-PM2.5 and associated PAHs levels. *Atmospheric Environment*, 160, 27 – 35. doi: <https://doi.org/10.1016/j.atmosenv.2017.04.004>

Sparkman, O. D., Penton, Z., & Kitson, F. G. (2011). *Gas chromatography and mass spectrometry: a practical guide* (2th ed.). San Diego, California: Academic Press. ISO 690

Srogi, K. (2007). Monitoring of environmental exposure to polycyclic aromatic hydrocarbons: a review. *Environ Chem Lett* 5(4), 169-195. doi: 10.1007/s10311-007-0095-0

Sundby, K. (2017). *Determination of nitrated and oxygenated polycyclic aromatic hydrocarbons in arctic air by GC/NICI-MS*. (Master's thesis). Ås: Norwegian University of Life Sciences.

Tang, N. S. L. & Poon, T. (2014). *Chemical Diagnostics From Bench to Bedside*. Berlin, Heidelberg: Springer

Termime-Roussel, B., Monod, A., Massiani, C. & Wortham, H. (2004). Evaluation of an annular denuder tubes for atmospheric PAH partitioning studies—1: evaluation of the trapping efficiency of gaseous PAHS. *Atmospheric Environment*, 38(13), 1913-1924. doi: 10.1016/j.atmosenv.2004.01.005

Thomas, H. V., Balaam, J., Barnard, N., Dyer, R., Jones, C., Lavender, J. & McHugh, M. (2002). Characterisation of potentially genotoxic compounds in sediments collected from United Kingdom estuaries. *Chemosphere*, 49(3), 247 – 258. doi: [https://doi.org/10.1016/S0045-6535\(02\)00316-8](https://doi.org/10.1016/S0045-6535(02)00316-8)

Tomaz S., Jaffrezo J., Favez O., Perraudin E., Villenave E. & Albinet A. (2017). Sources and atmospheric chemistry of oxy- and nitro-PAHs in the ambient air of Grenoble (France). *Atmospheric Environment*, 161(Supplement C). 144 – 154. doi: <https://doi.org/10.1016/j.atmosenv.2017.04.042>

Tröppner, O. (2017). Gas Chromatography coupled with Mass Spectrometry (GC/MS). Obtained from: <http://www.skz.de/en/research/technicalfacilities/pruefverfahren1/spektroskopie1/4870.Gas-Chromatography-coupled-with-Mass-Spectrometry-GCMS.html>

Tsapakis, M. & Stephanou, E. G. (2003). Collection of gas and particle semi-volatile organic compounds: use of an oxidant denuder to minimize polycyclic aromatic hydrocarbons degradation during high-volume air sampling. *Atmospheric Environment*, 37(35), 4935-4944. doi: <https://doi.org/10.1016/j.atmosenv.2003.08.026>

United Nations. (2012). *Moving towards a climate neutral UN - The UN system's footprint and efforts to reduce it*. Obtained from http://www.greeningtheblue.org/sites/default/files/2011CNeutral_UN_final_0.pdf

Valcárcel, M. (2000). *Principles of Analytical Chemistry – A Textbook*. Berlin: Springer -Verlag.

Wang, C., J. H. Yang, L. W. S. Zhu, L. Yan, D. Z. Lu, Q. Zhang, M. R. Zhao and Z. Y. Li (2017). Never deem lightly the "less harmful" low-molecular-weight PAH, NPAH, and OPAH - Disturbance of the immune response at real environmental levels. *Chemosphere* 168, 568-577. doi: 10.1016/j.chemosphere.2016.11.024

Wells, G. & Huston, C. (1995). High-Resolution Selected Ion Monitoring in a Quadrupole Ion Trap Mass Spectrometer. *Analytical Chemistry*, 67(20), 3650 – 3655. Obtained from:
<https://pubs.acs.org/doi/pdf/10.1021/ac00116a006>

Williams, D. & Fleming, I. (2008). *Spectroscopic methods in organic chemistry* (6th ed.). Berkshire, UK: McGraw-Hill Higher Education.

Yao, C. & Feng, Y.-L. (2016). A nontargeted screening method for covalent DNA adducts and DNA modification selectivity using liquid chromatography-tandem mass spectrometry. *Talanta*, 159, 93 – 102. doi: <http://dx.doi.org/10.1016/j.talanta.2016.05.074>

Zielinska, B. & Samy, S. (2006). Analysis of nitrated polycyclic aromatic hydrocarbons. *Analytical and Bioanalytical Chemistry*, 386(4), 883 – 890. doi: 10.1007/s00216-006-0521-3

Zeigler, C., MacNamara, K., Wang, Z. & Robbat Jr., A. (2008). Total alkylated polycyclic aromatic hydrocarbon characterization and quantitative comparison of selected ion monitoring versus full scan gas chromatography/mass spectrometry based on spectral deconvolution. *Journal of Chromatography A*, 1205(1-2), 109 – 116. doi: <https://doi.org/10.1016/j.chroma.2008.07.086>

Appendix

Appendix I

Table 18: Solvent information with CLPs and safety precautions

Name	Manufactory	Manufactory Location	Concentration	Phase	CLP	Precaution	Note
n-Hexane	WWR INTERNATIONAL	Oslo, Norway	≈ 100 %	Liquid		<ul style="list-style-type: none"> • Handling in fume hood • Use of safety goggles, latex gloves and protective work clothing • No eating or drinking in laboratory • Cleaning of hands after handling • Throw away in special waste – NOT IN SINK • Knowledge of nearest fire extinguisher station, eye wash station and emergency shower 	<i>Suspected of damaging the unborn child</i>
Dichloromethane	WWR INTERNATIONAL	Oslo, Norway	≈ 100 %	Liquid			
Acetone	WWR INTERNATIONAL	Oslo, Norway	≈ 100 %	Liquid			
Acetonitrile	SIGMA-ALDRICH	Oslo, Norway	≈ 100 %	Liquid			
Toluene	CHIRON AS	Trondheim, Norway	≈ 99 %	Liquid			
Isooctane	CHIRON AS	Trondheim, Norway	≈ 99 %	Liquid			
Nonane	Cambridge Isotope Laboratories, Inc.	Massachusetts, USA	≈ 99 %	Liquid			

Table 19: Stock standard information

Name	Manufactory	Manufactory location	Solvent	Phase	Concentration [ng/μL]	CAS no.
9,10-Anthraquinone	CHIRON AS	Trondheim, Norway	Toluene	Liquid	1000	84-65-1
Benzanthrone	CHIRON AS	Trondheim, Norway	Toluene	Liquid	1000	82-05-3
1,2-Benzo[a]anthraquinone	CHIRON AS	Trondheim, Norway	Toluene	Liquid	1000	2498-66-0
Benzo[a]fluoren-11-one	CHIRON AS	Trondheim, Norway	Toluene	Liquid	200	479-79-8
6H-Benzo[c,d]pyren-6-one	CHIRON AS	Trondheim, Norway	Toluene	Liquid	200	3074-00-8
4H-Cyclopenta[d,e]phenanthren-4-one	CHIRON AS	Trondheim, Norway	Toluene	Liquid	1000	5737-13-3
9-Fluorenone	CHIRON AS	Trondheim, Norway	Isooctane	Liquid	1000	486-25-9
1-Indanone	CHIRON AS	Trondheim, Norway	Toluene	Liquid	1000	83-33-0
2-Methyl-9,10-anthraquinone	CHIRON AS	Trondheim, Norway	Isooctane	Liquid	1000	84-54-8
1,4-Naphthoquinone	CHIRON AS	Trondheim, Norway	Isooctane	Liquid	1000	130-15-4
9,10-Phenanthrenequinone	CHIRON AS	Trondheim, Norway	Toluene	Liquid	1000	84-11-7
9-Fluorenone-d8	CHIRON AS	Trondheim, Norway	Toluene	Solid	1000	137219-34-2
2,7-Dinitrofluorene	CHIRON AS	Trondheim, Norway	Toluene	Liquid	100	5405-53-8
1,3-Dinitropyrene	CHIRON AS	Trondheim, Norway	Toluene	Liquid	100	75321-20-9
1,6-Dinitropyrene	CHIRON AS	Trondheim, Norway	Toluene	Liquid	100	42397-64-8
1,8-Dinitropyrene	CHIRON AS	Trondheim, Norway	Toluene	Liquid	100	42397-65-9

5-Nitroacenaphthene	CHIRON AS	Trondheim, Norway	Toluene	Liquid	1000	602-87-9
2-Nitroanthracene	CHIRON AS	Trondheim, Norway	Toluene	Liquid	200	3586-69-4
9-Nitroanthracene	CHIRON AS	Trondheim, Norway	Toluene	Liquid	100	602-60-8
7-Nitrobenz[a]anthracene	CHIRON AS	Trondheim, Norway	Toluene	Liquid	100	20268-51-3
6-Nitrobenzo[a]pyrene	CHIRON AS	Trondheim, Norway	Toluene	Liquid	100	63041-90-7
4-Nitrobiphenyl	CHIRON AS	Trondheim, Norway	Toluene	Liquid	100	92-93-3
6-Nitrochrysene	CHIRON AS	Trondheim, Norway	Toluene	Liquid	100	7496-02-8
2-Nitrofluoranthene	CHIRON AS	Trondheim, Norway	Toluene	Liquid	100	13177-29-2
3-Nitrofluoranthene	CHIRON AS	Trondheim, Norway	Toluene	Liquid	100	892-21-7
2-Nitrofluorene	CHIRON AS	Trondheim, Norway	Toluene	Liquid	100	607-57-8
1-Nitronaphthalene	CHIRON AS	Trondheim, Norway	Toluene	Liquid	100	86-57-7
2-Nitronaphthalene	CHIRON AS	Trondheim, Norway	Toluene	Liquid	100	581-89-5
9-Nitrophenanthrene	CHIRON AS	Trondheim, Norway	Isooctane	Liquid	1000	954-46-1
1-Nitropyrene	CHIRON AS	Trondheim, Norway	Toluene	Liquid	100	5522-43-0
2-Nitropyrene	CHIRON AS	Trondheim, Norway	Toluene	Liquid	100	789-07-1
4-Nitropyrene	CHIRON AS	Trondheim, Norway	Toluene	Liquid	100	57835-92-4
9-Methylcarbazole	CHIRON AS	Trondheim, Norway	Toluene	Liquid	1000	1484-12-4
2-Nitrobiphenyl-d9	CHIRON AS	Trondheim, Norway	Toluene	Solid	1000	38537-53-0
1,2,3,4-TetraCN	Cambridge Isotope Laboratories, Inc.	Massachusetts, USA	Nonane	Liquid	100	20020-02-4

Table 20: Equipment information

Type	Size	Manufactory	Distributor location
Laboratory equipment			
Soxhlet extraction tubes with heating mantles and cooling system	100mL	<i>Unknown</i>	
Round bottom flasks	500 mL	<i>Unknown</i>	
Glass Pasteur pipettes	230 mm	VWR International, New York, USA	VWR International, Oslo, Norway
Jencons sealpette Automate pipette	200 – 1000 µL	Jencons Scientific, Pennsylvania, USA	VWR International, Oslo, Norway
Jencons sealpette Automate pipette	10 – 100 µL	Jencons Scientific, Pennsylvania, USA	VWR International, Oslo, Norway
Jencons sealpette Automate pipette	1 – 10 µL	Jencons Scientific, Pennsylvania, USA	VWR International, Oslo, Norway
Beakers and Erlenmeyer flasks	various volumes	<i>Unknown</i>	
Chromacol fixed insert vial, clear, crimp top	300 µL	Thermo Fisher Scientific, Massachusetts, USA	Teknolab, Ski, Norway
Snap ring cap blue, soft, red rubber/PTFE beige, 45°	11 mm	VWR International, New York, USA	VWR International, Oslo, Norway
Aluminium cap, Natural, rubber/butyl/IPTFE, 45°	11 mm	VWR International, New York, USA	VWR International, Oslo, Norway
CL sorw vial w/inert	300 µL	Agilent Technologies	Germany
Vortex Genie 2 Vortex Mixer		Scientific Industries, New York, USA	Fisher Scientific AS, Oslo, Norway
Reacti-Vap I #TS-18825 Nitrogen Evaporation Unit		Thermo Fisher Scientific, Massachusetts, USA	Teknolab, Ski, Norway
Stainless steel needles		Thermo Fisher Scientific, Massachusetts, USA	Teknolab, Ski, Norway
EBA 20 Centrifuge		Hettich Instruments, LP	Tuttlingen, Germany
Glass test tubes	15 mL	<i>Unknown</i>	

32 position test tube stand		<i>Unknown</i>	
TurboVap Classic II Concentration Workstation		Biotage IST	Uppsala, Sweden
TurboVap Tubes with 0,5 endpoint stem	250 mL	Biotage IST	Uppsala, Sweden
SPE manifold with vakuüm flask and vakuüm pump		Thermo Fisher Scientific	Teknolab, Ski, Norway
SPE SiOH glass cartridges, 500 mg	3 mL	CHROMABOND	Ski, Norway
GC/MS system			
7890B GC-system		Agilent Technologies	Santa Clara, CA, USA
7000C Triple Quadrupole Mass spectrometer		Agilent Technologies	Santa Clara, CA, USA
G4513A Autosampler injector with 16-sample standalone turret		Agilent Technologies	Santa Clara, CA, USA
Agilent Gold Standard Injection Syringe	10 µL	Agilent Technologies	Santa Clara, CA, USA
Agilent 5190-2293 Ultra Inert Liner with glass wool		Agilent Technologies	Santa Clara, CA, USA
Agilent J&W HP-5ms 50m x 0.25mm, 0.25 µm film ((5%-phenyl)-methylpolysiloxane) GC column		Agilent Technologies	Santa Clara, CA, USA
Agilent DB-WAX 60m x 0,32mm, 0,50 µm film (Polyethylene glycol (GEC)) GC column		Agilent Technologies	Santa Clara, CA, USA
Computer software			
Agilent MassHunter Qualitative Analysis B.07.00		Agilent Technologies	Santa Clara, CA, USA
Agilent MassHunter Quantitative Analysis B.07.01		Agilent Technologies	Santa Clara, CA, USA
Microsoft Excel 2016		Microsoft Office	Elkjøp XL, Fredrikstad, Norway
Sampling, Kjeller, Norway			
High volume air sampler*	<i>Unknown</i>	Digitel Elektronik AG, Hegnau, Switzerland	Industriell Maaleteknikk as, Lørenskog, Norway
Polyurethane foam		<i>Unknown</i>	
Filter		Unknown	

*Information of air sampler obtained from professor Roland Kallenbord, NMBU

Appendix II

Table 21: Overview of EI analysis of standard solutions with Chromatographic peaks and according m/z peaks ranked in order of magnitude

P ₁	1-Indanone						File 0076																	
	Peak	1	2	3	4	5																		
	EI scan [min]	11,247	11,934	12,629	13,972	9,055																		
P ₂	1-Indanone												File 0077											
	Peak	1	2	3	4	5	6	7	8	9	10	11	12											
	EI scan [min]	11,934	12,612	13,958	15,603	16,545	16,982	18,719	32,087	33,432	34,733	36,714	37,735											
P ₂	9-Fluorenone: Just noise												File 079						File 080					
	4H-Cyclopenta[def]phenanthren-4-one												File 0082											
	Peak	1	2	3	4	5	6	7	8	9	10	11	12											
P ₁	EI scan [min]	11,662	11,920	12,159	12,977	14,122	16,893	17,321	18,259	19,044	31,550	32,186	32,024											
	m/z	102,2 97,1 57,3 92,4 97,3 91,2 73,3 163,4 214,3	97,3 57,2 123,2 180,1	97,2 57,3 99,4 109,2 102,3 67,3 91,3 79,4 143 214, 5	97,2 57,3 123,2 81,2 180,2	205,1 220,1 145,2 57,3	97,2 57,2 121,2 177,1	97,2 57,3 99,3 121,2 183,3 214,5	97,2 57,3 83,3 123,2 99,3 179,3 250,2	97,2 57,3 99,4 79,3 157,1 213,2	87,3 74,3 55,3 143,1 69,2 83,4 97,2 57,4 255,1 199,1	56,3 256,9 73,3 129,3 239,7 312,2 185,3	97,2 83,3 69,3 111,3 55,3 61,3 224,5											
	4H-Cyclopenta[def]phenanthren-4-one												File 0083											
P ₂	Peak	1	2	3	4	5	6	7	8	9	10	11	12	13	14									
	EI scan [min]	12,175	12,954	14,127	16,902	17,319	18,266	19,067	31,546	32,173	34,011	34,731	36,833	37,903	44,293									
	m/z	97,2 57,3 109,2 87,3 102,3 77,2 69,3 91,2 143,3	97,2 57,3 123,3 108,3	205,1 220,1 145,2 57,3	92,2 57,3 99,4 121,2 177,1	97,3 57,3 99,4 121,2 116,1 114,5	97,3 57,3 123,2 99,4 99,4 83,1 179,3 250,3	97,2 57,3 99,4 157,2 79,3 213,1	87,2 74,3 143,2 55,3 73,3 57,3 129,3 199,0 255,0	56,3 257,0 73,3 57,3 69,3 111,3 55,3 139,7 185,3 312,7	83,3 97,3 69,3 107,3	135,2 149,1 107,3	73,3 56,3 285,0 129,3 87,2 89,3 57,3 267,7 185,1 340,5 241,7	73,3 89,4 87,3 133,3 97,3 83,3 177,4	204,2 176,1 89,4 73,3 87,2 88,4 133,4 265,5									
1,2-Benz[a]anthraquinone												File 0085												
P ₁	Peak	1	2	3	4	5	6	7	8	9	10	11	12											
	EI scan [min]	12,262	13,032	14,148	16,966	17,378	18,408	19,123	31,669	32,335	34,2	34,704	37,218											
	m/z	97,3 57,3 99,4 109,2 102,2 67,4 91,2 79,3 143,2 129,0 163,3 214,4	97,3 57,3 123,2 180,1	205,1 220,2 145,1 57,3	97,2 57,3 99,4 121,2 83,2 91,3 79,3 177,3	97,2 57,3 99,4 121,2 79,3 116,2 214,6	97,2 57,3 123,2 83,3 69,4 137,0 109,0 179,4 250,5	97,2 57,3 99,4 79,2 93,2 123,0 179,2	87,2 74,3 97,4 55,3 143,3 83,2 109,2 59,3 255,0 298,3 199,0	56,3 250,3 73,3 129,3 219,1 224,5	83,2 97,3 69,3 55,3 111,2 206,5	135,2 73,3 107,2 89,3 206,5	73,3 89,3 56,3 117,3 103,3 129,3 285,0 267,6 340,4 185,1											

1,2-Benz[a]anthraquinone														File 0086													
Peak	1	2	3	4	5	6	7	8	9	10	11	12															
EI scan [min]	12,248	13,022	14,147	16,938	17,348	18,387	19,102	31,630	32,306	34,161	34,697	37,207															
m/z	97,3 57,3 109,2 99,4 67,2 91,2 79,1 143,1	97,3 57,3 123,2 179,4	205,1 220,1 145,2 57,3	97,2 99,4 57,3 121,1 83,4 79,3 214,3	97,3 57,3 99,4 121,2 214,5	97,3 57,3 12,2 83,3 69,3 111,2 179,1 250,3	97,2 53,3 123,2 179,2	87,2 74,4 55,3 97,3 69,2 81,2 143,0 255,2 298,2 198,9	56,3 257,1 73,3 239,6 129,3 219,2 185,2 312,6	83,3 97,2 69,3 55,3 111,4 61,3 57,3 149,2 224,3	135,2 73,3 89,3 107,2 149,1 206,5	73,3 89,3 285,0 59,3 117,3 133,4 185,3 340,2 267,8 267,3 241,0															
Benzanthrone														File 0088													
Peak	1	2																									
EI scan [min]	24,765	43,899																									
m/z	191,1 73,0 87,0 89,4 59,6 206,7	73,3 89,3 117,3 59,3 183,3 258,1 202,1																									
Benzanthrone														File 0089													
Peak	1																										
EI scan [min]	24,517																										
m/z	191,1 89,5 206,1 73,0 133,3 59,5 254,1																										
9,10-Anthraquinone														File 0091													
Peak	1	2																									
EI scan [min]	9,555	42,791																									
m/z	105,2 106,2 77,3 51,3 73,3	73,3 89,3 117,3 59,3 183,3 258,1 202,1																									
9,10-Anthraquinone														File 0092													
Peak	1	2	3	4	5	6																					
EI scan [min]	9,555	14,754	19,028	19,346	21,289	42,713																					
m/z	106,2 105,2 77,3 51,3 175,2	97,3 57,1 123,2 179,3	97,2 57,0 89,3 72,9 83,2 207,0	97,2 73,2 89,5 57,1 207,2	97,3 57,3 123,0 179,1	208,2 89,3 73,3 180,2 152,2 265,4																					
9,10-Phenanthrenquinone														File 0093													
Peak	1	2																									
EI scan [min]	9,553	12,899																									
m/z	106,2 105,2 77,3 51,4 206,8	79,3 108,3 73,4 89,1 165,1																									

P ₂	9,10-Phenanthrenquinone								File 0094									
	Peak	1	2	3														
	El scan [min]	9,533	12,906	15,892														
	m/z	106,2 105,2 77,3 51,4	79,2 108,2 107,4 77,1 73,3 91,3 89,3	97,3 57,2 89,3 73,3 123,1 179,7														
1,4-Naphtoquinone: Empty								File 0097				File 0098						
P ₁	2-Methyl-9,10-anthraquinone								File 0100									
	Peak	1	2	3	4	5	6	7	8	9	10	11	12	13	14			
	El scan [min]	11,109	11,635	12,311	13,688	16,148	16,602	17,409	18,287	31,702	33,674	34,451	36,537	37,549	44,525			
	m/z	102,2 97,2 57,3 104,2 99,4 67,3 214,4 163,2	97,2 99,4 57,3 109,2 79,3 67,3 143,2 214,3	97,2 57,3 123,2 180,2	205,1 220,1 145,1 57,3	97,2 99,4 57,3 83,3 121,2	97,2 99,4 57,3 121,2 79,3 214,5	97,2 57,3 123,2 83,2 153,2 179,2 250,3	97,2 57,3 99,4 97,3 123,2 91,2 179,3	56,3 256,9 57,3 73,3 129,3 239,6 83,3 312,2	97,3 83,3 69,3 111,3 61,3 55,3 224,6	135,2 107,2 57,3 206,4	56,3 284,9 129,3 73,3 267,7 83,3 340,4	97,3 83,3 69,3 111,3 55,3 61,3 252,8	165,2 222,28 9,4 194,2 133,3			
P ₂	2-Methyl-9,10-anthraquinone								File 0101									
	Peak	1	2	3	4	5	6	7	8	9	10	11	12	13	14			
	El scan [min]	11,062	11,597	12,288	13,667	16,117	16,562	17,376	18,222	31,665	33,637	34,440	36,503	37,519	44,501			
	m/z	102,2 97,2 57,3 99,4 67,3 214,5 163,2	97,3 99,4 57,3 109,2 67,3 102,3 79,3 143,1 214,4	97,2 57,3 123,2 180,2	205,2 220,1 145,2 57,3	97,2 57,3 99,4 121,2 180,3	97,2 57,3 9,4 121,2 214,5	97,2 57,3 123,2 153,1 83,2 179,2 250,3	97,2 57,3 99,4 79,3 123,2 157,2 123,2 93,3 179,3	56,3 257,0 129,3 73,3 239,7 185,3 312,4	83,3 97,3 69,3 111,3 55,3 61,3 224,5	135,2 107,2 57,3 206,5	56,3 284,9 129,3 73,3 83,3 69,3 71,3 340,4	97,3 83,3 69,3 111,3 61,3 55,3 252,7	165,1 222,2 89,4 194,2 73,3 265,5			
P ₁	5-Nitroacenaphthene								File 0103									
	Peak	1	2	3	4	5	6	7	8	9	10	11	12	13	14			
	El scan [min]	11,624	12,133	12,902	14,023	16,748	17,167	18,132	18,875	31,914	31,914	33,810	34,498	36,683	37,730			
	m/z	102,3 97,2 57,3 99,4 104,1 67,3 91,2 109,2 77,2 214,6 163,0	92,2 57,3 99,4 109,1 67,3 143,2 214,4	97,2 57,3 123,2 179,4	205,1 220,1 145,1 57,2	97,2 57,3 99,4 121,2 177,2	97,2 57,3 99,4 121,2 214,5	97,2 57,3 83,3 123,3 137,1 179,4 250,4	97,2 57,3 99,4 123,2 179,2	87,3 74,3 97,3 55,3 143,1 255,1 198,8	56,3 256,9 73,3 236,6 129,3 83,0 312,4	135,2 107,2 206,5	135,2 107,2 206,5	56,3 284,9 111,3 129,2 287,287, 2 340,2	97,2 73,3 83,3 89,4 69,3 55,3 111,3 61,3 175,4			
P ₂	5-Nitroacenaphthene								File 0104									
	Peak	1	2	3	4	5	6	7	8	9	10	11	12	13				
	El scan [min]	11,612	12,092	12,877	14,004	16,710	17,120	18,082	18,832	31,229	31,898	33,774	36,659	37,688				
	m/z	102,2 97,2 57,3 67,3 214,5 163,4	97,2 57,3 99,4 109,2 97,3 214,3	97,2 57,3 123,2 179,5	205,1 220,1 145,2 177,2 91,2	97,2 99,4 57,3 83,3 121,2 177,3	97,2 57,3 99,4 121,3 214,5	97,2 57,3 123,2 82,2 179,4 250,1	97,2 57,3 99,4 123,3 179,3	74,3 87,2 143,1 97,3 255,0 298,5	56,3 256,9 73,3 129,3 239,7 83,3 312,3	83,3 97,3 111,3 61,3 55,3 129,3 125,3 149,2 224,5	56,3 73,6 284,9 129,3 97,2 267,6 340,4	83,3 97,2 73,3 89,3 69,3 69,3 55,3 111,3 177,3				
P ₁	9-Nitrophenanthrene								File 0106									
	Peak	1																
	El scan [min]	24,471																
P ₂	9-Nitrophenanthrene								File 0107									
	Peak	1	2	3														

	El scan [min]	15,607	15,949	24,054									
	m/z	205,1 73,4 97,3	97,3 73,3 57,3 87,1 122,8 179,2	191,2 73,3 206,1									
9-Methylcarbazole					File 0109								
P ₁	Peak	1	2	3	4	5	6						
	El scan [min]	13,146	14,299	14,869	19,883	23,268	38,278						
	m/z	97,2 57,3 99,7 73,2 91,3 79,1 109,0 143,1	97,2 57,3 123,1 179,4	205,3 220,3 145,0 177,2 97,2 57,3	97,3 57,3 99,4 121,3	191,1 57,2 97,3 206,2 163,1	181,1 180,2 152,1 89,3						
1,6-Dinitropyrene					File 0517								
P ₁	Peak	1	2	3	4	5	6	7	8				
	El scan [min]	18,88	10,367	10,511	24,700	30,999	31,761	33,213	36,821				
	m/z	91,0 105,9 77,1 65,1 151,0	91,0 105,9 77,1 63,1 51,2	91,0 105,9 77,0 102,9 63,0	97,0 57,2 122,9 83,0 136,9 96,1 179,8	96,9 99,1 56,9 73,1 86,9 149,7	96,9 56,9 99,2 89,0 72,8 83,0 120,7 135,0	96,9 57,1 79,0 89,3 130,9 69,2	190,8 89,0 73,1 59,1 205,9				
2,7-Dinitrofluorene					File 00519								
P ₁	Peak	1	2										
	El scan [min]	26,028	36,820										
	m/z	128,0 127,4 72,9 89,2 101,8 58,9	89,2 73,0 87,0 190,8 59,1										
2,7-Dinitrofluorene					File 00520								
P ₂	Peak	1	2	3	4	5	6						
	El scan [min]	19,568	20,503	24,699	31,76	33,214	39,164						
	m/z	115,5 90,8 114,6 88,8 89,2 72,8 58,9	105,6 76,9 104,9 51,1 91,0 72,8 132,7	97,1 57,1 123,1	97,0 99,1 56,9 89,2 73,0 133,0 121,2 177,0	97,0 89,1 57,0 73,0 79,0 133,0 212,6	89,1 73,1 87,1 59,1 105,1 133,2						
2-Nitrofluorene					File 0522								
P ₁	Peak	1											
	El scan [min]	20,487											
	m/z	105,0 76,9 105,9 51,0											
2-Nitrofluorene					File 0523								
P ₂	Peak	1	2	3	4	5	6	7					
	El scan [min]	20,485	24,697	31,002	31,767	33,215	33,686	39,179					
	m/z	106,0 77,1 105,0 51,0	97,0 57,2 122,8	89,1 96,8 87,0 73,1 59,0	96,9 89,1 73,1 57,1 102,8 133,0	96,9 57,1 73,0 89,0 132,8	91,0 89,1 73,0 59,0 132,8 182,2	73,1 89,2 87,1 59,0 132,8 256,7					
3-Nitrofluoranthene					File 0525								
P ₁	Peak	1	2	3	4	5	6	7	8	9	10	11	
	El scan [min]	13,296	24,280	24,715	29,329	31,001	31,759	33,216	39,183	40,410	43,121	44,652	
	m/z	104,0 78,0	97,1 57,1 99,2	97,0 57,1 123,0	204,7 2219,9 57,0	97,1 57,1 99,1	97,0 57,1 99,2 121,0	97,0 57,1 99,1 79,0 122,8	56,1 73,1 256,7 129,1	97,0 83,0 55,1 61,1	56,2 73,1 89,1	89,1 73,1 59,0 55,1	

		102,9 51,1	109,0 67,0	81,0 180,0	177,8 91,0	79,0 121,0 107,0				69,1 111,0	129,1 284,4	96,9 132,9			
P ₂	3-Nitrofluoranthene								File 0526						
	Peak	1	2	3	4	5	6	7	8	9	10	11			
	El scan [min]	13,288	24,287	24,716	29,334	31,001	31,754	33,220	39,189	40,426	43,127	44,659			
	m/z	104,0 103,9 78,0 51,0 50,4	96,9 57,1 109,0 76,9 91,0	97,0 57,1 122,9 179,0	204,7 219,8 90,9 14,9 57,1	97,0 57,1 99,1 121,0	97,0 57,0 99,1 120,8 78,9 91,0	96,9 57,1 99,1 69,1 91,1 122,8	56,1 97,1 256,4 57,1 65,1 128,2	83,1 97,1 55,1 69,1 61,1 111,0	56,1 73,1 27,1 89,1 87,1 284,4 129,0	89,1 73,0 59,2 87,0 133,1			
P ₁	2-Nitrofluoranthene								File 0528						
	Peak	1	2	3	4	5	6	7	8	9	10	11	12	13	14
	El scan [min]	10,111	10,292	10,437	13,283	24,275	24,698	29,318	50,995	31,955	33,199	39,182	40,416	43,125	44,649
	m/z	91,0 106,0 77,1 65,1	91,0 106,0 105,1 77,0 79,0	91,0 105,9 105,0 77,0	103,9 78,1 103,0 77,0 51,1	97,2 97,0 109,0 99,1 102,0 90,9	97,0 57,1 122,9 81,1	204,9 219,6 57,1 144,9 91,1 176,8	97,0 99,2 57,1 120,9 90,9	97,0 57,0 99,2 121,0	97,0 57,1 79,0 99,2 131,0	56,1 73,0 256,6 89,2 129,0	83,0 55,1 97,0 61,1 69,1 89,1 73,1 111,0 133,0	56,1 73,0 284,6 89,1 129,2 339,5	89,1 73,1 59,1 87,1 133,1
P ₂	2-Nitrofluoranthene								File 0529						
	Peak	1	2	3	4	5	6	7	8	9	10	11	12	13	14
	El scan [min]	10,111	10,289	10,437	13,280	24,268	24,268	29,310	30,939	31,752	33,204	39,176	40,404	43,110	44,645
	m/z	91,0 106,1 77,0	91,0 106,0 105,1 77,0	91,0 105,9 77,0 102,9 63,0	104,0 78,0 103,0 51,1	97,0 57,1 108,8 99,1 79,0 90,9	97,0 57,1 80,0 122,9 179,1	204,9 205,7 219,8 144,7 105,0	96,9 99,1 57,0 89,1	97,0 57,1 99,2 89,0 73,0 120,8	97,0 57,1 99,2 79,1 90,9 130,7	56,1 73,1 256,6 57,1 55,1 129,1	83,0 96,9 55,1 69,1 61,1 73,1 111,0 133,2	56,1 73,1 89,1 57,0 128,9 284,6	89,1 73,1 87,0 59,0 133,0
P ₁	6-Nitrochrystene								File 0531						
	Peak	1	2												
	El scan [min]	20,448	33,60												
	m/z	105,9 77,0 105,2 51,0	91,1 73,1 89,1 86,8 59,0 103,1												
P ₂	6-Nitrochrystene								File 0532						
	Peak	1	2												
	El scan [min]	20,440	33,627												
	m/z	105,8 104,8 77,0 51,1 90,9	90,8 73,0 89,0 87,0 59,0 133,0 182,0												
P ₁	4-Nitrobiphenyl								File 0534						
	Peak	1	2	3	4	5	6	7	8	9	10	11			
	El scan [min]	13,267	24,352	24,689	29,295	30,984	31,739	33,197	39,164	40,398	43,097	11,642			
	m/z	104,0 103,0 78,1 77,0 51,1	97,1 57,0 99,2 56,3 78,9 78,9 143,0	97,0 57,1 123,0 81,0 179,6	204,8 219,6 57,0 132,9 176,7 89,1	97,0 57,1 99,2 120,9	97,0 57,1 99,2 120,8	96,9 57,0 99,2 79,1 131,1	73,0 56,1 89,0 256,6 103,0 239,4	83,0 97,0 69,0 89,1 61,1 55,1 132,9	89,2 73,0 87,0 6,1 59,0 117,0 284,4	89,1 73,1 87,0 59,1 32,9			
P ₂	4-Nitrobiphenyl								File 0535						
	Peak	1	2	3	4	5	6	7	8	9	10	11			

	El scan [min]	13,258	24,246	26,800	29,885	30,999	31,735	33,189	39,159	40,391	43,108	44,637				
	m/z	104,0 78,1 103,0 57,0	96,9 57,1 108,9 77,0 99,0 67,0	97,0 57,1 122,9 179,0	204,7 219,8 205,7 128,8 90,8	97,0 57,1 99,2 73,0 89,0 83,1 78,9 121,2	96,9 57,1 99,1 89,1 79,1 156,8	97,0 57,1 99,2 79,1 156,8	73,1 56,0 89,2 256,6 129,0	83,1 89,1 155,2 96,9 61,1 73,1 133,1	73,0 89,1 87,0 56,1 133,0 284,5	89,1 73,1 59,1 87,0 33,0				
P ₁	6-Nitrobenzo[a]pyrene								File 0537							
	Peak	1	2													
	El scan [min]	20,411	28,449													
	m/z	77,1 105,9 104,7 51,0	79,0 108,0 77,1 107,1 89,0													
P ₂	6-Nitrobenzo[a]pyrene								File 0538							
	Peak	1	2	3												
	El scan [min]	20,406	24,670	28,444												
	m/z	105,0 104,0 76,9 51,1	97,0 57,0 122,7 73,1	79,0 107,9 77,0 107,0 132,5												
P ₁	7-Nitrobenz[a]anthracene								File 0540							
	Peak	1	2	3	4	5	6	7								
	El scan [min]	13,246	20,396	28,432	36,720	38,480	40,233	42,157								
	m/z	103,8 91,0 103,0 78,0 91,9 51,0 65,0	105,0 105,9 77,0 51,2 50,1 78,2	79,1 108,0 76,9 88,9	89,0 73,1 86,9 67,0 190,9 133,2	89,1 87,0 73,0 57,2 133,1	89,1 73,0 57,2	89,1 73,1 59,1 87,0								
P ₂	7-Nitrobenz[a]anthracene								File 0541							
	Peak	1	2	3	4	5	6	7	8							
	El scan [min]	13,243	20,387	24,663	28,425	36,713	38,488	40,239	42,150							
	m/z	103,9 103,0 90,9 78,1 91,7 63,0	105,0 105,9 77,0 57,1	97,0 57,0 122,7 80,6	79,0 107,9 107,3 89,0 77,1 72,9 106,6	89,2 57,0 73,1 59,1 86,9 190,8 132,9	89,2 73,0 57,2	89,0 73,1 86,9 57,1 71,1 59,1 133,0	89,1 73,0 59,0							
P ₁	9-Nitroanthracene								File 0543							
	Peak	1	2	3	4	5	6	7	8	9	10	11	12	13	14	15
	El scan [min]	10,013	10,97	10,344	13,199	24,218	24,696	29,251	30,963	31,721	33,180	39,158	40,394	43,102	44,633	53,568
	m/z	91,0 106,0 77,1 65,1	91,0 105,9 77,0 78,0 102,9	91,0 105,9 105,0 77,1	104,0 78,1 103,0 51,1	97,0 57,1 99,1 108,9 67,2	97,0 57,1 123,0 89,1 69,1 137,0	204,8 219,7 144,8 176,8 97,0	96,9 57,1 99,2 79,0 55,0 120,8	97,0 57,1 99,2 121,0 79,0	97,0 57,1 79,1 99,2	56,1 73,0 57,1 55,2 256,4 129,0	97,0 83,1 55,2 69,1 111,0	56,1 73,1 57,1 82,0 129,1 284,5	89,0 73,1 83,0 96,9	89,1 73,1 207,8 179,8 151,8
P ₂	9-Nitroanthracene								File 0544							
	Peak	1	2	3	4	5	6	7	8	9	10	11	12	13	14	15
	El scan [min]	10,000	10,184	10,331	13,192	24,214	24,695	29,251	30,976	31,727	33,178	39,161	40,391	43,109	44,637	53,562
	m/z	91,0 105,9 77,1	91,0 105,9 104,9 77,0	91,0 106,0 105,1 77,1	103,9 78,1 103,0 77,1	97,0 57,1 99,1 108,9	97,0 57,1 123,0 81,0	204,8 219,7 144,9 90,9	97,0 57,1 99,2 120,6 79,0	97,0 57,1 99,1 79,1 120,7	97,0 57,1 79,0 99,1	56,1 73,0 256,0 129,1 86,9	83,1 97,1 55,2 69,1	56,1 73,0 89,1 129,1	89,1 73,1 55,1 97,1	89,1 179,9 207,9 73,0 151,9
P ₁	4-Nitropyrene								File 0546							
	Peak	1	2	3	4	5	6	7	8	9	10	11	12	13	14	

	El scan [min]	9,995	10,179	10,326	13,182	24,203	24,681	29,241	30,961	31,719	33,174	39,159	40,386	43,103	44,630	
	m/z	91,0 106,0 78,0 65,1	91,0 105,9 105,1 77,1 51,1	91,0 105,9 105,0 77,0	103,9 78,0 103,0	97,0 57,1 99,1 108,9 102,0 79,0	97,0 57,1 122,9 179,8	204,8 213,8 144,9 91,0 114,8	97,0 57,1 99,1 120,8	69,9 57,0 99,1 121,0 83,1 79,1	97,0 57,1 99,2 79,0 83,1	56,1 73,0 256,6 129,1 89,1	83,0 97,0 55,2 69,0 61,1	56,1 73,0 57,2 55,0 89,1 284,4	89,1 73,0 83,0 87,1 97,0 55,1	
P ₂	4-Nitropyrene								File 0547							
	Peak	1	2	3	4	5	6	7	8	9	10	11	12	13	14	
	El scan [min]	10,002	10,187	10,332	13,181	24,197	24,680	29,240	30,963	31,713	33,168	39,164	40,394	43,107	44,636	
P ₁	2-Nitropyrene								File 0549							
	Peak	1	2	3	4	5	6	7	8	9	10	11	12	13	14	15
	El scan [min]	9,960	10,144	10,295	13,159	24,224	24,820	29,250	30,997	31,762	33,234	38,593	39,231	40,466	43,200	44,704
P ₂	2-Nitropyrene								File 0550							
	Peak	1	2	3	4	5	6	7	8	9	10	11	12	13	14	
	El scan [min]	9,942	10,130	10,278	13,148	24,226	24,833	29,241	30,998	31,770	33,248	39,234	40,477	43,215	44,702	
P ₁	1-Nitropyrene								File 0552							
	Peak	1	2	3	4	5	6	7	8	9	10	11				
	El scan [min]	13,166	24,180	24,661	29,213	30,949	31,702	33,159	39,143	40,368	43,086	44,620				
P ₂	1-Nitropyrene								File 0553							
	Peak	1	2	3	4	5	6	7	8	9	10	11				
	El scan [min]	13,161	24,176	24,659	29,215	30,948	31,700	33,160	39,144	40,367	43,082	44,620				
P ₁	2-Nitronaphthalene: Empty								File 0555				File 0556			
	1-Nitronaphthalene								File 0558							
	Peak	1	2													
P ₁	El scan [min]	20,284	42,356													
	m/z	105,39 105,0 77,0 51,1	89,1 114 73,0 126,8													
P ₂	1-Nitronaphthalene								File 0559							
	Peak	1	2													
P ₂	El scan [min]	20,278	42,347													

	m/z	77,0 105,0 106,0 51,2	89,1 115,0 73,1 126,38														
P ₁	6H-Benzo[c,d]pyren-6-one								File 00123								
	Peak	1	2	3	4	5	6	7	8	9	10	11	12	13	14	15	
	El scan [min]	9,939	10,120	10,268	13,119	20,272	24,646	28,306	29,184	30,969	31,698	33,151	39,124	39,347	40,343	43,056	
P ₂	6H-Benzo[c,d]pyren-6-one								File 00124								
	Peak	1	2	3	4	5	6	7	8	9	10	11	12	13	14	15	
	El scan [min]	9,659	9,895	10,188	13,093	20,254	24,156	24,620	29,160	30,904	31,650	33,105	39,109	40,332	43,035	44,581	
	m/z	90,9 105,9 91,9 65,0	90,9 105,9 76,9	91,0 105,8 91,9 105,0 72,0	104,0 78,0 102,9 76,9	105,9 105,0 77,0 51,1	97,0 122,9 83,0 122,9	57,1 107,8 77,1 106,9	204,8 219,8 144,6 57,1	97,0 57,0 99,2 88,9 120,8	96,9 57,1 99,1 120,9	69,9 57,1 122,8	56,1 89,1 256,4 129,0	89,1 59,1 87,0	83,0 55,1 96,1 69,1	73,0 56,1 89,1 87,0	
	1,3-Dinitropyrene: Empty					File 00126					File 00127						
P ₁	9-Fluorenone-d ₈								File 00129								
	Peak	1	2														
	El scan [min]	7,851	45,878														
	m/z	91,0 92,0 65,1	188,0 160,0 158,0 156,0 132,0 80,2														
P ₂	9-Fluorenone-d ₈								File 00130								
	Peak	1	2	3													
	El scan [min]	7,819	24,590	45,871													
	m/z	91,0 91,9 65,1 63,0	97,0 57,0	188,0 160,0 158,0 156,0 132,0													
P ₁	2-Nitrobiphenyl-d ₉								File 00132								
	Peak	1	2														
	El scan [min]	7,821	43,767														
	m/z	91,0 91,9 65,1	160,0 122,0 180,0 150,0 190,0														
P ₂	2-Nitrobiphenyl-d ₉								File 00133								
	Peak	1	2	3													
	El scan [min]	7,817	24,578	43,760													
	m/z	91,0 92,0 63,1	97,0 57,1 123,0	160,0 122,0 180,0 150,0 189,9													
P ₁	AG std place 5								File 00135								
	Peak	1	2	3	4												
	El scan [min]	9,956	20,186	28,204	53,243												
	m/z	90,9 106,0 64,9	105,0 106,0 77,0 51,2	79,1 108,0 77,0 51,2	207,8 151,8 179,8 89,1 73,1												
P ₂	AG std place 5								File 00136								
	Peak	1	2	3	4	5	6										

	El scan [min]	9,947	20,176	24,568	28,198	29,093	53,238				
	m/z	91,0 105,9 92,0 65,1	105,0 77,0 105,9 51,1 50,1	96,9 57,0 122,9	79,1 108,0 77,1 107,0	204,7 89,0 73,1 219,8 59,0	207,8 179,9 151,8 89,1 73,1				
P ₁	AG std place 6							File 00138			
	Peak	1	2	3	4	5	6				
	El scan [min]	9,937	10,113	10,254	13,051	20,163	28,183				
	m/z	91,0 105,9 92,0 77,0	90,9 105,9 91,9 105,0	90,9 105,9 92,0 105,1 77,0	104,0 77,8 78,0 103,0 91,0	105,0 106,0 77,0 51,2	79,0 77,1 108,0 107,0				
P ₂	AG std place 6							File 00139			
	Peak	1	2	3	4	5	6	7	8	9	
	El scan [min]	9,930	10,108	10,251	13,047	20,153	24,559	28,170	29,073	33,040	
	m/z	91,0 105,9 91,9	91,0 105,9 92,1 104,9 77,0	91,0 106,0 105,0 77,0	103,9 78,0 91,1 103,0	105,0 105,9 77,0 51,1	97,0 57,0 123,0 80,9	79,0 77,1 108,0 106,9	204,7 219,7 144,8 90,8	89,0 96,9 59,1 72,9	
P ₁	AG std place 7							File 00141			
	Peak	1	2	3							
	El scan [min]	20,138	28,159	51,189							
	m/z	105,0 106,0 77,1 51,1	78,9 108,0 76,8 77,1	89,1 73,1 87,0 59,1							
P ₂	AG std place 7							File 00142			
	Peak	1	2	3	4	5	6				
	El scan [min]	20,128	24,453	28,148	29,058	31,575	33,025				
	m/z	105,9 105,0 77,0 51,1	79,0 57,1 122,8	79,0 107,9 107,0 89,0 76,9	204,7 219,9 86,8 57,1	96,8 89,2 57,0 99,2 73,1	96,8 89,2 57,0 99,2 73,1				
P ₁	AG std place 8							File 00144			
	Peak	1	2	3							
	El scan [min]	9,919	20,117	28,183							
	m/z	91,0 106,0 65,0	105,0 105,9 77,1 51,1	203,8 89,1 175,7 73,1							
P ₂	AG std place 8							File 00145			
	Peak	1	2	3	4	5					
	El scan [min]	20,110	24,533	29,041	33,015	56,169					
	m/z	106,0 77,0 105,0 51,1	96,9 57,1 122,8	204,8 89,0 144,8 219,36	97,0 89,2 87,2 73,1 57,2	203,8 89,1 175,8 73,1					
P ₁	AG std place 9							File 00147			
	Peak	1	2	3	4	5	6	7	8	9	
	El scan [min]	12,949	24,526	29,030	30,814	31,551	33,007	39,018	40,231	45,726	
	m/z	104,0 103,0 78,1 76,9	96,9 57,1 80,9 122,9	204,8 73,1 89,1 219,5	96,9 89,1 73,0 57,2	97,0 89,1 73,0 57,2	89,1 57,1 73,1 89,0	89,1 73,0 59,1	89,1 73,1 59,1	179,8 151,8 151,0 149,8	
P ₂	AG std place 9							File 001848			

	Peak	1	2	3	4	5	6	7	8	9		
	El scan [min]	23,989	24,524	29,028	30,812	31,553	33,006	39,016	40,228	45,726		
	m/z	97,0 56,9 99,2 108,9	97,0 57,2 123,0	204,7 220,0 144,9 89,0	97,0 57,0 99,2 73,1 89,1	96,9 57,0 99,2 89,2	96,9 57,1 99,2 89,1	73,1 89,1 87,0 59,1 56,1	89,1 73,1 59,1 87,0	179,8 151,8 150,9 89,1 125,9		
	AG std place 10								File 001850			
P ₁	Peak	1	2	3	4	5	6	7	8	9	10	
	El scan [min]	9,896	12,985	20,076	24,519	28,087	29,018	31,510	32,995	39,008	40,219	
	m/z	91,0 106,0 92,0 65,2	103,9 78,0 103,0 51,1 90,9	105,9 105,0 77,0 51,1	97,0 57,1 122,9 83,0	79,0 108,0 77,0 107,0	204,7 219,9 89,2 73,0	131,9 104,0 103,0 78,0 77,0	97,0 57,1 99,1 79,1	73,1 56,1 89,1 59,1 87,1	89,1 73,1 83,0 59,1 97,0	
	AG std place 10								File 001851			
P ₂	Peak	1	2	3	4	5	6	7	8	9		
	El scan [min]	12,979	20,067	24,517	31,505	32,989	39,003	40,215	42,911	44,461		
	m/z	103,9 78,0 102,9 77,0 51,1	106,0 105,0 77,0 51,0 50,0 78,0	97,0 57,1 81,0 122,9	131,9 104,0 103,0 78,0	97,0 57,1 99,1 79,0	73,1 56,1 89,1 86,9 59,1	89,1 83,0 73,1 55,1 97,1	73,1 89,1 87,0 59,1	89,1 73,0 87,0 59,1		
	AG std place 11								File 001853			
P ₁	Peak	1	2	3	4	5	6	7	8			
	El scan [min]	9,226	9,501	11,197	11,929	24,498	28,353	32,973	56,646			
	m/z	57,0 71,8 89,0 266,4	57,0 94,8 73,0 84,7	59,0 57,0 115,1	85,0 57,0 54,8 72,8	97,0 57,0 83,0 69,1 122,8 179,1	71,2 89,1 73,1 86,9 57,1	97,0 89,1 73,1 86,9 57,1	164,8 122,8 193,8 89,1			
	AG std place 11								File 001854			
P ₂	Peak	1	2	3	4	5	6	7				
	El scan [min]	9,217	9,495	11,195	11,928	24,494	32,974	56,643				
	m/z	56,9 71,9 72,9 88,9 132,7	57,2 99,7 85,0 72,2	59,1 57,1 56,1 115,0	85,0 57,1 73,1	91,0 57,0 122,9 83,1	82,2 968 57,1 73,1	164,9 221,8 193,8 89,1				
	AG std place 12								File 001856			
P ₁	Peak	1	2	3								
	El scan [min]	7,825	8,529	10,863								
	m/z	91,0 91,9 63,1	58,1 57,0 90,9 71,1 100,0	59,1 55,0 73,1 57,0								
	AG std place 12								File 001857			
P ₂	Peak	1	2	3	4							
	El scan [min]	7,823	24,482	28,965	32,960							
	m/z	91,0 92,0 63,1	97,0 57,0 123,1 183,0	204,7 72,9 88,9 144,8 59,0	89,1 97,0 73,1 87,0 57,1 59,1							
	AG std place 13								File 001859			
P ₁	Peak	1	2	3	4	5						
	El scan [min]	9,811	10,920	11,510	20,001	28,006						
	m/z	90,9 92,0 105,9 65,0	59,1 55,1 73,1 90,9	69,0 90,9 87,1 92,0 56,1 84,0	105,0 106,0 77,0 51,1 50,1 74,0	79,01 08,0 107,0 77,1						
	AG std place 13: Empty								File 001860			

AG std place 14		File 001862						
P ₁	Peak	1	2	3				
	EI scan [min]	9,820	19,976	27,989				
	m/z	90,9 106,0 92,0 65,0	106,0 105,0 77,1 51,1	79,1 108,0 106,9 76,9 89,0				
AG std place 14		File 001863						
P ₂	Peak	1	2	3	4	5	6	
	EI scan [min]	9,804	19,973	24,450	27,984	28,926	32,924	
	m/z	90,9 105,8 92,0 65,1	104,9 106,0 77,1 51,1	97,0 57,1 81,0 122,9	79,0 77,0 108,0 107,0 89,1	204,9 219,9 89,0 73,0 149,9	96,9 73,0 59,1 89,1	
AG std place 15		File 001865						
P ₁	Peak	1	2	3	4	5		
	EI scan [min]	12,841	24,440	28,912	32,911	40,146		
	m/z	103,8 103,0 88,9 77,2 72,8	97,0 57,0 122,9 83,0	204,7 89,0 219,7 73,1	73,2 89,1 96,8 87,1 57,0	89,1 73,0 97,1 59,1 133,0		
AG std place 15		File 001866						
P ₂	Peak	1	2	3	4	5	6	7
	EI scan [min]	12,824	24,143	28,905	30,723	31,460	32,911	40,137
	m/z	103,8 103,1	97,0 57,1 122,9 83,0	204,8 220,9 58,9 144,7	97,1 89,1 72,9 59,0	97,0 89,2 99,0 73,0 59,1	96,9 57,1 89,1 73,1	89,1 73,0 59,1 87,0 133,1

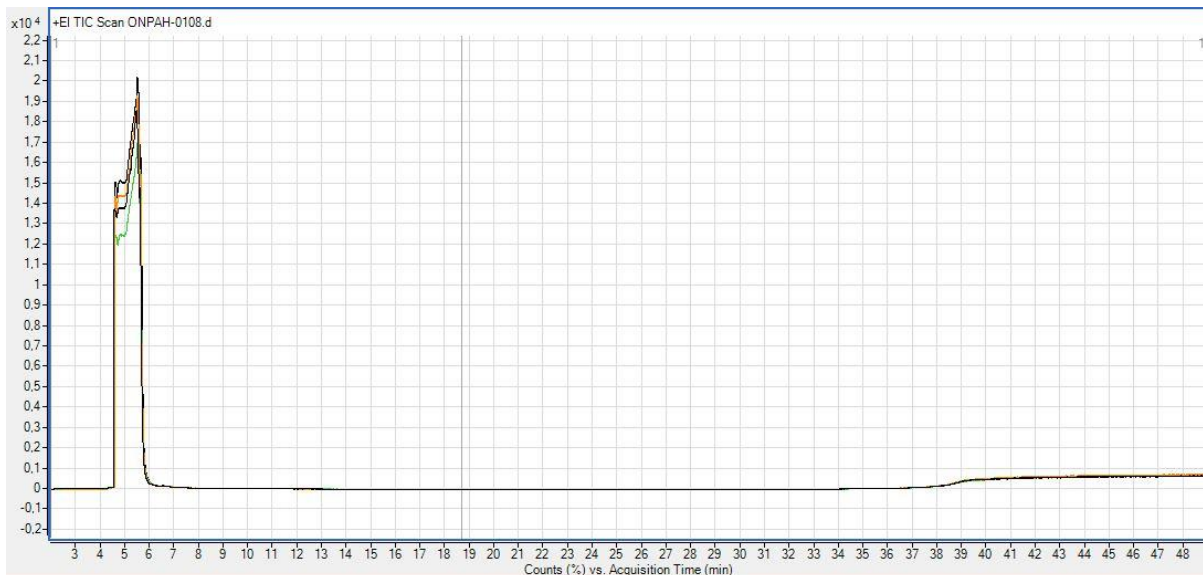


Figure 25: Chromatogram of four method blanks displayed on top of each other (file ONPAH-0078, ONPAH-0081, ONPAH-0084 and ONPAH-0108)

Appendix III

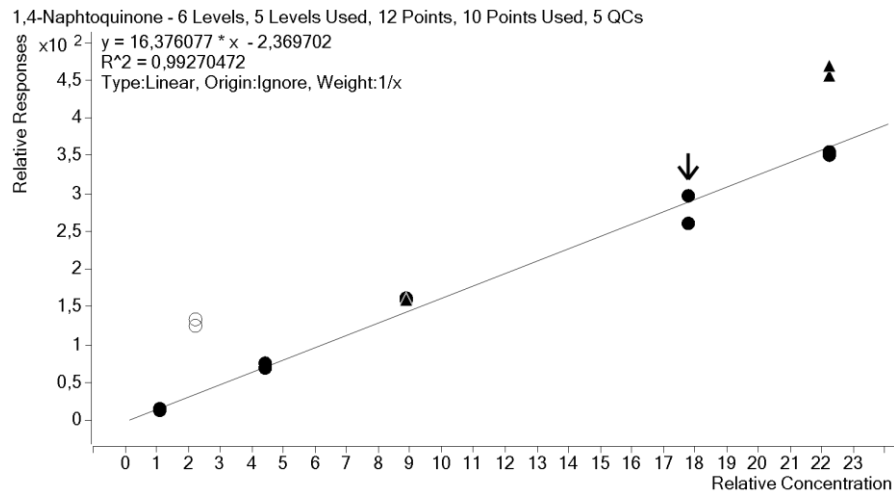


Figure 26: Calibration curve for 1,4-Naphtoquinone

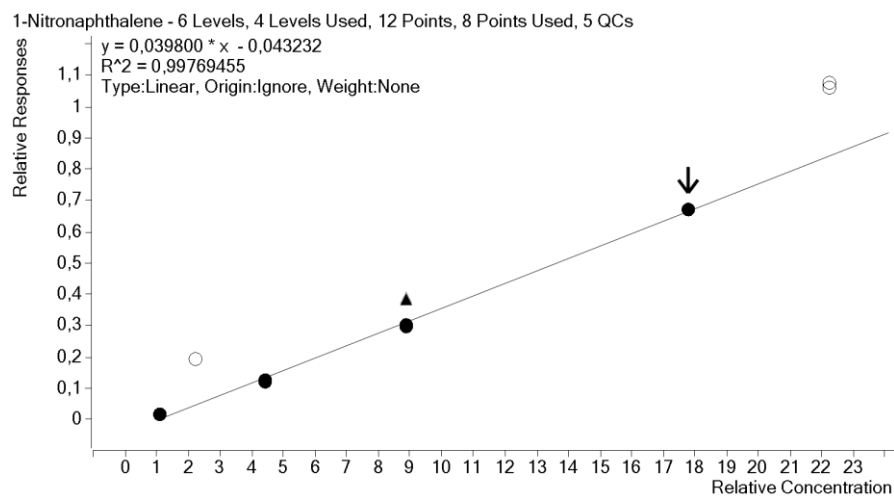


Figure 27: Calibration curve for 1-Nitronaphtalene

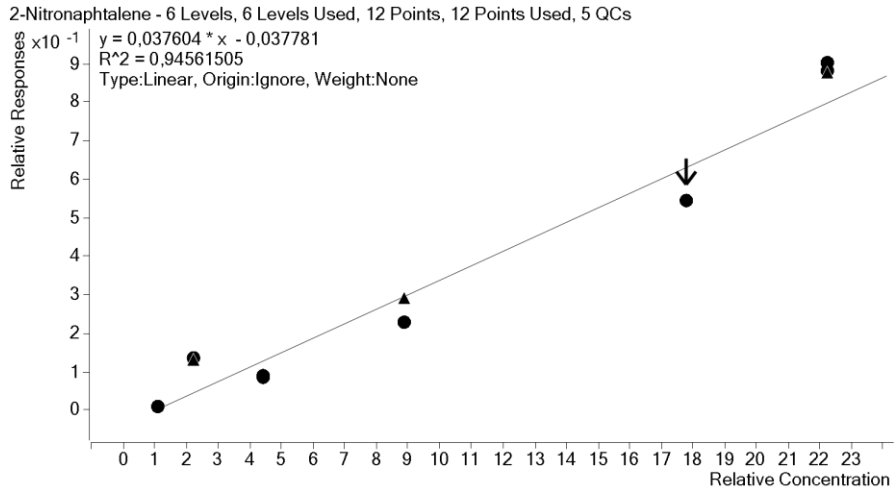


Figure 28: Calibration curve for 2-Nitronaphtalene

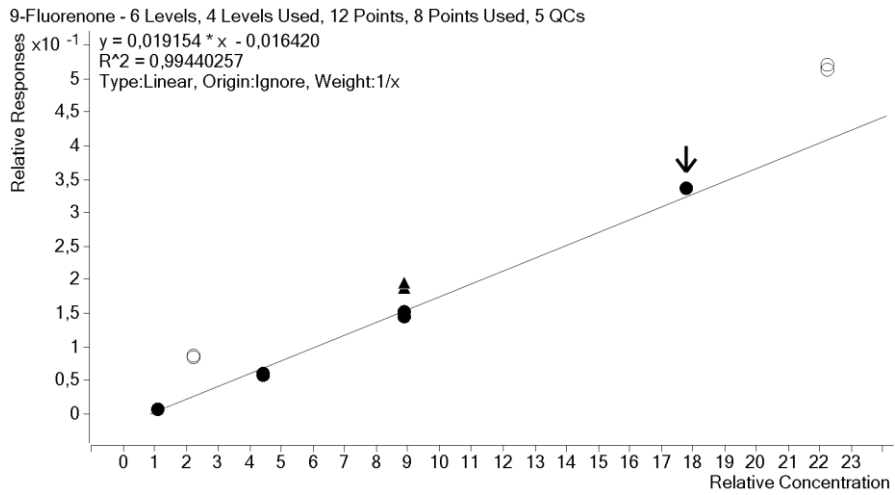


Figure 29: Calibration curve for 9-Fluorenone

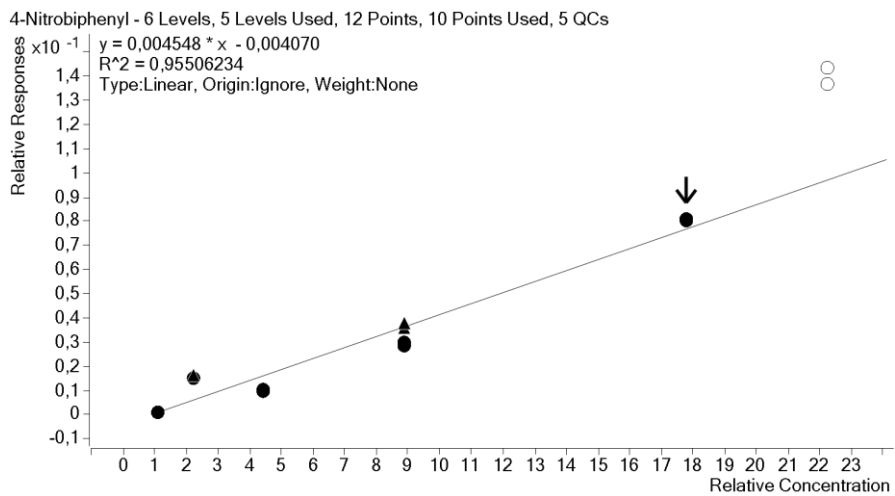


Figure 30: Calibration curve for 4-Nitrobiphenyl

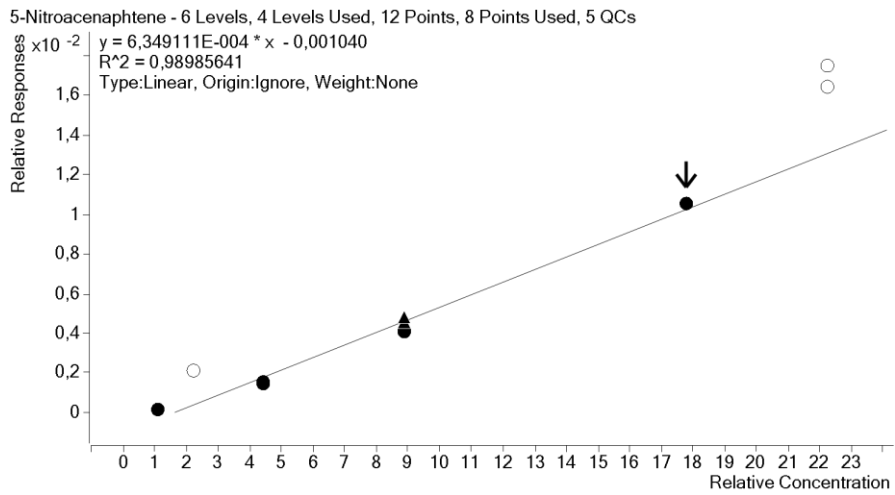
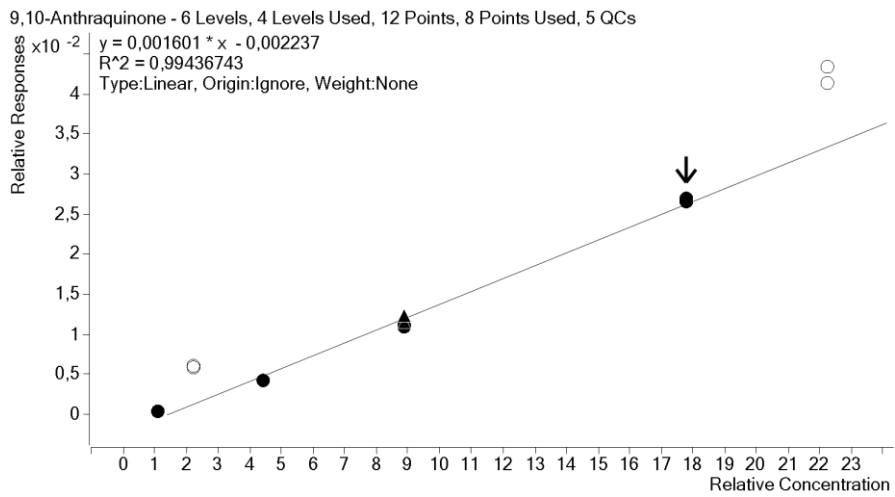


Figure 31: Calibration curve for 5-Nitroacenaphthene



Figur 32: Calibration curve for 9,10-Anthraquinone

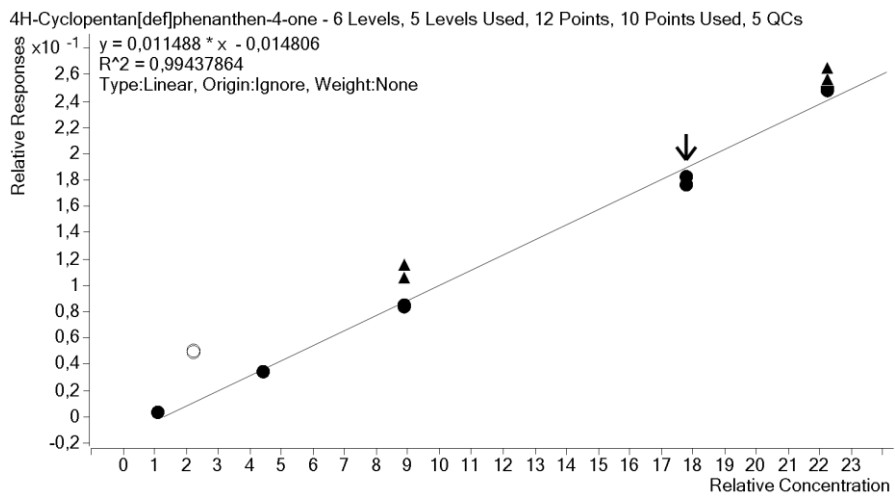


Figure 33: Calibration curve for 4H-Cyclopentan[def]phenanthen-4-one

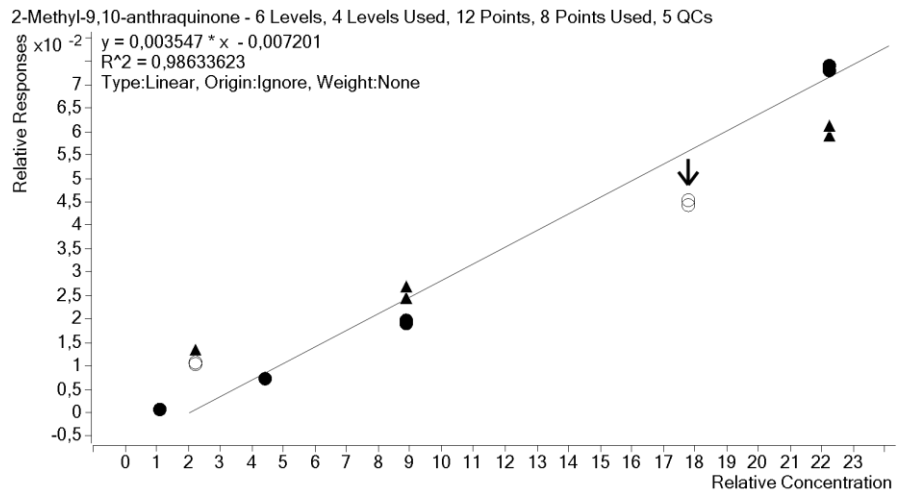


Figure 34: Calibration curve for 2-Methyl-9,10-Anthraquinone

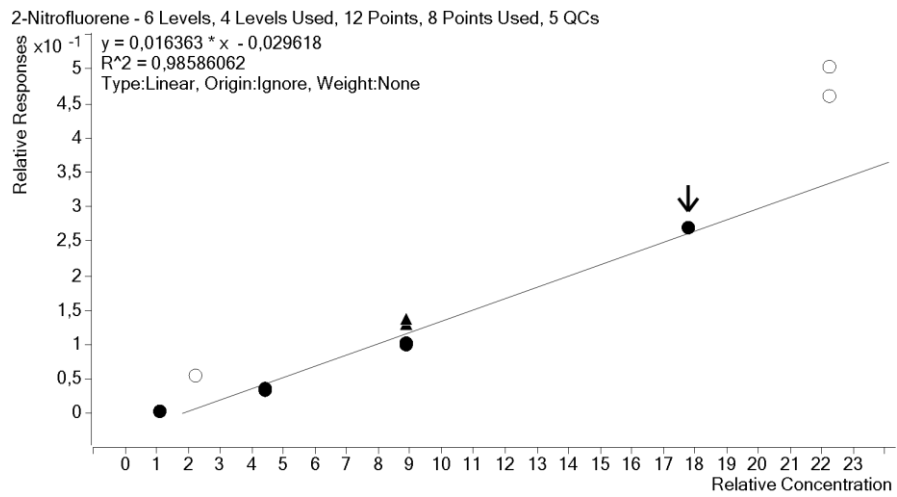


Figure 35: Calibration curve for 2-Nitrofluorene

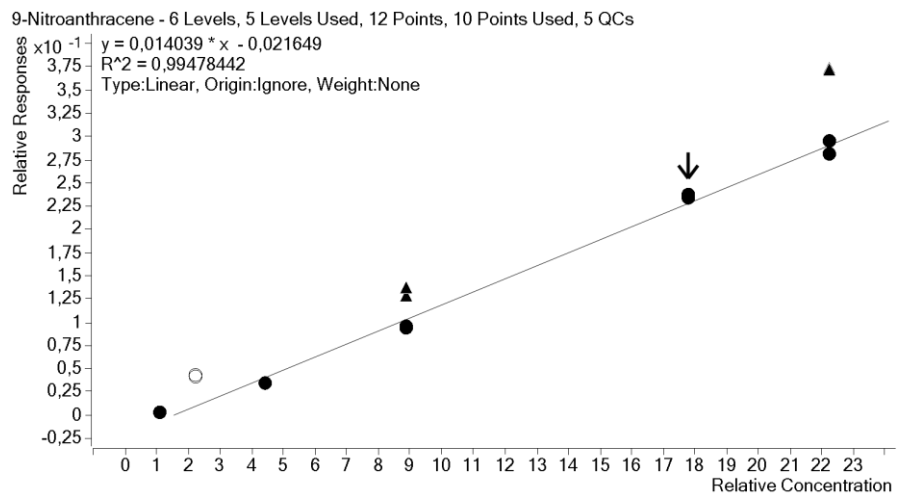


Figure 36: Calibration curve for 9-Nitroanthracene

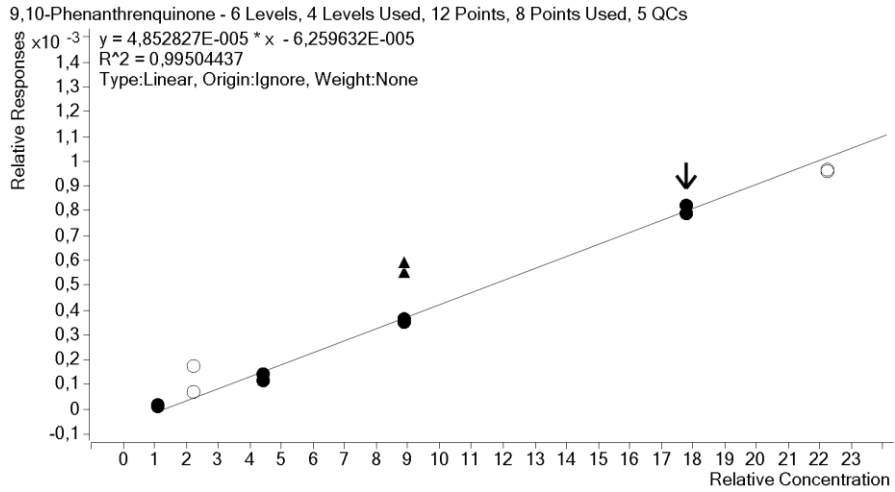


Figure 37: Calibration curve for 9,10-Phenanthrenquinone

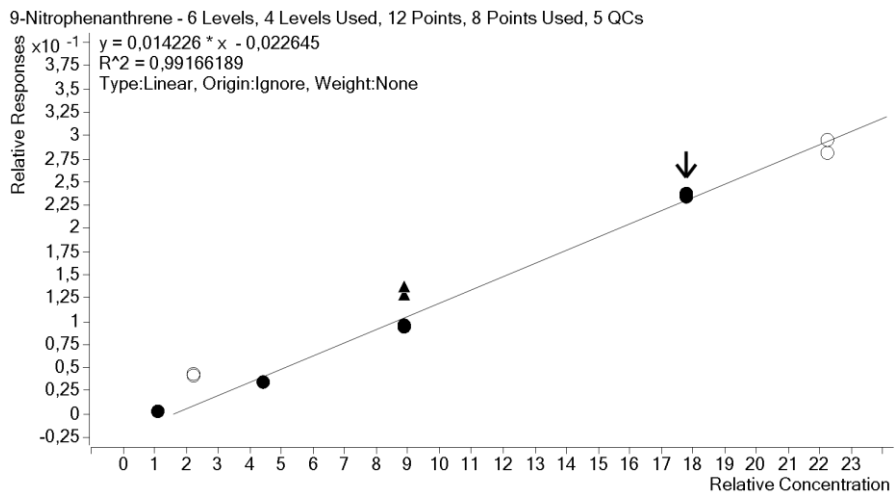


Figure 38: Calibration curve for 9-Nitrophenanthrene

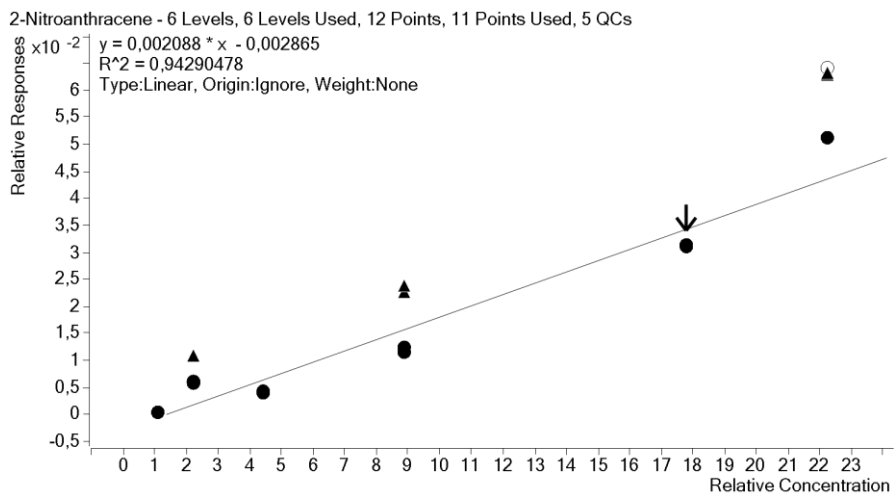


Figure 39: Calibration curve for 2-Nitroanthracene

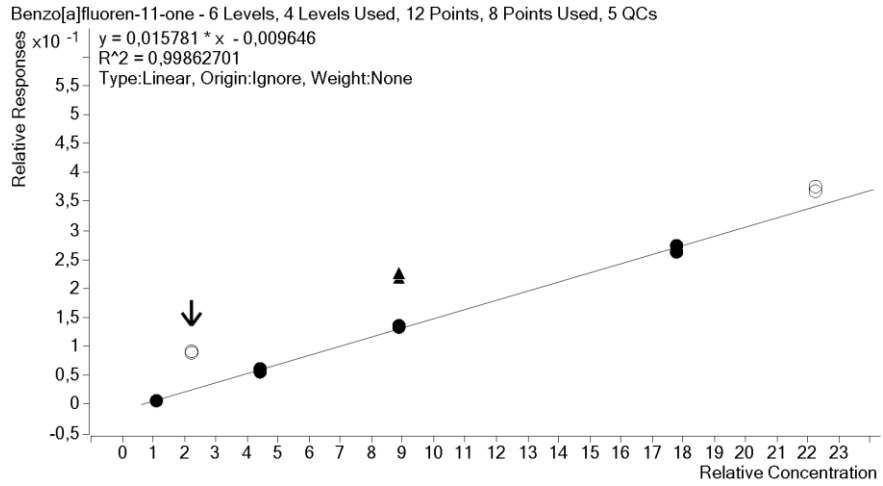


Figure 40: Calibration curve for Benzo[a]fluoren-11-one

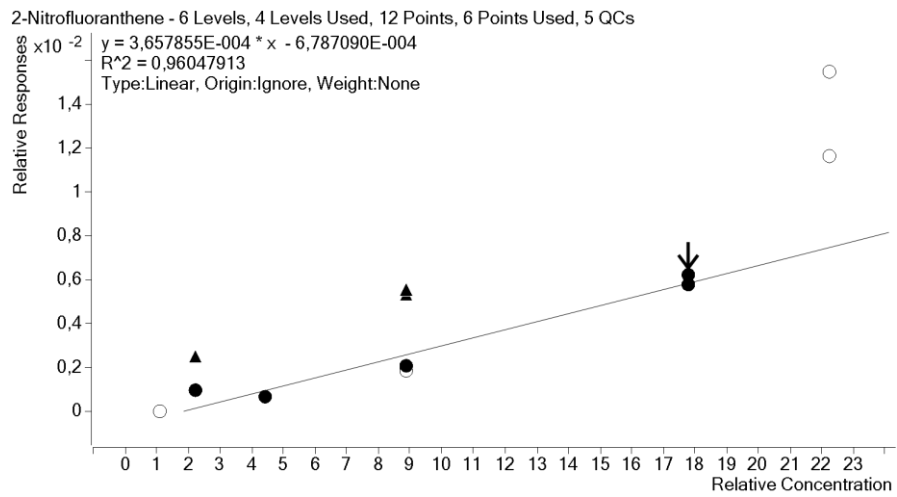


Figure 41: Calibration curve for 2-Nitrofluoranthene

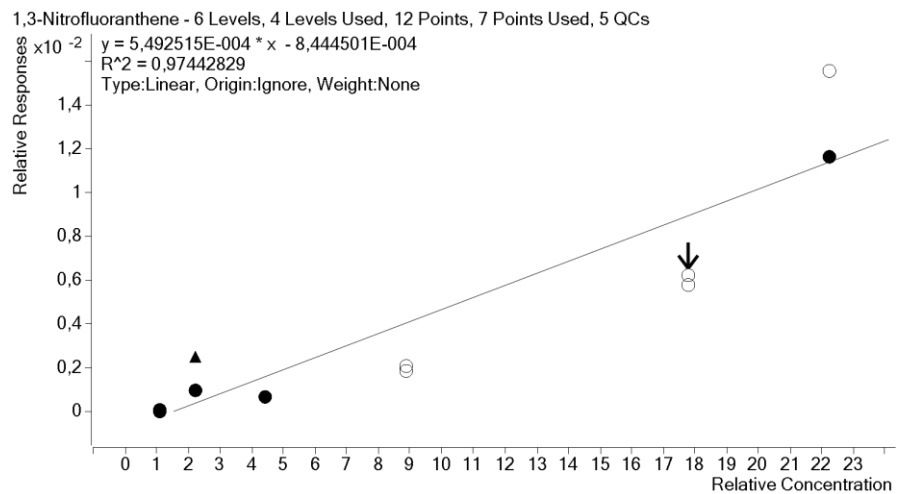


Figure 42: Calibration curve for 3-Nitrofluoranthene

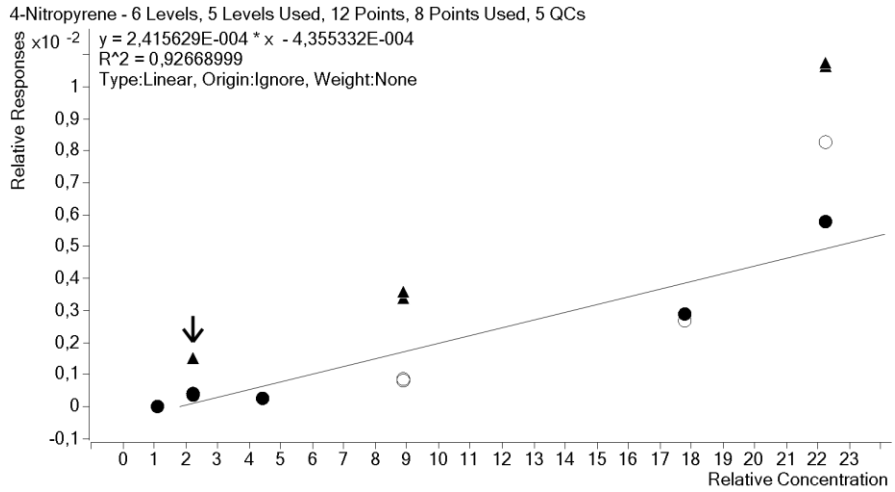


Figure 43: Calibration curve for 4-Nitropyrene

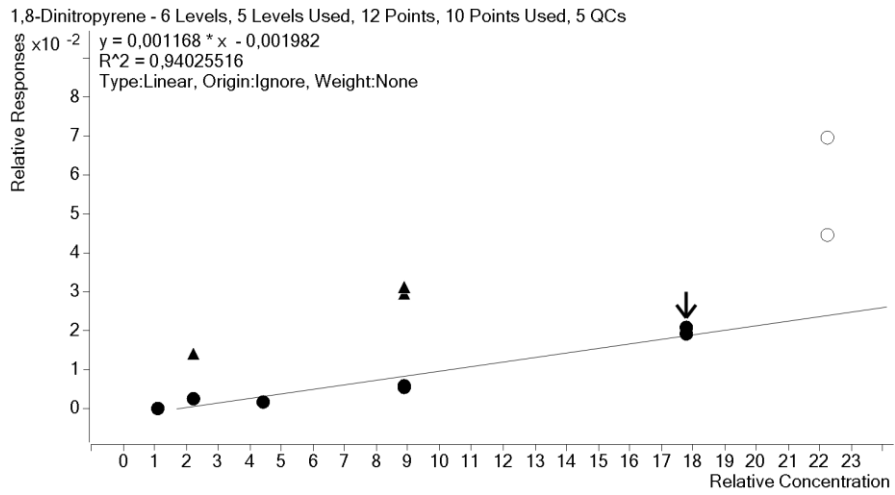


Figure 44: Calibration curve for 1,8-Dinitropyrene

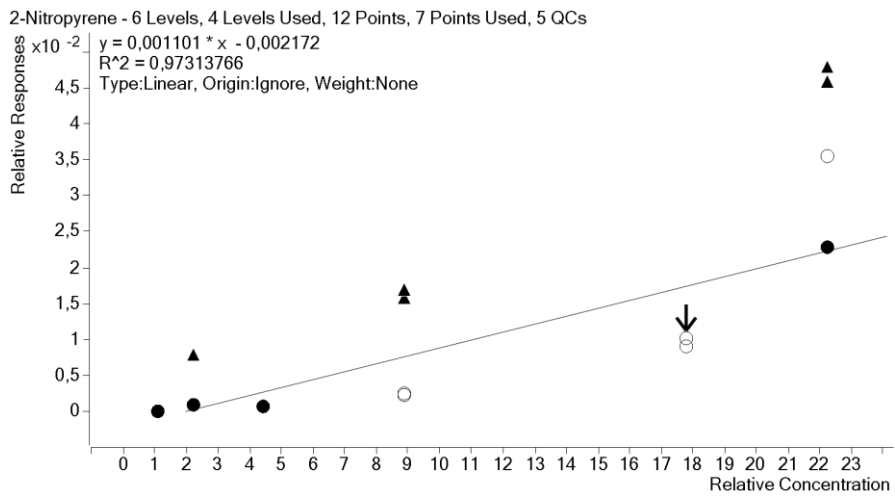


Figure 45: Calibration curve for 2-Nitropyrene

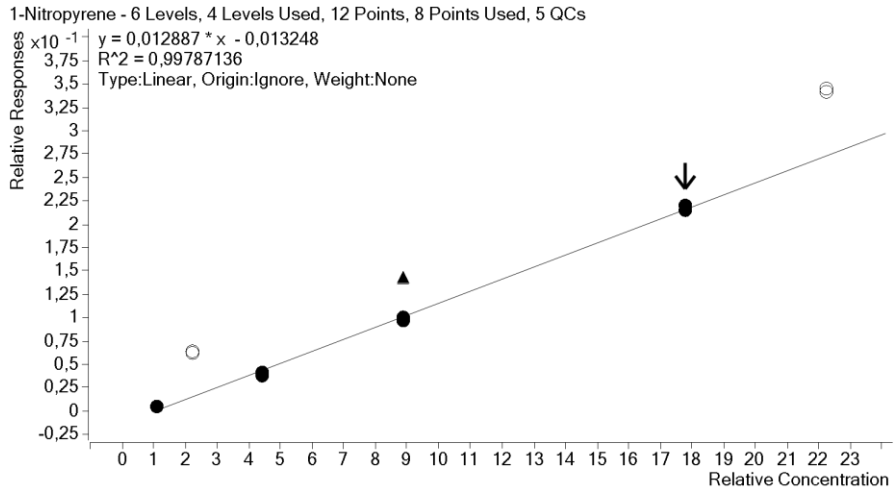


Figure 46: Calibration curve for 1-Nitropyrene

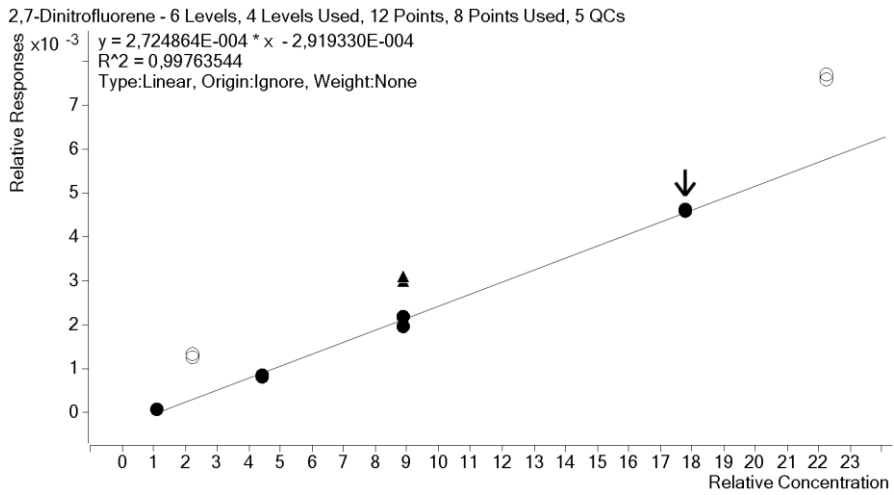


Figure 47: Calibration curve for 2,7-Dinitrofluorene

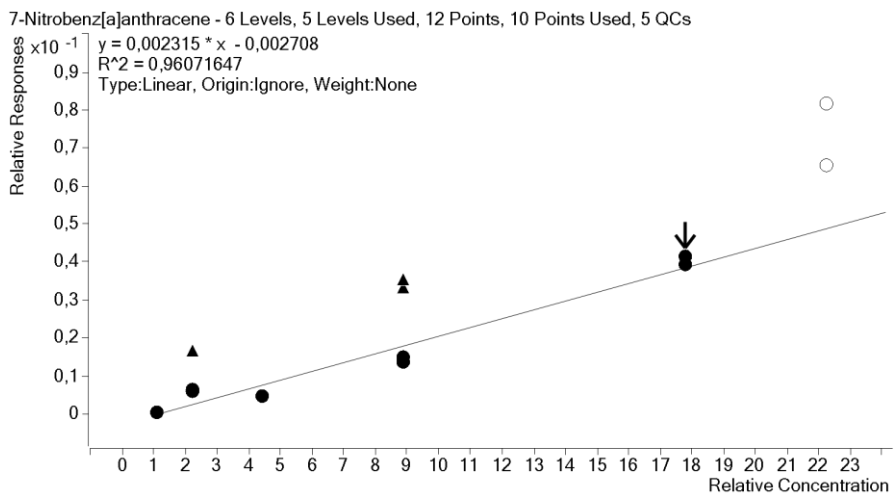


Figure 48: Calibration curve for 7-Nitrobenz[a]anthracene

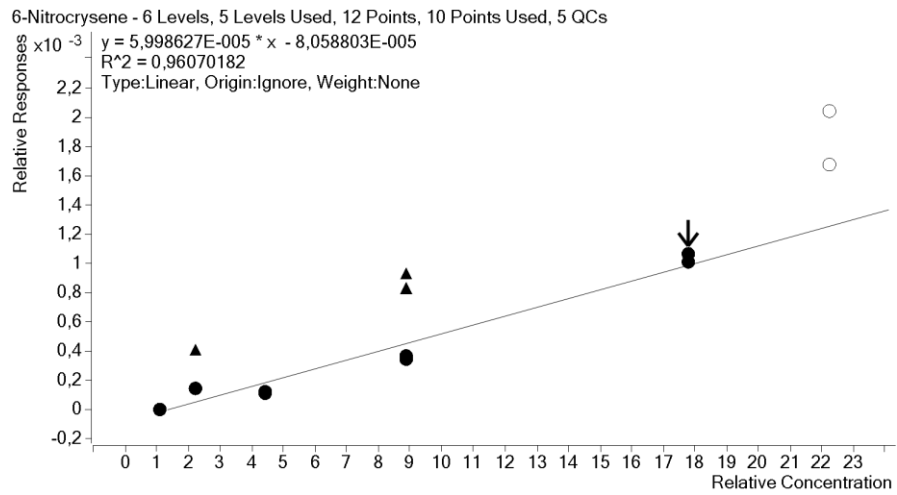


Figure 49: Calibration curve for 6-Nitrocrysene

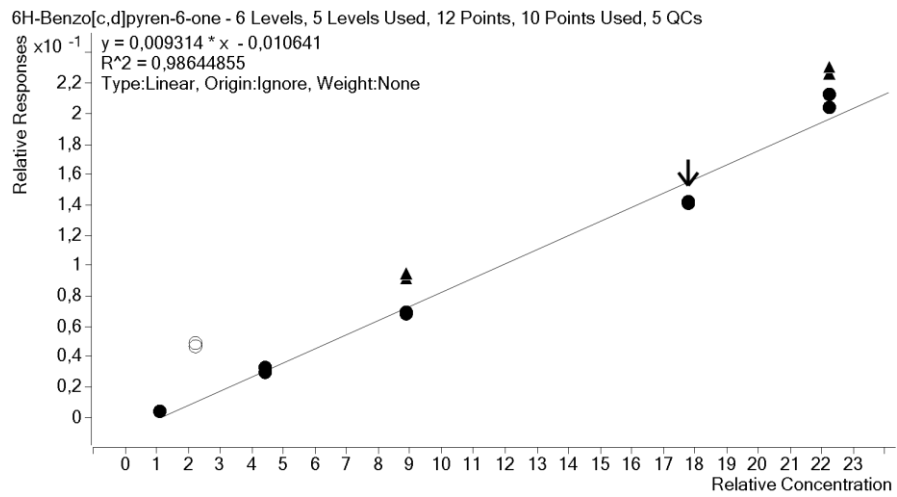


Figure 50: Calibration curve for 6H-Benzo[c,d]pyren-6-one



Norges miljø- og biovitenskapelige universitet
Noregs miljø- og biovitenskapelige universitet
Norwegian University of Life Sciences

Postboks 5003
NO-1432 Ås
Norway